Graduate School ETD Form 9
(Revised 12/07)

PURDUE UNIVERSITY
GRADUATE SCHOOL
Thesis/Dissertation Acceptance

This is to certify that the thesis/dissertation prepared

By Krystin Michelle Riha

Entitled
THE USE OF STABLE ISOTOPES TO CONSTRAIN THE NITROGEN CYCLE

For the degree of Doctor of Philosophy

Is approved by the final examining committee:

Greg Michalski
Chair

Linda Lee

Suresh Rao

Tim Filley

To the best of my knowledge and as understood by the student in the *Research Integrity and Copyright Disclaimer (Graduate School Form 20)*, this thesis/dissertation adheres to the provisions of Purdue University's "Policy on Integrity in Research" and the use of copyrighted material.

Approved by Major Professor(s): Greg Michalski

Approved by: Linda Lee 04/17/2013
Head of the Graduate Program Date

THE USE OF STABLE ISOTOPES TO CONSTRAIN THE NITROGEN CYCLE

A Dissertation

Submitted to the Faculty

of

Purdue University

by

Krystin M. Riha

In Partial Fulfillment of the

Requirements for the Degree

of

Doctor of Philosophy

May 2013

Purdue University

West Lafayette, Indiana

ProQuest LLC.
789 East Eisenhower Parkway
P.O. Box 1346
Ann Arbor, MI 48106 - 1346

To my mother for her

unconditional love and support

ACKNOWLEDGEMENTS

The success and final outcome of this project required a lot of guidance and assistance from many people and I am extremely fortunate to have received this throughout my time here. What I have accomplished during my time in graduate school is a reflection of the amazing people I have had the opportunity to work with who have changed my life in important ways and deserve recognition.

I would like to express the deepest appreciation to my advisor, Dr. Greg Michalski, for taking a chance on me and giving me the opportunity to work with him. As well as the guidance and knowledge that he provided throughout the years. I am also grateful to my extraordinary committee members, Drs. Tim Filley, Linda Lee and Suresh Rao, for their encouragement and faith in me as well as their generosity of time and vast knowledge which constantly challenged me over the years.

My thanks also go to collaborators in Arizona for the aiding in field work and sample collection as well as the generous sharing of knowledge: Drs. Kathleen Lohse, Erika Gallo, Paul Brooks and Tom Meixner.

I wish to express my since thanks to my friends and colleagues who have helped in this work in numerous ways. Especially the valuable assistance and contributions from Dan McMahon, Dr. Bethany Theiling, Michael King and Tanya Katzman.

TABLE OF CONTENTS

Page

Page

Page

LIST OF TABLES

LIST OF FIGURES

Figure Page

Figure Page

Figure Page

Appendix Figure

Appendix Figure Page

ABSTRACT

Riha, Krystin M. Ph.D., Purdue University, May 2013. The Use of Stable Isotopes to Constrain the Nitrogen Cycle. Major Professor: Greg Michalski.

Nitrogen (N) is a crucial element which is essential for life and is necessary for all organisms to live and grow. However, N compounds have also been acknowledged for their many detrimental impacts on the environment. Human activities have dramatically altered the global N cycle through energy production (fossil fuel combustion), production of synthetic fertilizers, and cultivation of legumes and other crops. In this study we aim to resolve sources of reactive N and its fate in semi-arid urban environments using stable isotopes abundances. We have shown conclusively, for the first time, that in semi-arid urban environments the fractional contributions of atmospheric nitrate dominate compared to biologically derived nitrate observed in runoff.

This study employs this use of nitrogen and triple oxygen isotopes of nitrate (NO_3^-) to infer changes in the nitrogen biogeochemical cycle (*e.g.* NO_3^- source appointment, processing, and atmospheric chemistry) in semi-arid urban environments. However, analytical and isotopic approaches come with their caveats many of which are overlooked. The recent isotopic analysis method which employs the use of denitrifying bacteria coupled with subsequent gold tube thermal decomposition has several

shortcomings. Adaptations have been made to: simultaneously analyze nitrogen and oxygen isotopes, discuss detection limits, determine the isotopic effects of sample preparation as well as improve calibration curves to encompass the full range of environmental samples and eliminate the need for extrapolation and improper corrections. One way to determine the sources of nitrogen input to these environments is through the use of multiple isotope analysis ($\delta^{15}N$, $\delta^{18}O$ and $\Delta^{17}O$). However, the commonly used 'dual isotope' approach for NO_3^- source appointment is based on of limited studies conducted in forested and coastal ecosystems and is not conclusive of all ecosystem NO_3^- values. Poor separation also occurs between NO_3^-sources, particularly atmospheric and nitrification, as well as misinterpretation of NO_3^- values due to fractionation occurring during NO_3^- processing. However, many N biogeochemical studies still employ this approach which can lead to inconclusive or incorrect results. Improvements to the dual isotope approach presented in this dissertation include isotopic constraints of NO_3^- sources including atmospheric samples from a variety of locations across the globe, a larger set of fertilizer NO_3^- samples, modeled nitrification NO_3^- $\delta^{18}O$ values, and inclusion of an alternative dual isotope approach using $\Delta^{17}O$ which allows for better source separation.

These NO_3^- source constraints were employed in a case study to determine the effects of urbanization on the coupled nitrogen hydrologic cycle in the semi-arid urban environment of Tucson, AZ. It was found that, contrary to an abundant amount of literature, variations in atmospherically derived NO_3^- was not controlled by changes in NO_x source emissions but rather by shifts in meteorological conditions and atmospheric

chemistry. Regardless of $\Delta^{17}O$ or $\delta^{18}O$ approach, the fraction of atmospheric NO_3^- exported from all the urban catchments, throughout the study period, were sustainably higher than in nearly all other ecosystems. Most studies trying to quantify atmospheric NO_3^- export have attempted to use elevated $\delta^{18}O$ values as a tracer of atmospheric NO_3^- with focus on forested and alpine ecosystems and have shown minimal to no atmospheric contribution to surrounding waterways. The variability in the fractional contribution in the study catchments changes over the course of the storm events suggesting different pools of nitrate are being mobilized during changing hydrologic conditions. The isotope data suggests that type of drainage substrate, such as concrete or vegetated washes, influences N cycling within the individual catchments.

CHAPTER 1. INTRODUCTION

This introduction briefly sets the framework for the research needs on nitrate stable isotope source constraints for nitrogen biogeochemical studies followed by detailing the research objectives and outlining the organization of this Ph.D. dissertation.

Nitrogen (N) is a critical element which is vital for life and is required for all organisms to live and grow. However, N compounds have also been recognized for their many harmful effects on the environment. Human activities have drastically altered the N cycle through anthropogenic activities including: energy production (fossil fuel combustion), production of synthetic fertilizers, and cultivation of legumes and other crops. And driven by energy and food production for an ever growing world population, anthropogenic fixation is projected to increase 60% by 2020 (mainly from developing countries). The magnitude of this production raises critical questions as to the consequences and the fate of new reactive N in the environments. With the cycling of N containing seven oxidation states, numerous mechanisms for interspecies conversion, and a variety of environmental transport/storage processes, nitrogen has arguably the most complex cycles of all the major elements. This complexity makes tracking anthropogenic nitrogen through environmental reservoirs a challenge. However, such studies are of importance due to

nitrogen's role in all living systems and in several environmental issues (*e.g.* greenhouse effect, smog, stratospheric ozone depletion, acid deposition, coastal eutrophication and productivity of freshwaters, marine waters and terrestrial ecosystems).

The use of nitrogen and triple oxygen isotopes of nitrate (NO_3^-) have been used to deduce changes in the nitrogen biogeochemical cycle (*e.g.* NO_3^- source appointment, processing, and atmospheric chemistry). However, analytical and isotopic approaches come with their limitations many of which are neglected. The recent isotopic analysis method which utilizes denitrifying bacteria coupled with subsequent gold tube thermal decomposition has gained widespread use due to its rapid analysis time and small sample size demand and therefore more N isotopic studies have emerged. However, this method has several shortcomings many of which will lead to miscalculation of isotopic values due to poor calibrations this limitation can lead to misinterpretation during N biogeochemical studies.

One way to determine the sources of nitrogen input to these environments is through the use of multiple isotope analysis ($\delta^{15}N$, $\delta^{18}O$ and $\Delta^{17}O$). The $\delta^{15}N$ of NO_3^- can be used to differentiate sources and when combined with $\delta^{18}O$ better separation can be attained due to distinct isotopic signatures. However, the commonly used 'dual isotope' approach for NO_3^- source appointment was designed off of a few N studies conducted in forested and coastal ecosystems and is therefore not conclusive of all ecosystem NO_3^- values. Even when combining both $\delta^{15}N$ and $\delta^{18}O$, NO_3^- sources still overlap, particularly those from atmospheric and nitrification, as well as the potential for values to plot outside source ranges due to fractionation occurring during NO_3^- processing. Because of this poor

separation, misinterpretation of NO_3^- sources and processing can occur. However, many N biogeochemical studies still employ this approach which can lead to inconclusive or incorrect results.

1.1 Objectives

1. Adapt current instrumentation and methodology consisting of the denitrifier method coupled with gold tube thermal decomposition to a) simultaneous measure nitrogen and triple oxygen isotopes of nitrate b) construct better calibration curves encompassing the full range of environmental samples c) provide detection limits and d) determine isotopic effects of sample preparation.

2. Improve on the dual isotope approach of nitrate source identification by constraining nitrate isotopic values for different sources. This includes investigation of the isotopic composition of fertilizer NO_3^- used in agriculture, atmospheric NO_3^- deposited as acid rain and aerosols, and NO_3^- generated by nitrification. Also I will determine the triple oxygen isotope composition ($\Delta^{17}O$) and develop a three isotope mixing model approach.

3. Demonstrate the feasibility of improved dual isotope and three isotope mixing models for understanding the N cycle through a case study of nitrate in runoff collected in semi-arid urban environment.

1.2 Organization

This dissertation is composed of seven chapters, including this introduction, organized as follows:

- CHAPTER 2: A literature review on the nitrogen cycle, stable isotopes and their use in understanding the nitrogen cycle.

- CHAPTER 3: Improving current methodology for nitrate isotopic analysis is discussed. [In review: Riha, K.; King, M.Z.; and Michalski, G. **2013**, *Standardization of $\Delta^{17}O$ and $\delta^{15}N$ using the denitrifier method and gold tube thermal decomposition*]

- CHAPTER 4: This chapter is a brief review of nitrate isotopic data used in constraining nitrate sources which can be utilized in isotopic mixing models and in the typical dual isotope approach as well as the $\Delta^{17}O$ three isotope approach [Submitted: Michalski, G.; Kolanoswski, M; Riha, K. **2013**, *Triple oxygen isotope composition of fertilizer nitrate*, In Press: Michalski. G.; Mase, D.; Riha, K.; and Waldschmidt, H., **2013**, *Assessing peroxy radical chemistry and N_2O_5 uptake using oxygen isotope anomalies in atmospheric nitrate*. Proceedings of the National Academy of Sciences – Physical Science., In Preparation: Michalski, G. and Riha, K., **2013**, *Spatial and temporal variations in oxygen isotopes during ammonia oxidation: Isoscapes of nitrification*., In Preparation: Michalski, G.; Li, B.; and Riha, K., **2013**, *Multiple isotope mixing model for source apportionment of nitrate*, In Preparation: Michalski, G.; Mase, D.; Riha, K.; Wang, F.;

Kolanowski, M; **2013**, *The global isotopic composition of nitrate in precipitation*.]

- CHAPTER 5: This chapter studies the seasonal variations of aerosol nitrate $\delta^{15}N$ composition in a semi-arid urban environment and utilizes it to show seasonal variations are related to atmospheric chemistry not N sources. [In review: Riha, K and Michalski, G., **2013**, *Seasonal variations in NO_3^- $\delta^{15}N$ of $PM_{2.5}$ and PM_{10}: Insights into isotope exchange during NO_x chemistry*.]

- CHAPTER 6: The effects of urbanization on sources of nitrate delivered to waterways are discussed. [In Preparation: Riha, K.M.; Lohse, K.A.; Gallo, E.L.; Brooks, P.D.; Meixner, T.; and Michalski, G., **2013**, *Linkages between the atmospheric and biospheric nitrogen cycles in arid urban ecosystems*.]

- CHAPTER 7: The major findings of the present study on constraining nitrate stable isotope sources for N biogeochemical studies are summarized followed by highlighting future research needs.

CHAPTER 2: LITERATURE REVIEW

2.1 Nitrate and the Nitrogen Cycle

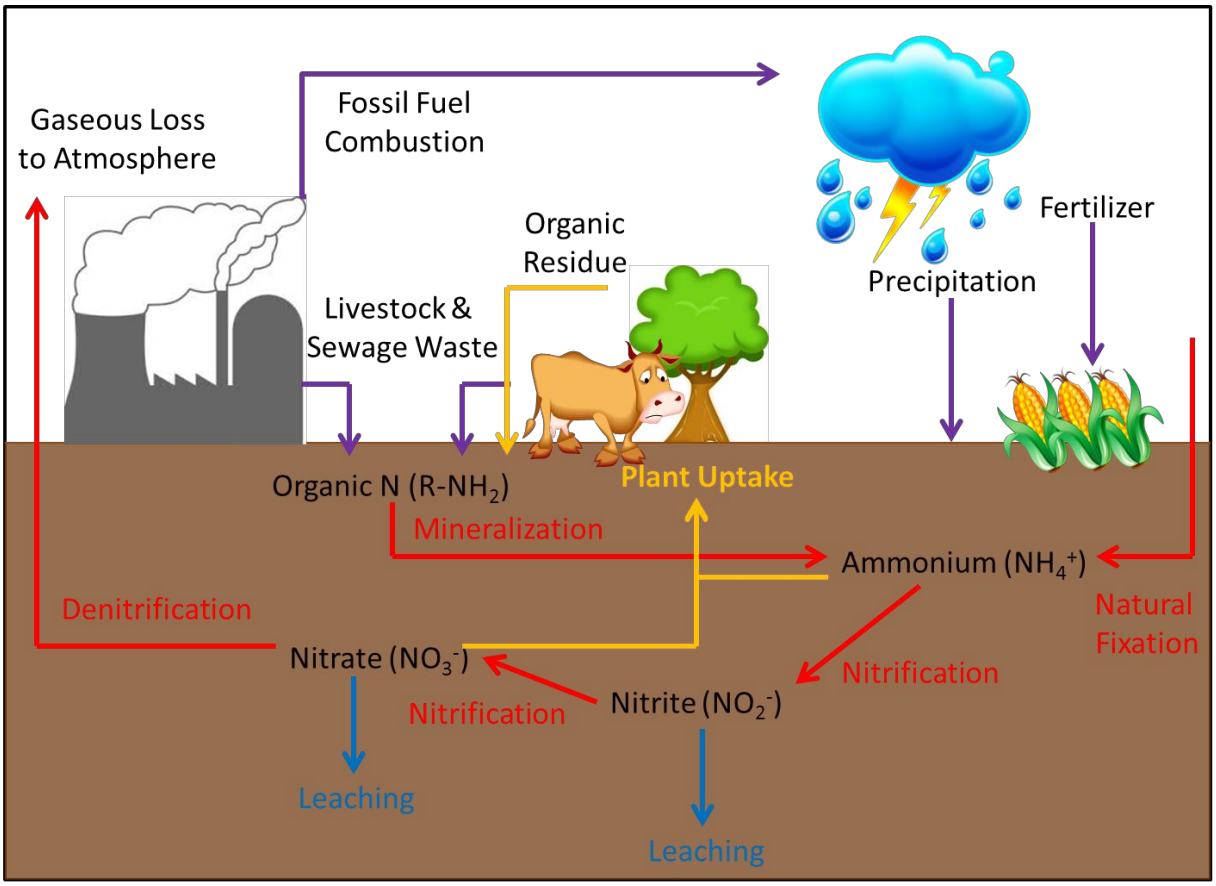

Figure 2.1. The terrestrial nitrogen cycle, where red arrows denote microbial transformations of nitrogen, purple arrows show anthropogenic influences to nitrogen in the environment, orange arrows indicate natural, non-microbial processes affecting the form and fate of nitrogen, and blue arrows designate physical forces acting on nitrogen.

Terrestrial Nitrogen Cycle – Nitrogen (N) is a crucial element essential for life (Keeney et al., 2001). It is a critical component of DNA, RNA and proteins, the building blocks of life, and is necessary for all organisms to live and grow (Galloway et al., 2002; Harrison, 2003). And while nearly 80% of the total mass of the atmosphere is made up of N_2, this form of nitrogen is biologically unavailable to most organisms due to the strong triple bond between the N atoms (Galloway et al., 2002). Breaking this triple bond is a high energy-requiring reaction and in nature only a few select species of microorganisms have developed the capability to covert N_2 to more chemically available forms of N, ammonium (NH_4^+), nitrate (NO_3^-), organic nitrogen $(NH_2)_2CO$ also known as *fixed N*. Fixed N is incredibly versatile, existing in both organic and inorganic forms as well as many different oxidation states (+5 as NO_3^- to -3 as NH_3). The movement of N between the atmosphere, biosphere and geosphere in different forms is described by the nitrogen cycle (Figure 2.1), one of the major biogeochemical cycles on Earth. Throughout the nitrogen cycle, N undergoes a variety of redox reactions that are performed by different organisms (mainly bacteria, archaea and fungi) via five main processes: nitrogen fixation, nitrogen assimilation, mineralization, nitrification and denitrification (Bothe et al., 2007). As microbially mediated processes, the rates of transformations are dependent on environmental factors controlling microbial communities, such as temperature, soil moisture, and resource availability.

Atmospheric NO_x Cycle – Negative consequences of urban growth include increasing emissions of primary airborne pollutants such as nitrogen oxides (NO_x) which can lead to the formation of secondary pollutants (O_3, particulate matter). NO_x is emitted from a variety of sources (mainly anthropogenic) and during the daytime is rapidly converted

between nitric oxide (NO) and nitrogen dioxide (NO_2) through oxidation reactions by ozone (O_3) or peroxy radicals (HO_2 and RO_2) (R1 and R2) and photolysis (R3)

$$NO + O_3 \rightarrow NO_2 + O_2 \quad \text{(R1)}$$

$$NO + HO_2 \text{ (or ROO)} \rightarrow NO_2 + OH \text{ (or RO)} \quad \text{(R2)}$$

$$NO_2 + h\nu \rightarrow NO + O \quad \text{(R3)}$$

The formation of HNO_3 is the main sink for NO_x in the atmosphere. During the daytime NO_2 is oxidized by OH to form nitric acid (HNO_3) (R4) or by O_3 to form NO_3 (R5). During the nighttime, NO_3 reacts with NO_2 to form dinitrogen pentoxide (N_2O_5) (R6), which subsequently hydrolyzes on aerosol surfaces to form HNO_3 (R7). A third, usually minor pathway, is that of hydrogen abstraction by nitrate radicals (R8).

$$NO_2 + OH + M \rightarrow HNO_3 + M \quad \text{(R4)}$$

$$NO_2 + O_3 \rightarrow NO_3 + O_2 \quad \text{(R5)}$$

$$NO_2 + NO_3 \leftrightarrow N_2O_5 \quad \text{(R6)}$$

$$N_2O_5 + H_2O + \text{surface} \rightarrow 2HNO_3 \quad \text{(R7)}$$

$$NO_3 + VOC \rightarrow HNO_3 + R \quad \text{(R8)}$$

Gaseous HNO_3 is highly water soluble and reactive and therefore is easily scavenged from the atmosphere by precipitation as wet deposition or on aerosol particles as dry deposition. Through the removal of NO_x, by the formation and subsequent removal of HNO_3, O_3 and OH mixing ratios are changed and aerosol production is altered (Dentener

et al., 1993). This dissertation research is focused on gaining a better understanding of the nitrogen cycle, in particular assessing the impact of human activities on the movement on N within urban ecosystems.

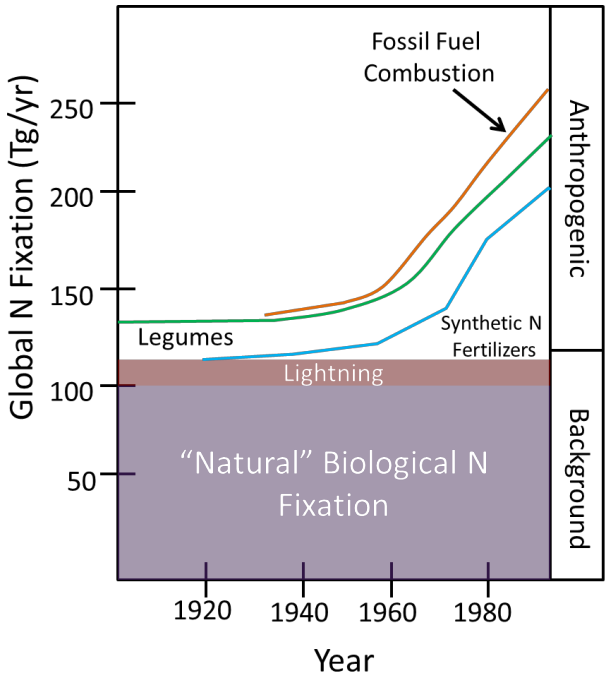

Figure 2.2. Recent increases in anthropogenic N fixation in relation to natural N fixation (Image: adapted from (Vitousek et al., 1997)).

While N is required to sustain life, N compounds have also been acknowledged for their many detrimental impacts on the environment (Keeney et al., 2001). Globally, humans fix N_2 at the same rate as biotic N_2 fixation (Galloway et al., 1995; Vitousek et al., 1997) (Figure 2.2). Anthropogenic activities contributing to the production of reactive N species include: energy production (fossil fuel combustion), production of synthetic

fertilizers, and cultivation of legumes and other crops. Human activities have dramatically altered the global N cycle, increasing both the availability and mobility of reactive N species over a large regions. Unsurprisingly, there is a notable anthropogenic N excess from developed countries, where vehicle emissions and industrial agriculture are most prevalent (Socolow, 1999). While excess N additions (whether intentionally through fertilization or unknowingly as a consequence of fossil fuel combustion) occur locally, their influence spreads regionally and even globally (Vitousek et al., 1997). Effects within the environment vary with the N form however the environmental repercussions are grave and long lived. Harmful impacts of excess N include increased concentrations of the greenhouse gas N_2O (Richardson et al., 2009) and drive photochemical smog production (Vitousek et al., 1997) and the destruction of stratospheric ozone (Lassey et al., 2007; Ravishankara et al., 2009), shifts in plant and microbial biodiversity as well as declines in sensitive organisms in both aquatic and terrestrial ecosystems (Fenn et al., 2003a; Tilman et al., 1996), soil acidification (Fenn et al., 2003a), eutrophication of coastal waters and estuaries (Rabalais, 2002), and degradation of surface waters and groundwater (Williams et al., 1996). And driven by energy and food production for an ever growing world population, anthropogenic fixation is projected to increase 60% by 2020 (mainly from developing countries), therefore causing a fertilizing effect on global ecosystems and changing ecosystem function in ways we still do not understand. This dissertation aims to resolve sources of reactive N and its fate in the environment using stable isotopes abundances.

2.2 Stable Isotopes of Nitrogen and Oxygen

The use nitrogen and triple oxygen isotopes of nitrate have been used to infer changes in the nitrogen biogeochemical cycle. Nitrogen has two stable isotopes with mole fractions of: ^{14}N (0.9963) and ^{15}N (0.0037) whereas oxygen has three stable isotopes: ^{16}O (0.9976), ^{17}O (0.0004) and ^{18}O (0.0020) (Criss, 1999). The natural abundances of stable isotopes are quite small and to compensate instruments have employed a technique of quickly measuring and comparing differences in intensities from the sample to the standard rather than measuring absolute intensities for each sample. For these reasons it is common to report the measured difference in the isotopic composition of the sample (*x*) and an accepted standard (*std*) in terms of dimensionless δ-values, defined as by the following formula (Criss, 1999):

$$\delta_x = 1000 \cdot \left(\frac{R_x - R_{std}}{R_{std}}\right)$$

where R is the ratio of the rare isotope to the abundant isotope (*e.g.* $^{15}N/^{14}N$). Nitrogen and oxygen δ values are made in comparison to N_2-air and Vienna Standard Mean Ocean Water (VSMOW), respectively (Coplen et al., 2002). Delta (δ) notation is a way of making comparisons between the isotopic ratios of two materials. These minuscule differences in isotopic abundances are a significant way of discerning transformations in biogeochemical systems such as the nitrogen cycle.

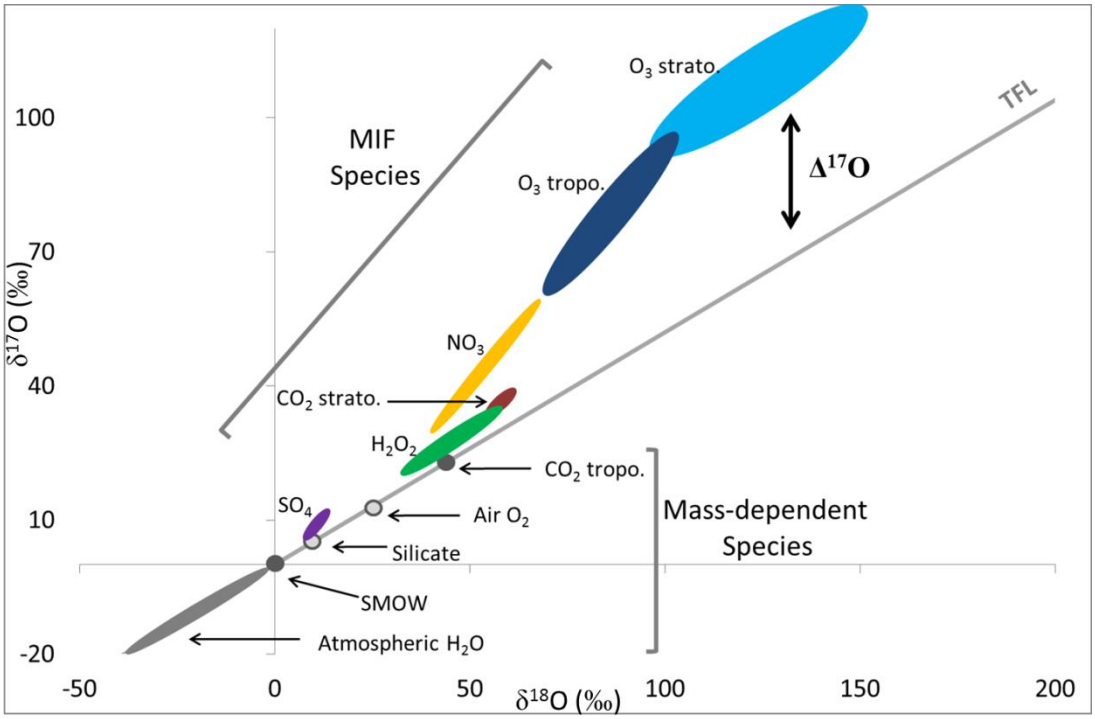

Figure 2.3: Oxygen isotopic compositions of atmospheric species that have been measured to date. TLF represents the oxygen terrestrial fractionation line based on mass dependent fractionation ($\delta^{17}O = 0.52 \bullet \delta^{18}O$) and MIF (mass independent fractionation) species are atmospheric derived oxygen sources that are equally enriched in ^{17}O and ^{18}O. The deviation from the TLF and MIF species is denoted $\Delta^{17}O$ ($\Delta^{17}O \sim \delta^{17}O - 0.52 \bullet \delta^{18}O$). (Image adapted from: (Thiemens, 2006))

The use of triple oxygen analyses to further gain insight into biogeochemical studies is a recent advancement. The three stable isotopes of oxygen typically fractionate in a mass dependent manner, therefore an almost linear relationship exists between changes in $\delta^{17}O$ and $\delta^{18}O$ (Miller, 2002a) which can be expressed as: $\delta^{17}O = 0.52 \bullet \delta^{18}O$. A dual isotope plot of $\delta^{17}O$ and $\delta^{18}O$ of the main oxygen reservoirs on Earth (H_2O, silicate

and carbonate rocks, and air O_2) verifies this theoretical relationship. The resulting line is referred to as the oxygen terrestrial fractionation line (TFL) (Figure 2.3). One well-known exception to the mass dependence rule is the isotope fractionation that arises during ozone formation (Thiemens et al., 1983) in which ^{17}O and ^{18}O become equally enriched in the resulting product (Figure 2.3). This process has been designated a mass independent fractionation (MIF) since both minor oxygen isotopes are impartially enriched, independent of their mass differences. MIF is denoted by $\Delta^{17}O$ and can be quantified by (Miller, 2002a):

$$\Delta^{17}O = \left[ln\left(1 + \frac{\delta^{17}O}{1000}\right) - 0.52 \cdot ln\left(1 + \frac{\delta^{18}O}{1000}\right)\right] \cdot 1000$$

Chapter 4 of this dissertation details the development of a new method for simultaneous $\delta^{15}N$, $\delta^{18}O$, and $\Delta^{17}O$ analysis of nitrate.

2.2.1 Isotopic Exchange and Equilibrium Fractionation of N and O Stable Isotopes

Isotope effects are only observed when reactions do not go to completion, such that not all N (or O) atoms in a substrate go into the products of the reaction. Variations in stable isotope ratios are a result of equilibrium and kinetic isotope effects. Equilibrium isotope effects arise because a larger activation energy is required, during a physical or chemical process, to dissolve an isotopically heavy chemical species (*e.g.* ^{15}N, ^{17}O and ^{18}O) compared to a lighter species (*e.g.* ^{14}N and ^{16}O) therefore an isotopically lighter species will be bound less strongly at equilibrium (Bigeleisen, 1952; Bigeleisen, 1965). A simplified example of an equilibrium exchange is:

$$A^*X + BX \leftrightarrow AX + B^*X$$

where A and B are different phases (e.g. $H_2O_{(g)}$ and $H_2O_{(aq)}$) or products and reactants and '*' represents the trace isotope. In this simplified reaction, isotopic fractionation of compound *A* relative to compound *B* can be expressed as a fractionation factor:

$$\alpha_{A-B} = \frac{R_A}{R_B}$$

The isotopic fractionation factor can be represented by the enrichment factor (ε), which describes the isotopic enrichment of the product relative to the substrate in parts per thousand symbolized as ‰:

$$\varepsilon_{A-B} = (\alpha_{A-B} - 1) \cdot 1000$$

An example of an equilibrium isotope exchange is the exchange of ^{15}N between NH_3 and NH_4^+ in an aqueous solution:

$$^{14}NH_3 + {}^{15}NH_4^+ \leftrightarrow {}^{15}NH_3 + {}^{14}NH_4^+$$

and the fractionation would be calculated by the ratios:

$$\alpha_{NH3-NH4} = \frac{\left(\frac{^{15}NH_3}{^{14}NH_3}\right)}{\left(\frac{^{15}NH_4^+}{^{14}NH_4^+}\right)}$$

Kinetic isotope effects arise because heavier molecules react more slowly than their lighter counterparts. Kinetic isotope fractionations are also described by α, however in this case it is sometimes (confusingly) defined by the ratio between the rates of the process for light and heavy isotopes (k_L and k_H, respectively):

$$\alpha = \frac{k_L}{k_H}$$

2.2.2 Tracing Nitrate Sources and Cycling Through the Use of N and O Stable Isotopes

Table 2.1. Nitrogen isotope effects for microbial processes in pure cultures (Adapted from (Casciotti, 2009; Hogberg, 1997))

Process	Reaction	$^{15}\alpha_k$	$^{15}\varepsilon_k$ (‰)	References
Nitrate reduction (denitrification)	$NO_3^- \rightarrow NO_2^-$	1.013 – 1.030	+13 – +30	(Barford et al., 1999; Delwiche et al., 1970; Granger et al., 2006)
Nitrite reduction (denitrification)	$NO_2^- \rightarrow NO$	1.005 – 1.025	+5 – +25	(Bryan et al., 1983; Casciotti, 2009)
Nitrous oxide reduction (denitrification)	$N_2O \rightarrow N_2$	1.004 – 1.013	+4 – +13	(Barford et al., 1999; Ostrom et al., 2007)
Nitrate reduction (nitrate assimilation)	$NO_3^- \rightarrow NO_2^-$	1.005 – 1.010	+5 – +10	(Granger et al., 2004b; Needoba et al., 2004; Waser et al., 1998)
Nitrogen fixation	$N_2 \rightarrow N_{org}$	0.998 – 1.002	-2 – +2	(Delwiche et al., 1970; Hoering et al., 1960; Meador et al., 2007)
N assimilation	$NH_4^+ \rightarrow N_{org}$ $NO_3^- \rightarrow N_{org}$	1.000 – 1.027	+1 – +27	(Hoch et al., 1992; Hogberg, 1997; Waser et al., 1998)
N mineralization	$N_{org} \rightarrow NH_4^+$	~1.000	+1	(Hogberg, 1997)
Ammonium oxidation (nitrification)	$NH_4^+ \rightarrow NO_2^-$	1.014 – 1.038	+14 – +38	(Casciotti et al., 2003; Delwiche et al., 1970; Mariotti et al., 1981; Yoshida, 1988)
Nitrite oxidation (nitrification)	$NO_2^- \rightarrow NO_3^-$	0.9872	-12.8	(Casciotti, 2009)
Ammonia volatilization	$NH_3 \leftrightarrow NH_4^+$	1.029	+29	(Hogberg, 1997)
Ionic equilibrium (ammonia volatilization)	$NH_4^+ \leftrightarrow NH_3$ (in solution)	1.020 – 1.027	+20 – +27	(Hogberg, 1997)
Diffusion	NH_4^+, NH_3, NO_3^- (in solution)	~1.000	0	(Hogberg, 1997)

N_2 Fixation – Nitrogen fixation is the process of converting N_2 into biologically available nitrogen. N_2 gas is an especially stable compound due to the strength of the triple bond and consequently requires a considerable amount of energy to oxidize it into

bioavailable inorganic N. The whole process requires eight electrons and at least sixteen ATP molecules (Bothe et al., 2007):

$$N_2 + 8H^+ + 8e^- \rightarrow 2NH_3 + H_2$$

As a result, only a select few microorganisms are capable of performing this energetically demanding process (Galloway et al., 2002) along with abiotic processes such as lightening and fossil fuel combustion (Vitousek et al., 1997). ^{15}N fractionation during nitrogen fixation is relatively small (Table 2.1) even though there are discrepancies between 'normal' fractionation and inverse fractionation (where heavy isotopes preferentially go into product) factors. These are mainly attributed to differences in bacterial strain, nutrient supply, and soil moisture (Bergersen et al., 1986; Ledgard, 1989; Steele et al., 1983). Humans fix N_2 into NH_3 using the Haber-Bosch process, which uses high temperatures and catalysts. Data shown in Chapter 4 of this dissertation shows that there is little to no isotope fractionation during this process.

Nitrogen Assimilation – Nitrogen assimilation occurs both in plants and microorganisms and is the formation of organic N (*e.g.* amino acids) from inorganic N (NH_4^+ and NO_3^-). Assimilation by plants or microorganisms acts as a temporary holding reservoir for nitrate, which can then be regenerated by mineralization or nitrification. Fractionation factors involved in assimilation can vary greatly (Table 2.1). These discrepancies are due to plant and microbial competition for substrate, substrate availability, substrate selectivity (NH_4^+ versus NO_3^-), and supply and demand of substrate (Hogberg, 1997). However, it has been shown that if assimilation is occurring by algae, bacteria, and possibly plants that both the $\delta^{15}N$ and $\delta^{18}O$ of the residual nitrate (plotted on a dual isotope plot) will increase in a linear relationship with a slope of 1 (Granger et al.,

2004a). Thus 1:1 trends in the $\delta^{15}N$ and $\delta^{18}O$ can be used as evidence of assimilation in ecosystem studies. Chapter 6 of this thesis uses this technique to assess the importance of assimilation in urban catchments located in Tucson, AZ, USA.

Nitrogen Mineralization – Nitrogen mineralization is the process in which organic N (*e.g.* proteins in dead plant material) is converted to ammonium. Very little evidence supports isotopic fractionation during nitrogen mineralization (Table 2.1).

Ammonia Volatilization – Ammonia volatilization is a physicochemical process where ammonium is in equilibrium between the gaseous and hydroxyl forms (Reddy et al., 1984):

$$NH_3(aq) + H_2O \leftrightarrow NH_4^+ + OH^-$$

This reaction is pH dependent where alkaline pHs support the presence of the aqueous or gaseous forms (NH_3) and at acidic or neutral pHs ammonium is primarily in the ionic form (NH_4^+). Once converted to gaseous forms, the transfer of dissolved ammonia in aqueous solution to the atmosphere is dependent on the differences in the respective partial pressures and a net transfer to the atmosphere will occur until an equilibrium is reached in concert with Henry's law (Reddy et al., 1984). Several steps during ammonia volatilization involve possible isotopic fractionation of N including: the equilibrium of $NH_4^+ \leftrightarrow NH_3$ in solution, diffusion of NH_3 to the site of volatilization, volatilization of NH_3, and diffusion of NH_3 away from the site of volatilization (Hogberg, 1997). The combined effect of these processes can impart a large net fractionation (Table 2.1). These fractionations are largely dependent on the rate limiting step of the reaction (*e.g.* pH of substrate, temperature, wind velocity at the surface of water and substrate supply (Reddy et al., 1984)). However, where ammonia volatilization is a significant process, it will

leave the residual N enriched in ^{15}N. In Chapter 5 of this dissertation the data show that NH_3 equilibrium is not important in the $\delta^{15}N$ of aerosol NH_4NO_3.

Nitrification – Nitrification in soil predominately occurs via chemolithic autotrophic ammonia oxidizing bacteria (AOB) and nitrite oxidizing bacteria (NOB). Nitrification is the conversion of ammonia (NH_3) to nitrate (NO_3^-) which occurs in a two-step process, in which AOB (*e.g. Nitrosomonas* or *Nitrosospira*) convert NH_3 to nitrite (NO_2^-) (Norton et al., 2011):

$$NH_3 + O_2 + 2H^+ + 2e^- \rightarrow NH_2OH + H_2O \rightarrow NO_2^- + 5H^+ + 4e^-$$

While NOB (*e.g. Nitrobacter* or *Nitrospira*) covert NO_2^- to NO_3^- (Norton et al., 2011):

$$NO_2^- + H_2O \rightarrow NO_3^- + H_2O + 2H^+ + 2e^-$$

Currently there are no known AOB which can covert NH_3 directly to NO_3^- (Hooper et al., 1997). In general, AOB and NOB populations are coupled in a way that inhibits accumulation of NO_2^- in soils except under transient conditions that have decreased the population or suppresses the activity of NOBs (*e.g.* NH_3 toxicity due to fertilizer applications (Norton et al., 2011), low pH enhancing production of HNO_2 (Venterea et al., 2000)). However, since AOB require NH_4^+/NH_3, CO_2 and O_2 to proliferate and grow ammonia oxidation is the rate limiting step in nitrification due to limited substrate availability (Norton et al., 2011). And at low O_2 concentrations, it has been shown that AOB can produce significant amounts of N_2O (Bremmer et al., 1978), NO (Goreau et al., 1980) and possibly N_2 (Poth, 1986) and it is argued that fraction of these by-product gases may account for as a comparable a fraction from denitrification (Anderson et al., 1986).

Nitrification and $\delta^{15}N$ − Nitrification has been associated with fairly large isotope effects (α), with respect to ^{15}N, ranging from 1.015 – 1.036 (Table 2.1) during the ammonia oxidation step. Since nitrite oxidation is not rate limiting, it has been suggested that there should be no further fractionation (Hogberg, 1997), however, recently Casciotti (2009) observed an inverse kinetic isotope fractionation (0.9872, Table 2.1) during bacterial nitrite oxidation in a strain of marine NOB (Casciotti, 2009). Inverse kinetic isotope effects are rare and it was suggested to expand these observations to determine if this inverse fraction is universal amongst NOB to further constrain N cycling within marine and terrestrial environments. This suggests in ecosystems where nitrification readily progresses and NO_2^- does not accumulate that ^{15}N will be enriched in NO_3^- compared to NH_3.

Nitrification and $\delta^{18}O$ – During bacterial nitrification, oxygen from H_2O and O_2 are incorporated into the product NO_3^-. O_2 is incorporated during the oxidation of NH_3 to hydroxylamine (NH_2OH) while H_2O is acquired during the subsequent oxidation to NO_2^- (Anderson et al., 1986; Andersson et al., 1983). The remaining oxygen atom incorporation from the oxidation of NO_2^- to NO_3^- is derived from H_2O (Hollocher, 1984; Kumar et al., 1983). Based on simple stoichiometry of oxygen incorporation the oxygen isotopic composition of NO_3^- generated by nitrification can be determined by a two component mixing model (Bohlke et al., 1997; Durka et al., 1994; Kendall, 1998a; Mayer et al., 2001; Wassenaar, 1995):

$$\delta^{18}O_{NO3} = \frac{2}{3}(\delta^{18}O_{H2O}) + \frac{1}{3}(\delta^{18}O_{O2})$$

Where $\delta^{18}O_{O2}$ is the isotopic composition of air O_2 which are essentially spatially and temporally constant at 23‰ (Horibe et al., 1973; Kroopnick et al., 1972) and the $\delta^{18}O_{H2O}$ values are the isotopic composition of soil water which is a function of precipitation $\delta^{18}O$ values and enrichment from evapotranspiration. Precipitation $\delta^{18}O$ values vary spatially and temporally as a function of water vapor source, temperature, and altitude and typically span -20 to 5‰ (Gat, 1996). While this straightforward stoichiometric approach has worked for some researchers in the natural environment (Mayer et al., 2001) it does not account for possible oxygen isotopic exchange with NO_2^- and water. It has been shown that NO_2^- equilibrates with water and is a strong function of pH (Bunton et al., 1952) in which rapid exchange occurs at lower pH and exchange requiring months at higher pH. If complete isotopic exchange occurs then any memory of the $\delta^{18}O$ value of O_2 incorporated during the oxidation of NH_3 to NH_2OH would be erased therefore altering the stoichiometric ratio. It has also been suggested that variations in the $\delta^{18}O$ values of oxygen atom donors (O_2 and H_2O) as well as oxygen isotopic exchange and fractionation will change the resulting $\delta^{18}O$ values of NO_3^-. This includes possible kinetic isotope effects ($^{18}\varepsilon$) of : 1) the selection of NH_2OH 2) selection of NO_2^- 3) incorporation of oxygen atoms from O_2 4) and 5) incorporation of oxygen from H_2O (Buchwald et al., 2010; Casciotti et al., 2009). While these isotope effects have been studied, it was determined that there was an isotopic fractionation occurring during either the incorporation of O_2 or H_2O but it varied substantially by AOB species (Casciotti et al., 2009) and an inverse kinetic isotope effect among NOB species (similar to ^{15}N) (Buchwald et al., 2010). In Chapter 4 of this dissertation several models were developed

to predict the spatial and temporal variation of $\delta^{18}O$ values of NO_3^- produced by soil nitrification.

Denitrification – Denitrification is the sole process in the nitrogen cycle which removes bioavailable N and returns it to the atmosphere; it is the biological reduction of NO_3^- to N_2 gas via heterotrophic bacteria under anaerobic conditions. It is a form of microbial respiration in which during anaerobic conditions, when oxygen levels are depleted, NO_3^- (or NO_2^-) serves as an alternative to O_2 as the final electron acceptor in the oxidation of organic matter (Reddy et al., 1984):

$$5(CH_2O) + 4NO_3 + 4H^+ \rightarrow 5CO_2 + 2N_2 + 7H_2O$$

However, due to gaseous loss as NO and N_2O due to incomplete denitrification and varying microbial populations the general sequence is accepted for biochemical denitrification (Reddy et al., 1984):

$$NO_3^- \rightarrow NO_2^- \rightarrow NO + N_2O \rightarrow N_2$$

The reduction of NO_3^-, thus completes the nitrogen cycle by returning fixed N to the atmosphere as N_2, NO, and N_2O. Other forms of NO_3^- removal have been proposed and confirmed in natural ecosystems (*i.e.* dissimilatory reduction of nitrate to ammonium (DNRA) and anammox) and it has been suggested that these pathways are being underestimated due to the complexities with denitrification (Burgin et al., 2007). However, the current state of isotopic research has not been able to constrain ^{15}N and ^{18}O fractionations occurring within these different NO_3^- removal pathways (Casciotti, 2009). Chapter 3 of this dissertation details the use of denitrifying bacteria as a way of determining the isotope composition of NO_3^-.

Denitrification and $\delta^{15}N$ and $\delta^{18}O$ – Denitrification is associated by significant isotope fractionation because organisms preferentially utilize the light isotope. The reported ^{15}N fractionation factors (Table 2.1) have been found to be highly variable. Possible explanations for these discrepancies include differences in concentrations of electron acceptors and donors, variations in temperature, different soils leading to dispersion effects (Hogberg, 1997). Whatever the cause behind these deviations in reported ^{15}N fractionations, they all result in enrichment of the residual NO_3^-. And in systems where denitrification occurs over time, the residual NO_3^- will become enriched (in both ^{15}N and ^{18}O) following a Rayleigh distillation (Kendall, 1998a; Mariotti et al., 1981). In which the combination of these two Rayleigh distillation processes gives a linear relationship termed fractionation ratio, such that during denitrification both the $\delta^{15}N$ and $\delta^{18}O$ of the residual nitrate (on a dual isotope plot) will increase along a trend line with a slope of 0.5 (Bottcher et al., 1990; Chen et al., 2005)

2.2.3 Tracing Nitrate Sources Through the use of $\Delta^{17}O$

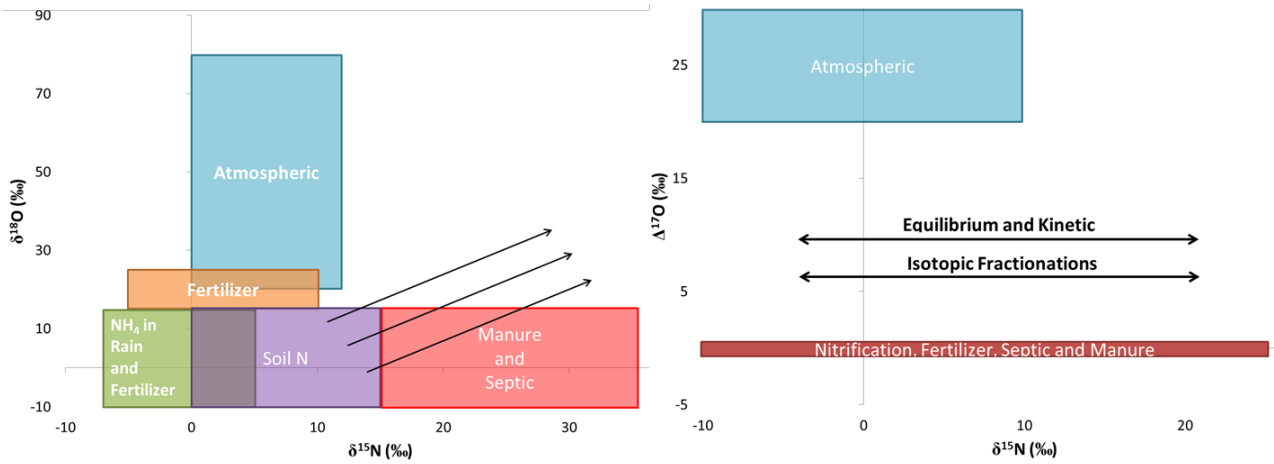

Figure 2.4 Comparison of the typical dual isotope plot of $\delta^{15}N$ and $\delta^{18}O$ (Kendall, 1998a) (Left) and $\Delta^{17}O$ (Michalski et al., 2003b) (Right) with differing NO_3^- sources with arrows indicating kinetic and equilibrium mass dependent isotope fractionations (Image adapted from: (Michalski et al., 2003b)).

While the dual isotope approach is often used in deconvoluting NO_3^- sources (*e.g.* fertilizer, atmospheric deposition, soil N) and processes (denitrification and assimilation) (Figure 2.4, left) (Bottcher et al., 1990; Granger et al., 2004b; Kendall, 1998a), it can often lead to error due to overlapping $\delta^{15}N$ and $\delta^{18}O$ values of NO_3^- sources, particularly atmospheric nitrate and NO_3^- originating from nitrification. As well as kinetic and equilibrium isotope fractionations which will enrich (or deplete) residual NO_3^- and can usually led to misinterpretation when $\delta^{15}N$ and $\delta^{18}O$ values fall outside the range and can be considered a mixing of two NO_3^- sources. Through the use of $\Delta^{17}O$ values the dual isotope approach can be significantly simplified (Figure 2.4, right) (Michalski et al., 2003b). $\Delta^{17}O$ values for NO_3^- sources originating from fertilizers, manure, and

nitrification (i.e. soil N) are equal to zero (Michalski et al., 2003b; Michalski et al., 2004d). $\Delta^{17}O$ values will remain unaltered by postdepositional isotopic fractionation effects (e.g. denitrification) as they will obey the well-established mass dependent fractionation law. Therefore, the $\Delta^{17}O$ can be used as a conservative tracer of atmospheric NO_3^-. Chapter 6 of this dissertation details how $\Delta^{17}O$ was used to assess the importance of atmospheric NO_3^- in Tucson catchments and how that relates to N cycling under different land use types in urban environments.

CHAPTER 3: STANDARDIZATION OF $\Delta^{17}O$ and $\delta^{15}N$ USING THE DENITRIFIER METHOD AND GOLD TUBE THERMAL DECOMPOSITION

3.1 Introduction

Stable isotope abundance variations in nitrate ($\Delta^{17}O$, $\delta^{15}N$, and $\delta^{18}O$) are useful in nitrogen (N) studies as they can be used to infer changing nitrate (NO_3^-) sources, biogeochemical processes and atmospheric chemistry. Various NO_3^- sources can have different $\delta^{15}N$ values which can be used to apportion N sources in mixtures (Elliott et al., 2007). When NO_3^- $\delta^{15}N$ values are used in conjunction with $\delta^{18}O$ values, denitrification and assimilation can often be differentiated (Bottcher et al., 1990; Sebilo et al., 2003a) as well as refining source apportionment. NO_3^- $\Delta^{17}O$ values can be used to differentiate HNO_3 oxidation pathways in the atmosphere (Alexander et al., 2009; Michalski et al., 2003b; Morin et al., 2008) and to determine the fraction of atmospheric NO_3^- in stream and soil samples (Michalski et al., 2003b; Michalski et al., 2004d) Therefore, a quick, accurate, and precise method of NO_3^- isotopic analysis of small samples would be useful in N biogeochemical studies.

The denitrifier method is a recent isotopic analysis method for NO_3^- (Casciotti et al., 2002; Sigman et al., 2001). The approach uses denitrifying bacteria (*Pseudomonas aureofaciens*) to convert NO_3^- into N_2O that is then collected from a headspace vial and

analyzed using an isotope ratio mass spectrometer to determine the nitrate's $\delta^{15}N$ and $\delta^{18}O$ values. This method has been used extensively to understand NO_3^- cycling in a variety of systems (ocean, soil, groundwater, etc.) (Amoroso et al., 2010; Casciotti et al., 2007; Jarvis et al., 2009; Morin et al., 2012; Wankel et al., 2010). Conversion of N_2O into O_2 and N_2 by gold catalyzed thermal decomposition (Kaiser et al., 2007) was recently developed in order to analyze $\Delta^{17}O$ because analysis of N_2 and O_2 avoids isobaric interferences that occurs when N_2O is the analyte (Michalski, 2010). This study, however, had several limitations. First, it only focused on triple oxygen isotope analysis and did not integrate simultaneous $\delta^{15}N$ analysis that would be beneficial in N studies. Secondly, the isotopic references used for calibrating oxygen isotopes did not fully encompass the isotopic range of nitrates usually found in the environment. Finally, the method's calibration also did not fully examine the detection limit for $\Delta^{17}O$ nor did it discuss any effects of sample preparation or purification might have on NO_3^- isotopes. The objectives of this paper are to further develop the denitrifier method with gold tube thermal reduction and address the following problems left unanswered by previous studies.

3.2. Bacterial Preparation

A modified version of the denitrifier method detailed by Casciotti et. al. (2002) was carried out but with several small modifications. The bacteria are cultured in 4 autoclaved 250 mL polycarbonate centrifuge bottles (Fisher Scientific, 300 Industry Drive, Pittsburgh, PA 15275, USA) containing 250 mL of amended tryptic soy broth growth medium for 7 days. The solutions are tested for the presence of NO_3^- using Aqua

Chek NO_3^- test strips (Hach Company, P.O. Box 389, Loveland, CO 80539-0389, USA) before the bacteria are harvested by centrifuging, decanting, and rinsing twice with 50 mL of NO_3^- free growth medium, then finally resuspending the bacteria in 130 mL of NO_3^- free growth medium. This solution is placed in a glass, fritted disc gas washing bottle and purged with helium at a rate of 10 mL/min for 2 hours. The bacteria solution is then placed into an autoclaved 130 mL glass bottle, sealed with a crimp cap and the headspace is flushed for 5 minutes with helium and allowed to incubate overnight at room temperature. The following day, the solution is purged with helium at a rate of 10 mL/min for 2 hours. One mL of bacteria is then pipetted into 12 mL exetainer screw top septum vials (Labco Limited, Unit 3 Pont Steffan Business Park, Lampeter, Ceredigion, SA487HH, United Kingdom) that are then capped and flushed with helium at a rate of 40 mL/min for 4 minutes. This flushing routine reduces blank analysis to below the detection limit of 1 nmol. The sample, consisting of 1 mL of NO_3^- solution (containing 250 – 500nmol NO_3^-) is then added to the vials and incubated for 2 hours and then lysed with 0.5 mL of 1% NaOH. Samples are then loaded into the headspace extraction system.

3.3 Instrumentation

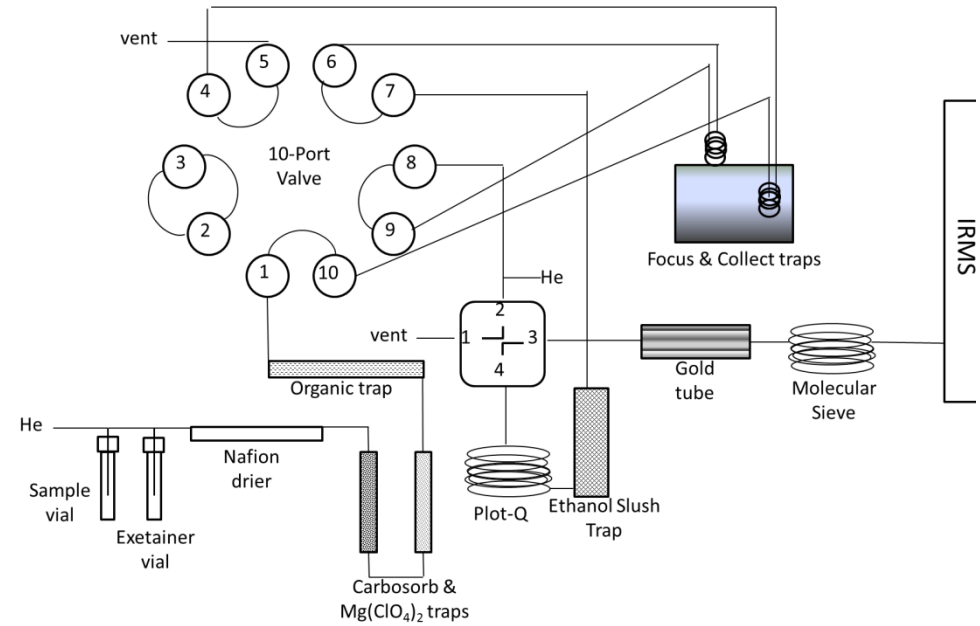

Figure 3.1. N_2O headspace extraction apparatus.

N_2O produced from NO_3^- denitrification in the sample vial is extracted from the headspace, cryogenically collected, and purified, before entering the isotope ratio mass spectrometer (IRMS) (Figure 3.1). Each sample vial is flushed with a helium carrier gas (20 mL/min for 12 minutes) using a double needle. The He/N_2O mixture passes through a second double needle inserted into a vacant exetainer vial, so that any liquid that might exit the sampling vial will be isolated and not contaminate the subsequent purification traps. The gas stream then passes through a Nafion drier, 7 mL of solid Carbosorb to remove CO_2, 7 mL of magnesium perchlorate to absorb trace water, and a Supelco Type F hydrocarbon purge trap that filters out volatile organic compounds. The gas stream then passes through a cryogenic loop immersed in liquid nitrogen. After 10.5 minutes the trap is thawed and the pre-concentrated N_2O/He is transferred and cryogenically collected (2

minutes) in a focusing loop. The focus loop is then thawed and the N_2O/He through an -80°C ethanol slush trap which is used as a final filter to reduce water and VOC's in the sample gas before it enters the HP-Plot-Q column (Agilent J&W GC Columns, 5301 Stevens Creek Blvd, Santa Clara, CA 95051, USA) where it is separated from any other gases, including CO_2. When analyzing for $\delta^{15}N$ and $\delta^{18}O$, the sample gas is injected into a custom open-split interface and analyzed in the IRMS. When analyzing for $\delta^{15}N$, $\delta^{18}O$ and $\delta^{17}O$, the sample gas is first passed through a 25 cm long, 2mm I.D. gold tube (Depths of the Earth, 6314 E. Morning Vista Lane, Cave Creek, AZ 85331-6701, USA) that has four, 10cm long pieces of gold wire braided together inserted into its center. The tube is housed in a 35.5cm long quartz capillary tubing (O.D 7mm, I.D. 2mm) which is fixed inside a furnace heated to 900°C and connected to the GC system with stainless steel Swageloks fitted with Teflon ferrules. The N_2O is disproportionated to N_2 and O_2 within the gold tube and then are separated using a molecular sieve capillary GC column (Agilent J&W GC Columns, 15m length and 0.32mm ID) before analysis by a Delta-V Plus IRMS. The IRMS is equipped with an 11-cup collector configuration which allows for N_2 ($^{29}N/^{28}N$) and O_2 ($^{33}O/^{32}O$ and $^{34}O/^{32}O$) isotopes to be measured without peak jumping (magnet adjustment). With a sample analysis time of 20 minutes, the automated N_2O system is capable of running 72 samples in a 24 hour period.

3.4. Stable Isotopes

The denitrifier method combined with gold tube thermal reduction yields N_2 and O_2 which can be analyzed for $\delta^{15}N$, $\delta^{18}O$ and $\delta^{17}O$, where $\delta = (R_{sample}/R_{standard} - 1)\bullet 1000$ and R is the ratio of the rare isotope relative to the abundant isotope of the sample and the

standard. It has been shown that atmospheric NO_3^- is anomalously enriched in ^{17}O.(Michalski et al., 2003b) This ^{17}O enrichment is denoted by $\Delta^{17}O$, where

$$\Delta^{17}O = \left[ln\left(1 + \frac{\delta^{17}O}{1000}\right) - 0.52 \cdot ln\left(1 + \frac{\delta^{18}O}{1000}\right)\right] \cdot 1000$$

of approximately $\Delta^{17}O = \delta^{17}O - 0.52 \bullet \delta^{18}O$ (Miller, 2002a). The approximation can lead to error when $\delta^{18}O$ and $\delta^{17}O$ values are far from zero or when the defining reference for the delta scale is changed (Bohlke et al., 2003; Miller, 2002a). Therefore to avoid error in $\Delta^{17}O$ calculation the full calculation should be used.

3.5 Using nitrate reference materials for standardization of $\Delta^{17}O$

$\Delta^{17}O$ values of environmental NO_3^- typically span 0 – 33‰, therefore having working reference nitrates encompassing this range is important to ensure accurate measurements. Environmental NO_3^- samples generally fall into three groups: atmospheric, polluted biosphere, and pristine biosphere. Atmospheric NO_3^- (aerosols, dissolved NO_3^-, and gaseous nitric acid) $\Delta^{17}O$ values usually range from 20 – 33‰, where $\Delta^{17}O$ variation is linked to changes in oxidation chemistry in the atmosphere (Michalski et al., 2003b; Morin et al., 2008; Morin et al., 2009). Polluted biosphere NO_3^- (urban streams) $\Delta^{17}O$ values range from 5 – 15‰ and pristine biosphere NO_3^- samples (streams and soils) range from 0 – 4‰ (Michalski et al., 2004d). The NO_3^- $\Delta^{17}O$ values observed in the biosphere is the result of mixing of biogenic NO_3^- ($\Delta^{17}O$ = 0‰) and atmospheric NO_3^-.

For accurate measurement of all sample types, multiple working reference nitrates, which bracket these ranges, were developed (Table 3.1). Due to limited supply of international references (USGS32 and USGS34), three secondary NO_3^- reference salts were prepared and calibrated. The first was Hoffman (20H) nitrate fertilizer (Hi-Yield Nitrate of Soda), which is a sodium nitrate mined from ore deposits in the Atacama Desert in Northern Chile. The second is NC32, a mixture of potassium nitrate obtained from North Carolina State University (NCSU, prepared by equilibrating water and reagent grade HNO_3 per Bohlke et. al.(2003) to obtain a $\delta^{18}O$ of -23.5) and USGS32 (93:7 respectively). The third was Antarctica soil NO_3^- ($\Delta^{17}O$ = 32‰) (Michalski et al., 2005) used to bracket atmospheric samples. The $\delta^{18}O$ and $\Delta^{17}O$ values of all three working references were determined using the silver nitrate thermal decomposition method (Michalski et al., 2002) that was calibrated using USGS32, USGS34, and USGS35 NO_3^- isotope reference materials (Bohlke et al., 2003; Michalski et al., 2002). These secondary NO_3^- references were mixed to attain "working references" (Table 3.1), which expanded the range of ^{15}N, $\delta^{18}O$ and $\Delta^{17}O$ calibration curves so they bracketed most natural samples.

Table 3.1. Working NO_3^- references delta values, mixing model fractions and calibration ranges for environmental nitrate samples of desired $\Delta^{17}O$ values using appropriate mole fractions (x) of NC32 and Hoffman fertilizer (20H) nitrates using a two member mixing model: $\Delta^{17}O_{std} = x(\Delta^{17}O_{NC32}) + (1-x)(\Delta^{17}O_{20H})$.

sample type	reference	$\delta^{15}N$ (‰) vs N_2 air	$\delta^{18}O$ (‰) vs VSMOW	$\Delta^{17}O$ (‰) vs VSMOW	Fraction NC32	Fraction 20H
Pristine Biosphere	NC32	15.3	-18.8	0	1	0
	1H	14.6	-15.2	1	0.95	0.05
	2H	13.7	-11.1	2	0.91	0.09
Polluted Biosphere	5H	11.5	0.15	5	0.76	0.24
	10H	7.9	17.6	10	0.53	0.47
Atmospheric	20H	0.5	54.1	19.8	0	1
	Antarctic	-20	72.3	32		

3.6 Helium Effect on Triple Oxygen Isotopes

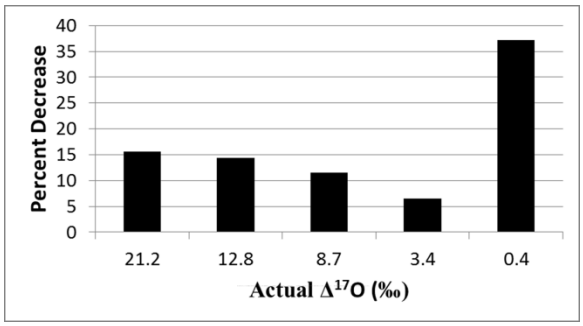

Figure 3.2. Percent error in $\Delta^{17}O$ measurement associated with the helium carrier gas.

To examine the possible effects of a helium background gas on triple oxygen isotope analyses experiments using the dual inlet interface at near vacuum (10^{-8} mbar) were performed. NO_3^- with positive $\Delta^{17}O$ were converted to O_2 and analyzed by dual inlet with and without helium gas present in the background (10^{-6} mbar). The $\Delta^{17}O$ precision was good with or without He (± 0.1‰) but there was a consistent 1‰ offset

and linear trend (0.84) resulting in consistently lower, inaccurate $\Delta^{17}O$ value when helium was present (Figure 3.2). Helium did not significantly impact the $\delta^{18}O$ values, thus the interference must be in mass 33 ($^{17}O^{16}O$), but it is unclear what causes this effect. It may be that the addition of He causes ion quenching reactions in the ion source and perhaps the ^{17}O is more readily quenched than the ^{18}O, which effectively would lower the expected delta value. Abe and Yoshida (2003) observed a partial pressure dependency on the isotopic composition of $O_{2,}$ which they concluded was most likely due to isotopic fractionation during emission from the ionization chamber into the flight tube of the mass spectrometer (Abe et al., 2003). This loss of $\Delta^{17}O$ accuracy can explain conflicting accounts of isotope exchange between bacteria and water. Casciotti et. al's. (2002) original study demonstrated that this exchange was usually less than 3%, which was confirmed by Kaiser et. al. (2007) However, Morin et. al. (2008) measured a $\Delta^{17}O$ in USGS35 that 26% was lower than the accepted value and attributed this to bacteria-water isotope exchange. The results presented here show that the lower $\Delta^{17}O$ values are likely due to the presence of the He gas in the ion source, and not analysis blank or isotope exchange. Quantifying the degree of bacterial exchange must be accounted for in $\delta^{18}O$ analysis because NO_3^- is found in waters with vastly different $\delta^{18}O$ values. Therefore, because of the helium effect, the bacterial exchange should be evaluated running a suite of water $\delta^{18}O$ references and not be based on shifts in $\Delta^{17}O$ values. The helium effect can be corrected for by measuring isotopic references and using calibration curves.

3.7 $\Delta^{17}O$ Calibrations

The $\Delta^{17}O$ measurements of the working reference nitrates yielded excellent calibration curves (Figure 3, r^2=0.99), resulting in a high degree of measurement accuracy and provided high limits of detection. However, there exists a slightly different calibration linearity within the $\Delta^{17}O$ ranges of the NO_3^- reference materials. Using a single calibration curve results in poor accuracy (Figure 3.3) for high $\Delta^{17}O$ values (too low) and low $\Delta^{17}O$ values (too high). Such a failure to properly calibrate has likely led to reporting of a low bias for nitrates with high $\Delta^{17}O$ values (rain and aerosol) and a high bias when actual $\Delta^{17}O$ values are low (soils and streams). Using correct calibration curve for the environmental samples that have the range of $\Delta^{17}O$ values of interest reduced this bias and improves the $\Delta^{17}O$ accuracy (Table 3.1). Using the low $\Delta^{17}O$ calibration at 0.3‰ precision, 1‰ can be differentiated from 0‰ but a 0.5‰ difference is within the 2σ uncertainty and cannot be distinguished from zero. Therefore the $\Delta^{17}O$ detection limit is 1‰ which equates to ~ 4% contribution of atmospheric NO_3^- to an ecosystem's total NO_3^- budget.

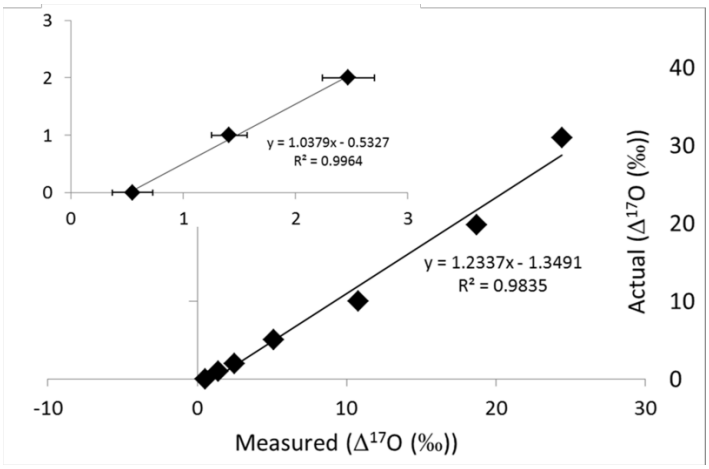

Figure 3.3 $\Delta^{17}O$ calibration with 1‰ bias effect on lower $\Delta^{17}O$ values, however 0, 1 and 2‰ are still distinguishable (inset). Different slopes and offsets demonstrate the need to bracket samples within the calibration range. A failure to do so can lead to biases in reported values, a raw value of 1‰ calibrated with 'pristine' references would lead to a corrected value of 0.5‰, yet; if this value were to be corrected with the entire range of references (0-32‰) a corrected value of -0.1‰ would be obtained.

3.8 Effect of Sample Size on $\Delta^{17}O$ Precision and Accuracy and Memory effects

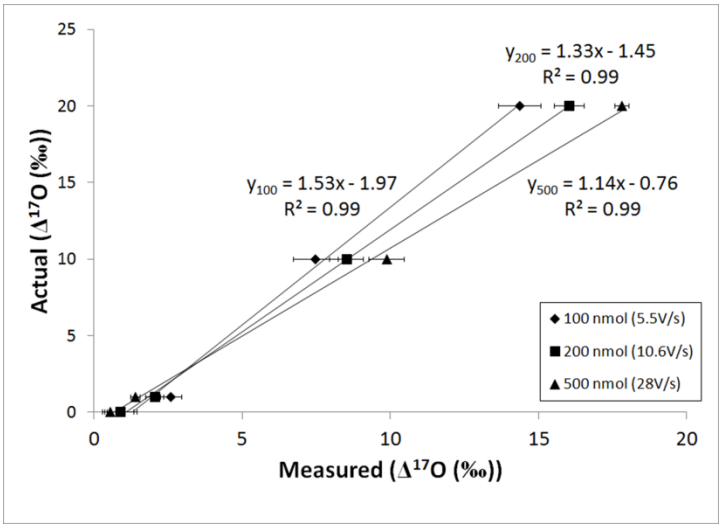

Figure 3.4. Precision and accuracy of $\Delta^{17}O$ values based on sample size.

The precision and accuracy of the $\Delta^{17}O$ analysis was also assessed as a function of sample size. It is well known that during IRMS analysis, sample gas peaks that are different sizes relative to the reference pulse can result in nonlinear responses in the feedback amplifier resistors and cause shifts in δ values (Brand, 2004). This is particularly important for oxygen isotopes because $\Delta^{17}O$ values are determined by the observed divergence from the linear relationship between $\delta^{18}O$ and $\delta^{17}O$ values (Miller, 2002a) and, therefore, false $\Delta^{17}O$ values can be generated by linearity effects. Kaiser et. al. (2007) previously investigated the effects of sample size linearity; however, they used artificially created N_2O gases (not bacterial derived) with very low oxygen values ($\delta^{18}O$ = -102 – -116‰ and $\Delta^{17}O$ = -25 – -33‰) that are not representative of calibration references or natural samples. The $\Delta^{17}O$ value precision was similar for sample sizes ranging from 100-500nmol of NO_3^- (±0.3‰) (Figure 3.4) but accuracy shifted with sample size. This is likely due to the divergence of the voltages between the 33 and 34 amu faraday cups with increasing ion flux, which in turn changes the calculated $\Delta^{17}O$ values. Slopes and offsets are size dependent indicating that the measurement uncertainty is larger than the calibration uncertainty, and that the measurement standard deviation is the limit between calibration curves. The best accuracy is therefore attained by limiting peaks area variation to ±10% of NO_3^-. Peak area variations greater than this require linearity corrections to attain good accuracy (Figure 3.5). The best $\Delta^{17}O$ precision and accuracy (r^2=0.99, ±0.3‰) were obtained by running samples at 500nmol of NO_3^- leading to a peak area of 45V/s in O_2.

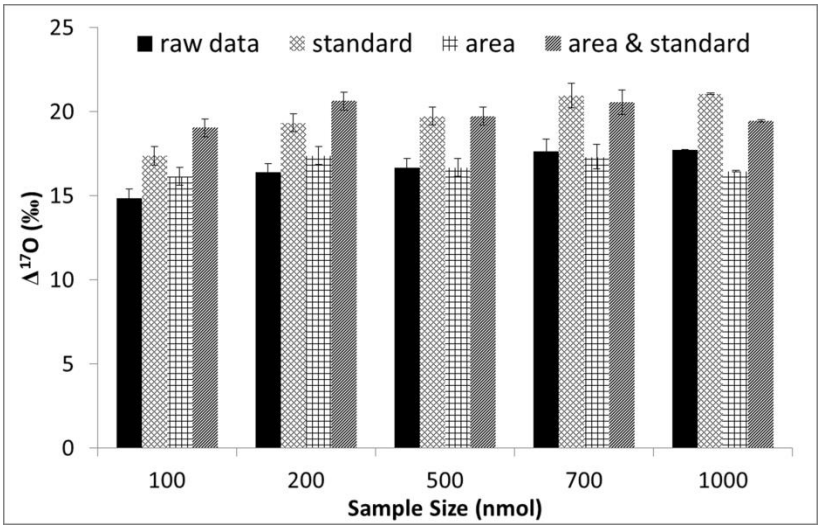

Figure 3.5. $\Delta^{17}O$ raw data (black) of 20 Hoffman at different sample sizes with applied different corrections for a 500nmol sample. Correcting with a reference only calibration (light grey) leads to an underestimation as well as correcting only with peak area (criss cross). However, correcting with both peak area and references (dark grey) leads to more accurate values across all sample sizes.

The headspace extraction apparatus showed no evidence of $\Delta^{17}O$ bias from the previous analysis (memory effect). Alternately analyzing nitrates (100nmol to 500nmol) with $\Delta^{17}O$ = 20‰ and 0‰) had no memory effect if proper vial extraction protocols were followed: flow 10 mL/min, 12 minute flush of the sample vial extraction, 8 minutes flush from a blank helium vial. At flushing rates lower than these a pronounced memory effect was observed (10% at 7 minute extraction). Thus, improper headspace extraction can cause memory effects, but no evidence of isotope memory was detected within the gold tube itself, in agreement with Kaiser et. al. (2007).

3.9 Effects of Sample Preparation on NO_3^- Isotopes

The effects of sample pre-concentration and purification procedures were tested to ensure that they did not impact the isotope values of NO_3^-. Sample pre-concentration is required if a sample's NO_3^-concentration is less than 100 μM because of limited headspace vial volume. Many natural NO_3^- samples are not neutral (alkaline soils, acid rain) which can lead to HNO_3 volatilization during pre-concentration or could kill the bacteria if pH is extreme, therefore reducing conversion of NO_3^- into N_2O leading to smaller peak size and error in calibration. Some samples may have both NO_3^- and NO_2^- and the denitrifier method is non-selective between these two species, therefore the NO_2^- must also be chemically removed for accurate analysis.

Isotope effects occurring during pre-concentration at different pH's were evaluated using the Hoffman NO_3^- reference in acidic, neutral, and basic solutions, which were pre-concentrated by either freeze drying, centrifuge concentration, or oven drying. When samples were acidified and pre-concentrated, ^{15}N, ^{17}O and ^{18}O isotopes became enriched. This was likely due to preferential volatilization of HNO_3 containing light isotopes (^{14}N and ^{16}O) leaving behind the isotopically enriched NO_3^- in the liquid. This could explain shifts in $\delta^{15}N$ and $\delta^{18}O$, but not $\Delta^{17}O$ since phase transitions should follow mass dependent isotope fractionation laws. The $\Delta^{17}O$ decrease maybe due to isotopic exchange between NO_3^- and water that occurs at very low pH (Bohlke et al., 2003; Bunton et al., 1952; Bunton et al., 1953). This could occur when acidic sample solutions evaporate to dryness and exponentially decrease in pH (Bunton et al., 1952). Basic solutions had less isotopic variability and were similar to neutral samples. Freeze drying,

centrifuging, and oven drying (35°C) of neutral and basic had no effects on NO_3^- isotopes outside normal precision.

Pre-concentration and isolation of NO_3^- using of ion chromatography (IC) was also tested for isotope effects. The IC (Alltech Model 626, Grace, 2051 Waukegan Road, Deerfield, IL 60015, USA) is controlled with PeakSimple software (SRI Instruments, 20720 Earl Street, Torrance, CA 90503, USA) and ran in preparative mode (45 minutes analysis time). Preparative analysis requires the entire volume of a sample to be pumped onto an analytical column where chloride, nitrite, nitrate, and sulfate anions are then separated based on their affinity for the column resin. The mobile phase is a 3.5mM/1.0mM solution of $NaHCO_3/Na_2CO_3$ (respectively) The 15 mL sample solutions are accessed by an autosampler (Gilson, Inc. 3000 Parmenter Street, P.O. Box 620027, Middleton, WI 53562-0027, USA - 176 vial capacity) and the ~ 12 mL of the solution is pumped through a SPE sorbent C_{18} (Omnifit/Diba Industries, 4 Precision Road, Danbury, CT 06810, USA) chromatographic tube to remove organics and onto the analytical column (4mm Dionex IonPac AS14, Thermo Scientific, 3000 Lakeside Drive Suite 116N, Bannockburn, IL 60015, USA), using a single head pump (Alltech Model 426) via a 6-port valve. The mobile phase then elutes the column at 2mL/min and flows through a chemical suppressor (4mm Dionex AMMS300 using a 50mN H_2SO_4) which eliminates the carbonate within the mobile phase. The detector (Alltech Model 650) measures the conductivity and the sample is then sent to the fraction collector where individual anion peaks are collected as a function of retention time. Due to the interference with nearby peaks, the largest sample size that could be separated was 1800nmol NO_3^-. However, due the similar affinity of the analytical column for NO_2^- and NO_3^-, samples containing both

species had a smaller limit of 450nmol NO_3. Precision for Cl^-, NO_3^-, and SO_4^{-2} was 0.01mg/L, 0.02mg/L, and 0.03mg/L, respectively. The preparative mode's NO_3^- collection efficiency and isotopic integrity was tested by separating and collecting 175nmol of Hoffman mixed with equimolar amounts of Cl^-, SO_4^{-2} and NO_2^-. IC separation showed no degradation of $\delta^{15}N$, $\delta^{18}O$, or $\Delta^{17}O$ in precision or accuracy.

The sulfamic acid technique (Granger et al., 2009) to remove NO_2^- was also tested to assess any effect on triple isotope analysis. Nitrite removal by sulfamic acid was sensitive to the time of reaction, and it was determined that an hour reaction time was sufficient to obtain accurate isotopic values (Figure 3.6). Precision of the method including centrifuged/freeze dried pre-concentration, IC separation and/or sulfamic acid NO_2^- removal are $\delta^{15}N$ (±0.4‰), $\delta^{18}O$ (±1‰), and $\Delta^{17}O$ (±0.3‰).

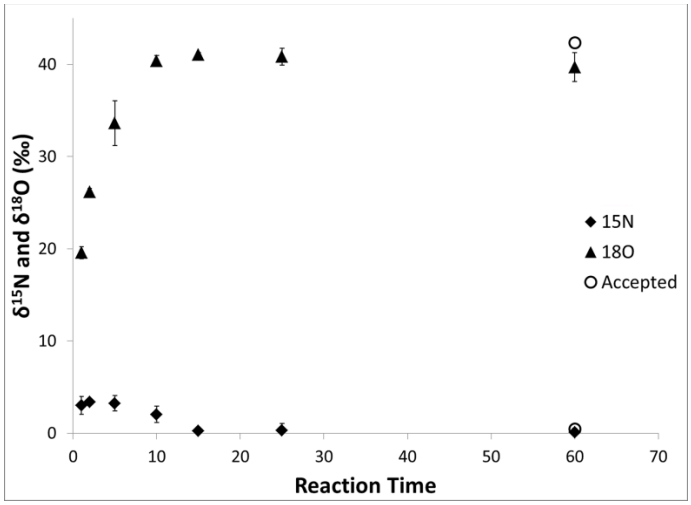

Figure 3.6. Time trial of sulfamic acid nitrite removal demonstrating that 1 hour was sufficient to remove NO_2^- from an initial 100nmol each NO_3^- and NO_2^- mixture.

3.10 $\delta^{15}N$ Analysis

Simultaneous N_2 analysis has been integrated into triple oxygen isotope analysis. $\delta^{15}N$ data would be beneficial in many N cycle studies and a simultaneous $\delta^{15}N$, $\delta^{18}O$, and $\Delta^{17}O$ analyses reduces sample size requirements and reduces instrument time and cost. Morin et. al. (2008) showed simultaneous analysis but calibration references did not encompass the full range of environmental samples and they did not discuss any linearity issues or details of their approach. Also their $\delta^{15}N$ calibration used USGS32 (180‰), USGS34 (-1.8‰), USGS35 (2.7‰) and a mixture of USGS34/35 (0.45‰) (Bohlke et al., 2003) and the 180‰ USGS32 disproportionately leverages the calibration curve effectively making it a two point linear regression. The internal references developed for this study have a $\delta^{15}N$ values that the range of -20 to +15.3‰ (Table 3.1) that encompasses that majority of natural abundance nitrates measured to date. The working reference $\delta^{15}N$ measurements yield excellent calibration curves (Figure 3.7 (top), r^2=0.99) with accuracy and precision that were similar for all sample sizes (r^2 = 0.96 - 1, ±0.4‰) (Figure 3.4) There is a linearity in the $\delta^{15}N$ values (Figure 3.7 (bottom)), similar to the $\Delta^{17}O$ calibration, the slopes and offsets differed as a functions of sample size indicating that the measurement uncertainty is larger than the calibration uncertainty and that the measurement standard deviation is the limit between calibration curves. Therefore, peaks can vary by 10% and still use one calibration curve before a linearity correction would need to be used or the sample would need to be reanalyzed. Linearity corrections are done the same way as with $\Delta^{17}O$ corrections. The most accurate values were obtained by running samples at 500nmol leading to a peak area of 65V/s in N_2.

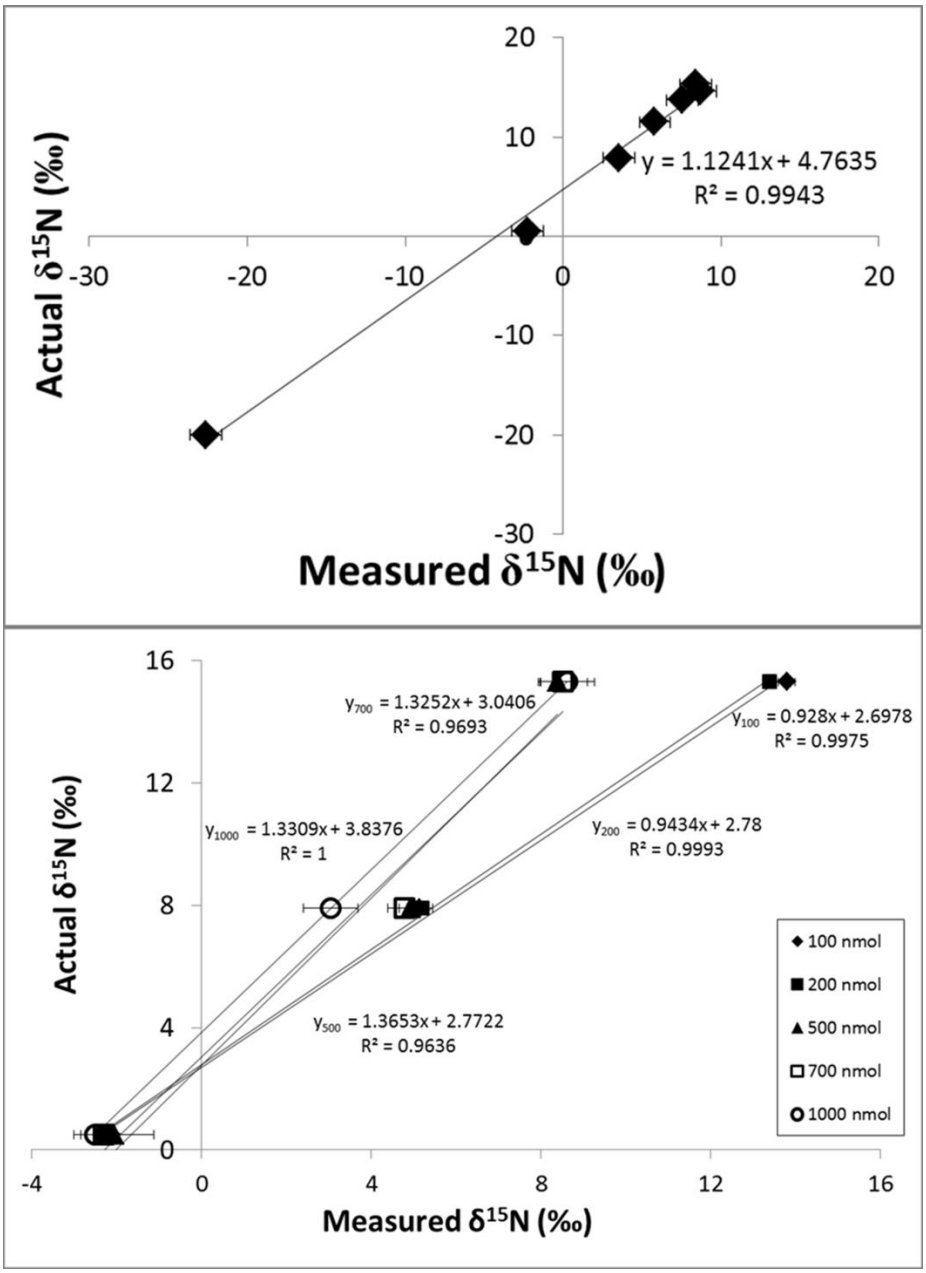

Figure 3.7. $\delta^{15}N$ calibration curve of working internal references at a sample size of 500nmol, demonstrating a high degree of measurement accuracy (top). Effect of sample size on accuracy of calibration (bottom)

3.11 Conclusion

Details of denitrifier method with gold tube thermal reduction were addressed with emphasis on introducing simultaneous N_2 isotopic analysis, improving calibrations and corrections and understanding the effects of sample preparation or purification on NO_3^- isotopic composition. References need to encompass the range of environmental samples of interest so that calibration curves are not extrapolated therefore inducing more error. And due to linearity and offset amongst isotope values, it is important to bracket samples within the desired ranges of references to obtain proper calibration. Also, the importance of consistent NO_3^- sample size during analysis to further eliminate errors as different sample sizes yield different isotopic values for the same sample of interest, and while this can be corrected for by a linearity correction, it should be avoided. There was a minimal observed effect with sample preparation/purification. Simultaneous N_2 analysis was implemented and it was observed that sample size linearity as well as offsets existed with $\delta^{15}N$ as it did with $\Delta^{17}O$.

CHAPTER 4: ISOTOPIC VARIATION IN NITRATE SOURCES FOR INPUTS INTO MIXING MODELS

4.1 Introduction

The discussion below is a brief synopsis of research that was conducted in order to constrain isotopic values for multiple nitrate sources. Through multiple collaborative efforts, the resulting research is currently being used to help us better constrain isotopic mixing models and multiple papers are under development. The key to elucidating nitrate (NO_3^-) dynamics in complex ecosystems is an understanding of the relative importance of NO_3^- loading from different sources. While NO_3^- concentration data informs us about changes in NO_3^- loads or losses, only stable isotopes can be used to infer which NO_3^- sources or loss process are changing. This is possible by utilizing isotope mass balance technique, where the NO_3^- $\delta^{15}N$, $\delta^{18}O$ and $\Delta^{17}O$ values are used in an isotope mixing plot (Kendall, 1998b). A multiple isotope mixing model requires knowledge of the $\delta^{15}N$, $\delta^{18}O$, and $\Delta^{17}O$ values for each NO_3^- source applying an isotope mixing equation:

$$\delta^{15}N_{runoff} = n_1\delta^{15}N_{atmospheric} + n_2\delta^{15}N_{biologic} + n_3\delta^{15}N_{fertilizer}$$

$$\delta^{18}O_{runoff} = n_1\delta^{18}O_{atmospheric} + n_2\delta^{18}O_{biologic} + n_3\delta^{18}O_{fertilizer}$$

$$\Delta^{17}O_{runoff} = n_1\Delta^{17}O_{atmospheric} + n_2\Delta^{17}O_{biologic} + n_3\Delta^{17}O_{fertilizer}$$

where n_1, n_2, and n_3 are the mole fraction of each NO_3^- source. Isotope analysis of stream runoff, an "isotopic source integrator", leads to quantification of the relative importance of each nitrate source to the total nitrogen budget in the ecosystem being flushed. This

chapter briefly discusses the isotope variation in the three main sources of NO_3^-: Photochemical (atmospheric), synthetic fertilizers, and nitrification (biogeochemical).

4.2 Methods

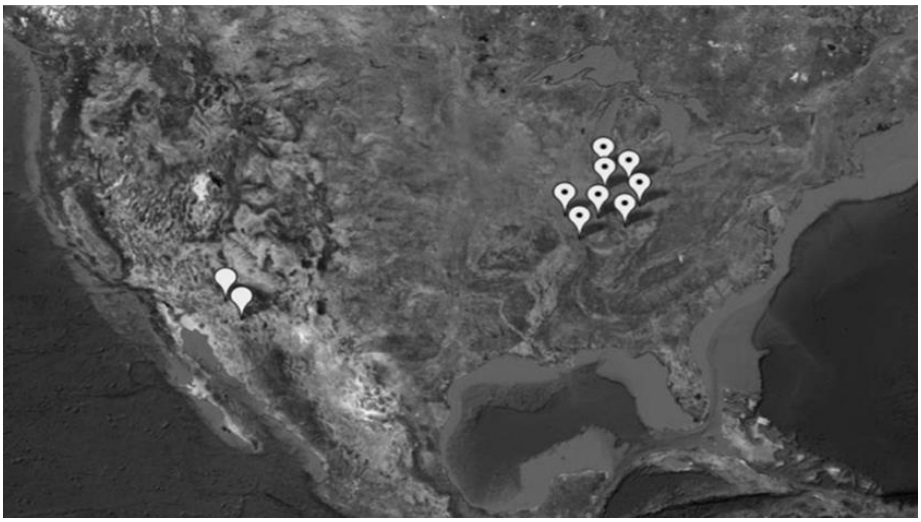

Figure 4.1. Midwestern United States (markers with dots, including Indiana, Illinois, Ohio, and Kentucky) and Arizona, US (solid markers, including Tucson and Phoenix) atmospheric NO_3^- sampling locations.

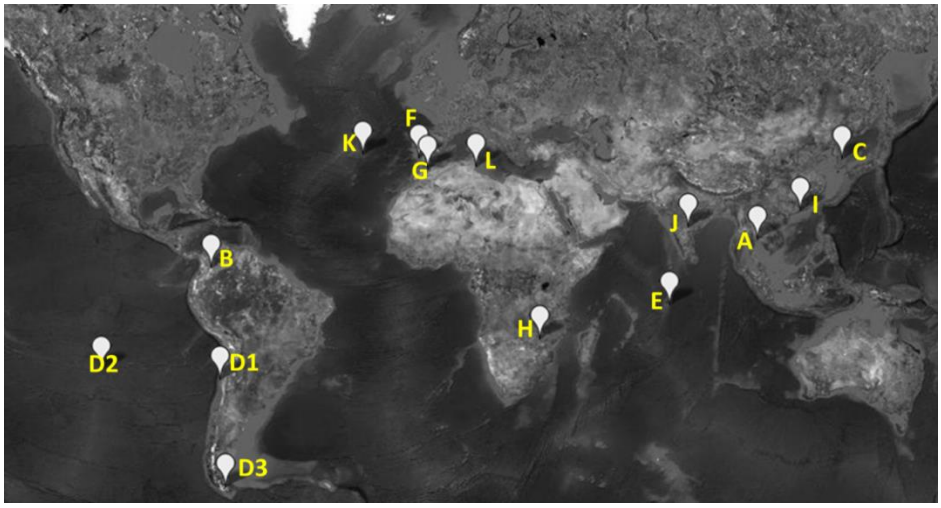

Figure 4.2. World rainfall sample locations. A – Bangkok, Thailand; B – Bagota, Columbia; C – Cheongju, Korea; D – Chile (D1 – La Serena, D2 – Easter Island, D3 – Punta Arenas); E – Diego Garcia, British Indian Ocean Territory; F – Faro, Portugal; G – Fes, Morocco; H – Harare, Zimbabwe; I – Hong Kong, China; J – Hyberabad, India; K – Ponta Delgada, Portugal; L – Sfax, Tunisia

Nitrate contained in rainwater and aerosols, and fertilizer nitrate were obtained for isotope analysis. Weekly composite precipitation samples for the Midwestern United States were obtained from the National Atmospheric Deposition Program (NADP) (Figure 4.1). At NADP sampling locations, wet deposition sampling is only initiated when precipitation is detected therefore preventing dry deposition contamination. As a result, NADP precipitation samples would be solely considered NO_3^- scavenging of the atmosphere during rain events. Daily event based precipitation samples (Tucson and Phoenix) as well as particulate matter (Tucson) for Arizona (Figure 4.1) were collected as part of a larger study to understand the effects of urbanization on the coupled nitrogen-

hydrologic cycle in semi-arid urban ecosystems and is detailed in Chapters 5 and 6. Monthly global precipitation samples were obtained from the Global Precipitation Climatology Project (GPCP) for multiple locations (Figure 4.2). At GPCP sampling locations, precipitation collectors are primarily used to record precipitation depth and consequently are left out to environmental conditions (*e.g.* microbial processing, heat) throughout the month long sampling period. Therefore these precipitation samples are subjected to dry deposition as well as wet deposition and can be considered composite deposition samples. Fertilizer samples (ammonium nitrate and urea ammonium nitrate) were obtained from the Office of Indiana State Chemist.

Isotopic preparative and analytical methods are detailed in Chapter 3, a brief synopsis follows. Samples were stored frozen until ready for preparation and analysis. Samples were filtered to 0.7μm and neutralized using Na_2CO_3. NO_3^- concentrations were determined using high pressure liquid chromatography with a precision of 0.02mg/L. Samples were then pre-concentrated to obtain 100μM of NO_3^-. NO_3^- isotopic analysis ($\delta^{15}N$, $\delta^{17}O$ and $\delta^{18}O$) was carried out using the denitrifier method and gold tube thermal reduction discussed in Chapter 3 (Casciotti et al., 2002; Kaiser et al., 2007). Isotope ratios were measured using the Delta V Plus ratio mass spectrometer that was calibrated using internal working reference standards that were previously calibrated to international standards USGS32, USGS35 and USGS34 (Riha et al., 2013). All subsequent $\delta^{15}N$ values are reported versus air N_2 and oxygen values ($\delta^{17}O$, $\delta^{18}O$, and $\Delta^{17}O$) are reported with respect to VSMOW. Precision of the $\delta^{15}N$, $\delta^{18}O$ and $\Delta^{17}O$ values were ±0.4‰, ±1.0‰, and ±0.3‰, respectively based on replicate analysis of the working standards and calibrations.

4.3 Atmospheric $\delta^{15}N$, $\delta^{18}O$ and $\Delta^{17}O$ values

The discussion below is a synopsis of all atmospheric NO_3^- isotope data generated using the analytical methods described in Chapter 3. Complete discussion of the data is presented in Chapter 5 and in three peer review articles in review or preparation: 1) Assessing peroxy radical chemistry and N_2O_5 uptake using oxygen isotope anomalies in atmospheric nitrate. Michalski G., D. Mase, K. Riha and H. Waldschmidt (Proceedings of the National Academy of Sciences). 2) *Tracing oxidation chemistry in an urban environment in the southwestern United States. Riha, K., D. Mase, and G. Michalski. (Atmospheric Environment). 3) The global isotopic composition of nitrate in precipitation. Michalski G, D. Mase, K. Riha, F. Wang, M. Kolonowski. (Atmospheric Chemistry and Physics).*

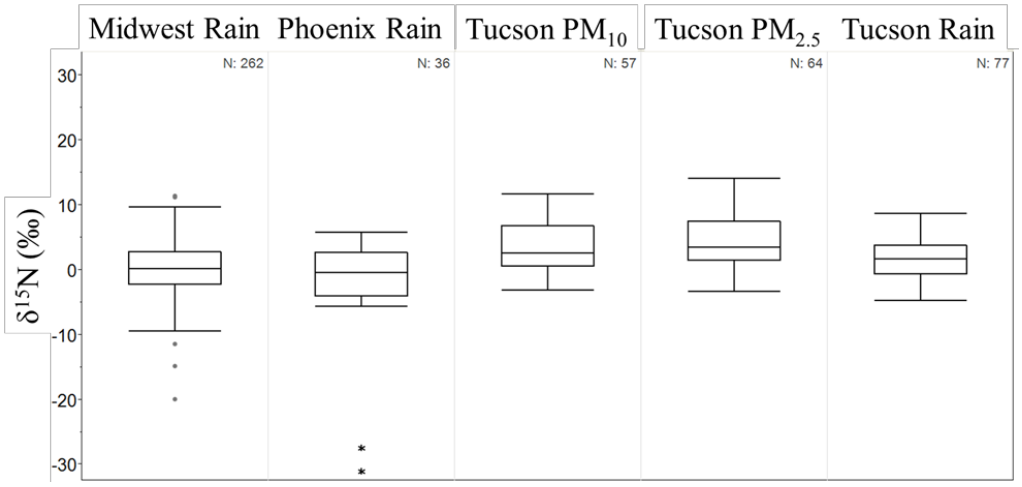

Figure 4.3. Box plots of atmospheric NO_3^- $\delta^{15}N$ from study sites within the Midwestern United States and Arizona, USA (See Figure 4.1 for collection locations).

Precipitation NO_3^- $\delta^{15}N$ values – Variations in atmospheric NO_3^- $\delta^{15}N$ values can be used to infer changes in NO_x sources or shifts in seasonal NO_x chemistry (see Chapter 5). Figure 4.3 shows atmospheric NO_3^- $\delta^{15}N$ values from the sampling locations within the United States. Midwestern precipitation NO_3^- $\delta^{15}N$ values averaged 0.25 ± 4.0‰ with a pronounced seasonal trend of higher values during the winter (-9.5 – 11.4‰) and lower values in the summer (-19.9 – 8.7‰). The NO_3^- $\delta^{15}N$ values of Tucson particulate matter (PM_{10} and $PM_{2.5}$) averaged 3.5 ± 3.8‰ (PM_{10}) and 4.4 ± 3.9‰ ($PM_{2.5}$) and displayed a distinct seasonal trend with higher values in the winter (PM_{10}: 8 – 12‰ and $PM_{2.5}$: 8 – 14‰) compared to the summer (PM_{10}: -3 – 0.5‰ and $PM_{2.5}$: -3 – 2‰). Phoenix precipitation NO_3^- $\delta^{15}N$ values averaged -1.8 ± 7.6‰ whereas Tucson values averaged 1.8 ± 3.2‰. These differences could be due to varying proportions of NO_x emissions between the two urban sites as well as varying importance of NO_x chemistry (i.e. varying ambient trace gas concentrations, heat island effect).

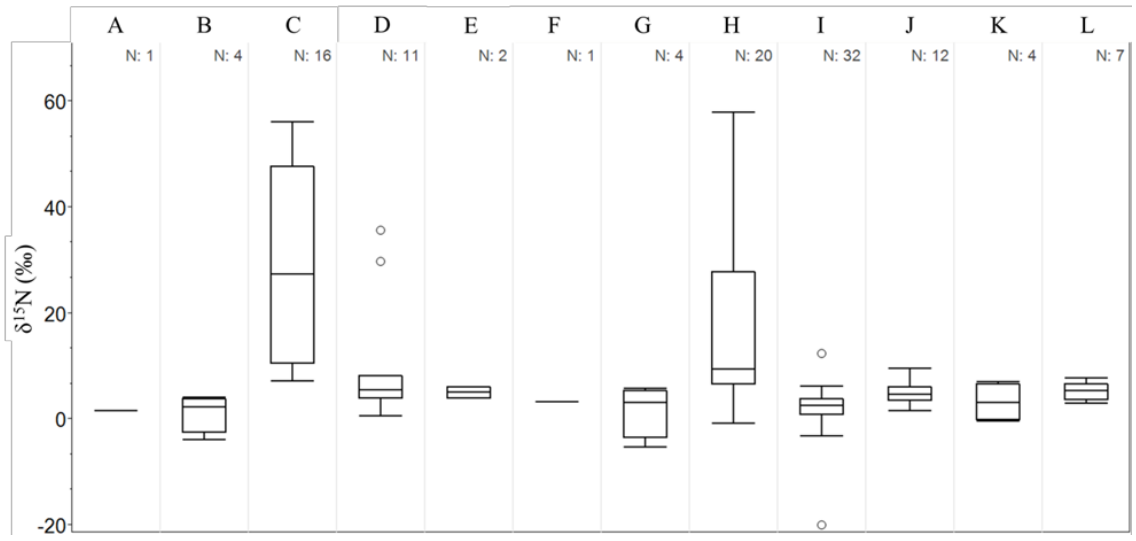

Figure 4.4. Box plots of atmospheric NO_3^- $\delta^{15}N$ from world rain samples (See Figure 4.2 for collection locations and letter correlations).

Figure 4.4 shows precipitation NO_3^- $\delta^{15}N$ values from individual sampling locations around the world. All world rain precipitation NO_3^- $\delta^{15}N$ values averaged 9.6 ± 13.7‰. All sites had $\delta^{15}N$ values representative of reported NO_x emissions except Sites C and H which had extremely elevated values (28.4 ± 16.8‰ and 16.9 ± 15.6‰, respectively). While these sites are in coastal areas which are more urban, which are subjected to heavier NO_x emissions both within city limits and cross ocean transport. However, these values suggest microbial processing therefore leaving precipitation samples enriched in ^{15}N. While it has been shown that unfiltered precipitation samples left out for two weeks remain isotopically unaltered with respect to NO_3^- (Spoelstra et al., 2004), the world rain samples are monthly composites and are often left in harsher environments that what was previously tested. Therefore the possibility of microbial processing cannot be eliminated.

Precipitation NO_3^- $\delta^{18}O$ and $\Delta^{17}O$ values − Spatial and temporal fluctuations in NO_3^- $\delta^{18}O$ and $\Delta^{17}O$ values can be attributed to a variety of atmospheric parameters (*e.g.* ozone and peroxy radical concentrations, relative humidity, solar flux, and temperature), as well as shifts in NO_3^- formation chemistry and transport effects. This is apparent when comparing NO_3^- $\delta^{18}O$ and $\Delta^{17}O$ values from the United States sites (Figure 4.5 and Figure 4.7) to those from around the world (Figure 4.6).

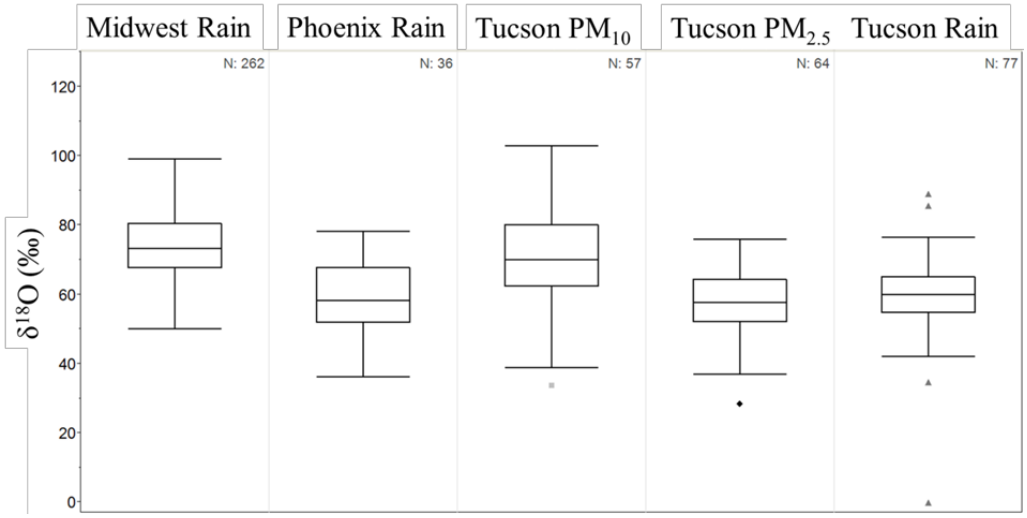

Figure 4.5. Box plots of atmospheric NO_3^- $\delta^{18}O$ from study sites within the Midwestern United States and Arizona, USA (See Figure 4.1 for collection locations).

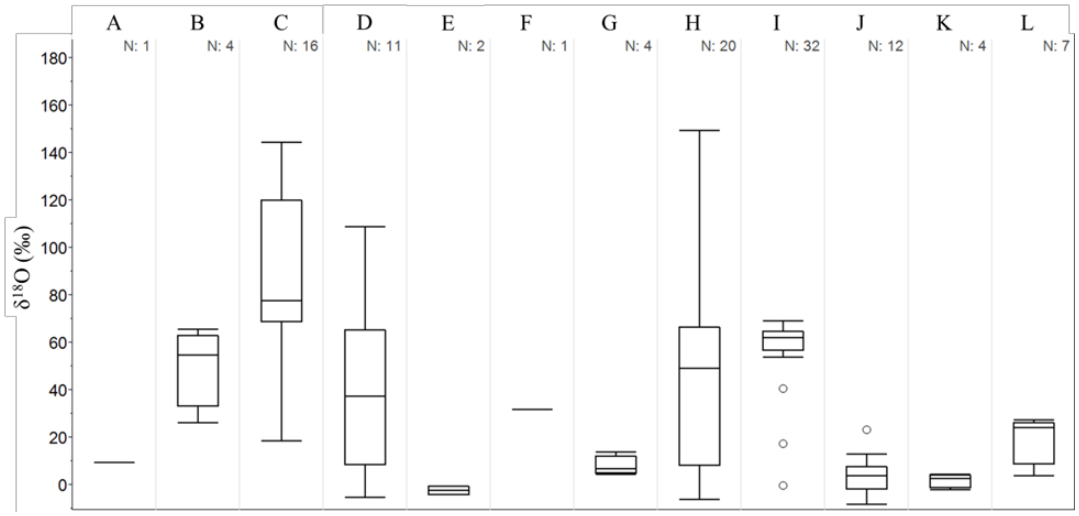

Figure 4.6. Box plots of atmospheric NO_3^- $\delta^{18}O$ from world rain samples (See Figure 4.2 for collection locations and letter correlations).

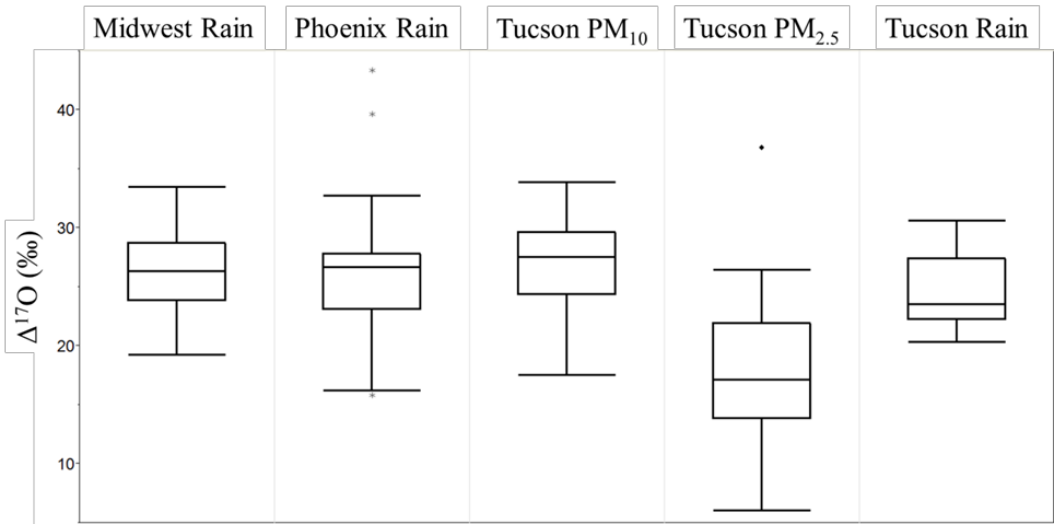

Figure 4.7. Box plots of atmospheric NO_3^- $\Delta^{17}O$ from study sites within the Midwestern United States and Arizona, USA (See Figure 4.1 for collection locations).

Midwestern precipitation NO_3^- $\delta^{18}O$ values averaged 74.1 ± 9.4‰ with a pronounced seasonal trend of higher values during the winter (65.8 – 99.1‰) and lower values in the summer (50.0 – 80.4‰). Precipitation NO_3^- $\Delta^{17}O$ values averaged 26.3 ± 3.1‰ with similar seasonal behaviors as $\delta^{18}O$ values (winter: 23.6 – 33.5‰ and summer: 19.2 – 27.8‰). This data will be submitted as a peer review manuscript in the summer of 2013 but is not discussed further in this thesis. Arizona precipitation $\delta^{18}O$ values averaged 59 ± 10‰ and $\Delta^{17}O$ values averaged 25 ± 3.2‰, all precipitation samples were taken during the summer monsoon season and therefore seasonal dependence cannot be evaluated. Tucson particulate matter (PM_{10} and $PM_{2.5}$) NO_3^- $\delta^{18}O$ values averaged 70.9 ± 13.5‰ (PM_{10}) and 56.9 ± 9.7‰ ($PM_{2.5}$) and exhibited a dampened and less pronounced seasonal trend than Midwestern samples with higher values in the winter (PM_{10}: 80.5 ± 10.3‰ and $PM_{2.5}$: 60.4 ± 10.1‰) compared to the summer (PM_{10}: 56.7 ± 10.7‰ and

$PM_{2.5}$: 56.3 ± 7.5‰). Particulate matter (PM_{10} and $PM_{2.5}$) NO_3^- $\Delta^{17}O$ values averaged 27.2 ± 3.7‰ and 18.4 ± 7.8‰, respectively and exhibited a similar seasonal trend as NO_3^- $\delta^{18}O$ values (i.e. winter (PM_{10}: 29.8 ± 2.2‰ and $PM_{2.5}$: 21.9 ± 11.3‰) and summer (PM_{10}: 22.6 ± 2.4‰ and $PM_{2.5}$: 13.9 ± 2.2‰)). All world sampling sites pooled together, precipitation NO_3^- $\delta^{18}O$ values averaged 44.9 ± 36.6‰, however, individual sites significantly varied. Sites B, C, D, F, H, and I all fall within the range of observed atmospherically derived NO_3^- (Chang et al., 2002; Durka et al., 1994; Kendall, 1998a; Mayer et al., 2001) (Figure 4.8).

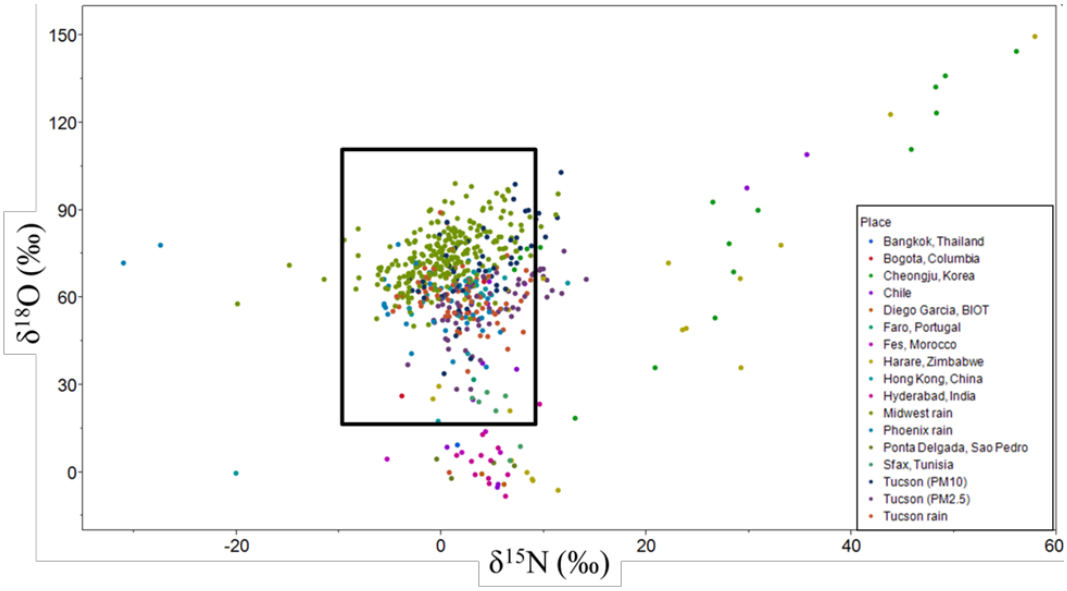

Figure 4.8. Dual isotope plot of all atmospheric NO_3^- samples, black box represents the classically accepted range of atmospheric NO_3^- (Chang et al., 2002; Durka et al., 1994; Kendall, 1998a; Mayer et al., 2001).

However, Sites C, D, and H vary more than all other sites and do fall below this range. These sites are coastal areas which could be subjected to strong seasonal wind patterns leading to $\delta^{18}O$ variations. Sites A, E, G, J, K and L all fall outside the atmospheric range

(<20‰). These sites are located near the Mediterranean Sea and Indian Ocean suggesting a stronger importance of water incorporation versus ozone incorporation during NO_3^- formation. There is also the possibility of microbial reactions altering the isotopic composition of bulk precipitation samples. If microbial processes (i.e. nitrification of deposited NH_4^+) this would 'erase' the atmospheric $\delta^{18}O$ and subsequently lower the NO_3^- $\delta^{18}O$ values and in part could explain the observed lower $\delta^{18}O$ values (-10 - 15‰)

4.4 Fertilizer $\delta^{15}N$ and $\delta^{18}O$ values

The discussion below is a synopsis of fertilizer NO_3^- isotope data generated using the analytical methods described in Chapter 3. Complete discussion of the data is found in a peer review article: The isotopic composition of nitrate fertilizers. Michalski G, M. Kolonowski, and K. Riha (Environmental Science and Technology).

Fertilizer NO_3^- $\delta^{15}N$ and $\delta^{18}O$ values − The isotopic composition of commercial N fertilizers will be representative of the chemical processes used in their production. Commercial N fertilizers are produced through the combined process of NH_3 production via the Haber-Bosch process followed by HNO_3 production by the Ostwald process. The Haber-Bosch process involves the reaction of N_2 with high pressure H_2 using iron based catalysts at high temperatures to form NH_3 (Appl, 2011). Due to high conversion rates, high temperatures, and the use of catalysts there is little ^{15}N isotopic fractionation. Approximately half of all NH_3 produced in the United States is then converted into HNO_3 through the Ostwald process (U.S.Environmental Protection Agency, 1995). This process uses a Pt/Rh catalyst at high pressure and temperature to oxidize NH_3 into NO_3 using air O_2 and H_2O as oxygen reagents ($NH_3 + 2O_2 \rightarrow HNO_3 + H_2O$) (Ostwald, 1902). Since the

$\delta^{18}O$ value of air O_2 is relatively constant at 23.5‰, the variation in the resulting oxygen isotopic composition will therefore be a result of local H_2O $\delta^{18}O$ values based on production plant locations. NH_4NO_3 is synthesized by the neutralization of the reaction $NH_3 + HNO_3 \rightarrow NH_4NO_3$ and its isotopic composition will largely reflect the effects of these two processes. Fertilizer NO_3^- $\delta^{15}N$ values averaged 0.1 ± 3.5‰ and $\delta^{18}O$ values averaged 22.7 ± 4.6‰ (Figure 4.9).

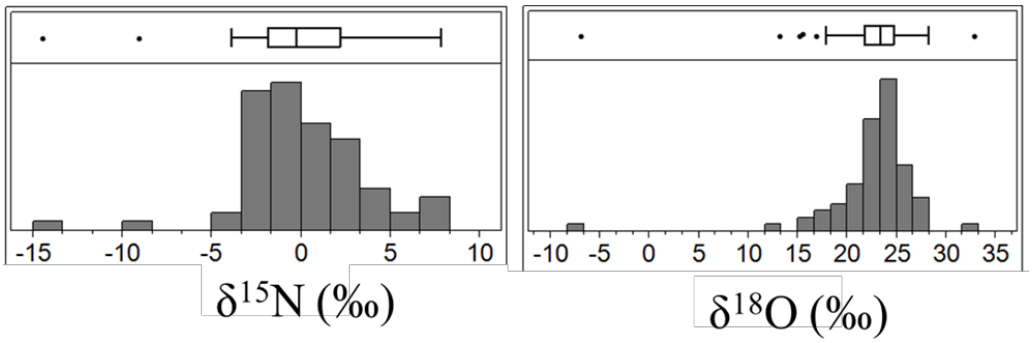

Figure 4.9. $\delta^{15}N$ and $\delta^{18}O$ histograms of fertilizer NO_3^- samples.

Fertilizer NO_3^- $\Delta^{17}O$ values – Most of the NO_3^- fertilizers had $\Delta^{17}O$ values near the terrestrial oxygen isotope fractionation line, ranging from -0.25 – 0.04‰. This suggests that air O_2 is the major oxygen reagent in during the Ostwald process since $\Delta^{17}O$ value of air O_2 is -0.223‰ (Luz et al., 1999; Luz et al., 2005) whereas oxygen isotope variation in meteoric water induced by evaporation and condensation follows mass dependent isotope fractionation rules and has a $\Delta^{17}O$ value of 0.0‰ (Meijer et al., 1998). While the majority of NO_3^- fertilizer had $\Delta^{17}O$ values near the terrestrial oxygen isotope fractionation line, a subset were anomalously enriched in ^{17}O. These fertilizers fell in a

narrow range of $\Delta^{17}O$ values 19 – 21‰. These fertilizers were naturally occurring ores located in the Atacama (Chile) and Turpan (China) deserts and are subjected to accumulation of photochemically produced HNO_3 and NO_3 aerosol deposition leading to larger $\Delta^{17}O$ values (Michalski et al., 2004c). These fertilizers make up only a trivial amount of the total N applied as fertilizer annually in the U.S. and therefore their contribution to NO_3^- loads in watershed scale studies can effectively be ignored.

4.5 Nitrification $\delta^{18}O$ isoscapes

The discussion below is a synopsis of a modeling paper by Michalski G., and K. Riha in preparation for submission to Global Biogeochemical Cycles.

Chemolithoautotrophic nitrification is a microbially facilitated multi-step oxidation of ammonium (NH_4^+) to nitrite (NO_2^-) and nitrate (NO_3^-) through the intermediate ammonia monooxygenase (NH_2OH). This process is carried out by chemolithoautotrophic microbes via an inorganic pathway in which NH_4^+ is used as an energy source according to the generalized equation:

$$NH_4^+ \rightarrow NH_2OH \rightarrow NO_2^- \rightarrow NO_3^-$$

Nitrification potentials and oxygen source appointment (H_2O versus O_2) in soils vary depending on environmental conditions, such as moisture, pH, temperature, availability of nutrients, soil chemical properties (i.e. C:N ratios and NH_3 supplies) and microbial communities (Mayer et al., 2001; Norton et al., 2011; Sharma et al., 1977). Three models were created and compared to determine the dependence of seasonality (April – September), oxygen isotope source apportionment, soil temperature (Stark, 1996) and soil pH (Bunton et al., 1959; Kool et al., 2011; Mayer et al., 2001; Snider et

al., 2010; Stark, 1996) on NO_3^- $\delta^{18}O$ values produced during nitrification. Model methodology and assumptions of choices, as well as oxygen isotopic values, are detailed in Michalski et. al. (Michalski et al., 2013). In brief, isoscapes of NO_3^- $\delta^{18}O$ values produced during nitrification were created in ArcGIS 10.1. Input parameters to the below models were obtained from the following sources: Water isotopes ($\delta^{18}O$ values) were obtained from the interpolation model of the Global Network of Isotopes in Precipitation (waterisotopes.org) (Bowen et al., 2002; Bowen et al., 2003); whereas, $\delta^{18}O$ of air O_2 was assumed to be a constant 23‰ (Horibe et al., 1973; Kroopnick et al., 1972). Monthly average maximum temperature normals (proxy for soil temperature) were attained through the PRISM Climate Group (PRISM Climate Group, 2004) and soil pH was acquired from the CONUS-SOIL dataset (Miller et al., 1998).

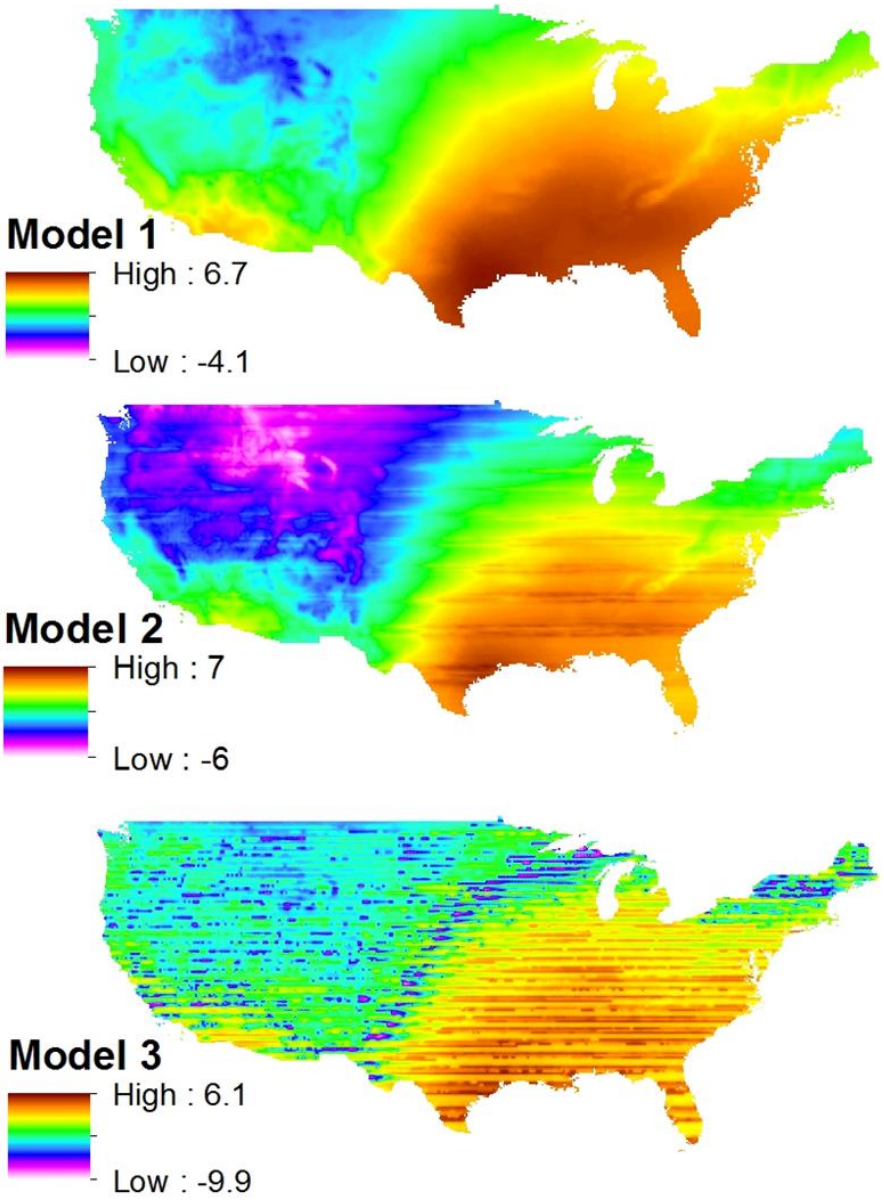

Figure 4.10. Isoscapes of modeled $\delta^{18}O$ values of NO_3^- produced from nitrification for August based on three predictive models (notice difference in scales). Model 1 is representative of the 2/3rd H_2O and 1/3rd O_2 source appointment, Model 2 demonstrates the effect of temperature and Model 3 shows the effect of both temperature and pH on $\delta^{18}O$ values.

Model 1 demonstrates the simplest of the three models in which NO_3^- $\delta^{18}O$ values produced during nitrification follow a simple two member mixing model of oxygen sources (Figure 4.10). Through multiple laboratory culture experiments it has been shown that oxygen from H_2O and O_2 are incorporated into NO_3^- produced during nitrification in a 2:1 ratio. It has been reported that the oxidation of NH_3 to NO_2^- derives one oxygen atom from H_2O and another from O_2 (Anderson et al., 1986). The remaining oxygen atom incorporation from the oxidation of NO_2^- to NO_3^- has been reported to derive from H_2O (Hollocher, 1984). Based on these experimental studies it has been suggested that the oxygen isotopic composition of NO_3^- generated by nitrification can be calculated by a two component mixing model (Bohlke et al., 1997; Durka et al., 1994; Kendall, 1998a; Mayer et al., 2001; Wassenaar, 1995):

$$\delta^{18}O_{NO3} = \frac{2}{3}(\delta^{18}O_{H2O}) + \frac{1}{3}(\delta^{18}O_{O2})$$

This 'source only' model was used to estimate the monthly average $\delta^{18}O$ values of NO_3^- produced from nitrification across the continental United States (Figure 4.10). While this mixing model was formulated from laboratory culture experiments few experimental data exists for the oxygen isotope composition of NO_3^- formed through nitrification in soils (Mayer et al., 2001). The data sets that do exist are either in accordance with the 2:1 ratio (Mayer et al., 2001) or deviate with the underlying mechanisms behind the variation of $\delta^{18}O$ values of NO_3^- remaining unclear (Snider et al., 2010). The remaining two models build off of this basic 2:1 mixing model approach and account for environmental factors that can cause differences in this ratio.

Model 2 incorporates the effect of potential isotopic exchange between NO_2^- and water on $\delta^{18}O$ values of NO_3^-. If complete isotopic exchange occurs then any memory of the $\delta^{18}O$ value of O_2 incorporated during the previous oxidation of NH_3 to NH_2OH would be erased therefore altering the simple 2:1 ratio. This model makes the assumption that NO_2^- equilibrates with H_2O faster than NO_2^- oxidizes to NO_3^-. The NO_2-H_2O oxygen isotope equilibrium is assumed to be temperature dependent and the enrichment factor was determined for temperatures at which nitrifying bacteria are active (278 – 320K) and was calculated by (Stark, 1996):

$$\varepsilon_{NO2} = -0.13[T(K)] + 50.4$$

This enrichment factor was incorporated into the previous 'source only' Model 1. No kinetic isotope effects were assumed during the final oxidation of NO_2^- to NO_3^-. Therefore the monthly average $\delta^{18}O$ values of NO_3^- produced by nitrification accounting for isotopic exchange between NO_2^- and water can be determined by (Figure 4.10):

$$\delta^{18}O_{NO3} = \frac{2}{3}(\delta^{18}O_{H2O} + \varepsilon(T)_{NO2-H2O}) + \frac{1}{3}(\delta^{18}O_{H2O})$$

Model 3 builds upon both the previous models but assumes the degree of NO_2-H_2O isotopic equilibrium is a function of soil pH. Incubation experiments demonstrate a strong dependence of oxygen isotope exchange on pH, with rapid exchange occurring at low pH and minimal exchange at higher pHs. Using experimental data from Bunton et. al. (Bunton et al., 1952), the isotope exchange fraction was assigned as a function of soil pH. Below pH 5, the exchange is fast enough that equilibrium always occurs and above pH 8 isotopic exchange is slow enough that it can be ignored. Between these pH ranges (pH 5 – 8) a linear function was fit to obtain f_{ex} (the fraction of NO_2^- that undergoes

exchange). This fraction (f_{ex}) was incorporated into the temperature dependent NO_2-H_2O exchange Model 2 to determine the monthly average $\delta^{18}O$ values of NO_3^- produced by nitrification accounting for pH effects on isotopic exchange between NO_2^- and water and can be determined by (Figure 4.10):

$$\delta^{18}O_{NO3} = \frac{2}{3}\left[\frac{1}{2}(\delta^{18}O_{H2O} + f_{ex} \cdot \varepsilon_{NO2}) + \frac{1}{2}\left(\delta^{18}O_{O2} \cdot (1 - f_{ex})\right)\right] + \frac{1}{3}(\delta^{18}O_{H2O})$$

$$= \frac{2}{3}(\delta^{18}O_{H2O}) + \frac{1}{3}\left[(f_{ex} \cdot \varepsilon_{NO2}) + \left(\delta^{18}O_{O2} \cdot (1 - f_{ex})\right)\right]$$

While the three models have similar spatial patterns (Figure 4.10) the resulting $\delta^{18}O$ values of NO_3^- produced by nitrification varied with Model 2 having the highest values and Model 3 having the lowest. The simplest source model is in accordance with other researchers 2:1 ratio assumptions that based on simple stoichiometry NO_3^- produced from nitrification should have a $\delta^{18}O$ values between -2 – 6‰ (Durka et al., 1994; Mayer et al., 2001) and these values are distinguishable from both fertilizer and atmospherically derived NO_3^-. However, while previous $\delta^{18}O$ values were based on experimental soil seepage $\delta^{18}O$ values which were not spatially distributed the $\delta^{18}O$ values presented here cover the continental United States and can further contribute to confining NO_3^- source appointment in mixing models. It is not surprising that Model 2 has the highest $\delta^{18}O$ values, as this model only accounted for temperature in NO_2-H_2O isotopic exchange and therefore areas such as the Southeastern and Southwestern United States would have elevated $\delta^{18}O$ values. Once pH is accounted for in the NO_2-H_2O isotopic equilibrium (Model 3), the $\delta^{18}O$ values range more closely resemble those of Model 1 however the spatial distribution differs. Major distinctions include the Northeastern, Midwestern and Great Plains areas of the United States. These differences

are most likely due to the acidic soil conditions brought on by air pollution and intense agriculture in these areas.

A comparison of $\delta^{18}O$ values from sixteen major watersheds in the northeastern United States (Mayer et al., 2002), in which atmospheric NO_3^- contributions were ruled out due to low $\delta^{18}O$ values and the resulting NO_3^- was concluded to be the result of nitrification. The reported $\delta^{18}O$ values for nitrification were 12 – 18‰, these values are too high to fit any of the three proposed models and suggest that there are atmospheric NO_3^- contributions. Through a simple mass balance:

$$\delta^{18}O_{sample} = x(\delta^{18}O_{nit}) + (1 - x)(\delta^{18}O_{atm})$$

where $\delta^{18}O_{sample}$ is the reported nitrification value for the sixteen watersheds (12 – 18‰), $\delta^{18}O_{nit}$ is equal to the average of the modeled nitrification values for the northeastern United states (6.5‰), $\delta^{18}O_{atm}$ is the average of the range of reported atmospheric NO_3^- values (70‰) and *x* is the fractions of nitrification and atmospheric NO_3^-. It is determined that the watersheds in the northeastern United States would be subjected to 8.6 – 18.2% atmospheric contribution despite no detected signal through the use of $\delta^{18}O$ values (further discussed in Chapter 6).

CHAPTER 5: SEASONAL VARIATION IN NO_3^- $\delta^{15}N$ of $PM_{2.5}$ AND PM_{10}: INSIGHTS INTO ISOTOPE EXCHANGE DURING NO_x CHEMISTRY

5.1. Introduction

Urbanization results in increased sources of primary airborne pollutants such as nitrogen oxides (NO_x) that can lead to generation of secondary pollutants. Nitric oxide (NO) is emitted from a variety of sources (mainly anthropogenic) and is converted to nitrogen dioxide (NO_2) in the troposphere through reactions with ozone (O_3) or oxygenated radicals (Finlayson-Pitts et al., 1986; Seinfeld et al., 2006). NO_2 rapidly photolyzes producing oxygen atoms that reform ozone, making these reactions a null reaction sequence, but leads to high ozone levels when volatile organic compounds, elevated in urban environments, are present (Leighton, 1961; Singh, 1987). The main sink for NO_x is by its conversion into nitric acid (HNO_3), primarily via NO_2 oxidation by OH in the daytime and N_2O_5 hydrolysis during nighttime (Brown et al., 2006; Crutzen, 1979). Because gaseous HNO_3 is highly soluble and reactive it is removed from the atmosphere through precipitation as wet deposition, a major component of acid rain (Elliott et al., 2007) or on aerosol particles as dry deposition. Aerosol nitrate is particularly common in arid and semi-arid regions where alkaline dust and NH_3 (Sorooshian et al., 2011) can build up and neutralize HNO_3 as particulate nitrate (Dentener et al., 1996). The removal of NO_x by the production and removal of HNO_3 changes OH and O_3 mixing ratios, and alters aerosol production (Dentener et al., 1993).

Since O_3 and particulates are criteria air pollutants (U.S.Environmental Protection Agency, 2012a) that are detrimental to the environment and human health (Pope et al., 2006), understanding the formation of atmospheric nitrate (HNO_3, NO_3^-, particulate NO_3^-) is a fundamental concern in the atmospheric sciences.

Atmospheric nitrate formation rates are a complex function of increases/decreases in NO_x emissions, atmospheric chemistry and meteorological. The relative importance of NO_x sources can change throughout the year. For example, in the southwestern United States, biogenic NO emissions (denitrification) and forest fires usually increase during the spring and summer (Crimmins et al., 2004; McCalley et al., 2008; Westerling et al., 2006) while automobile NO_x emissions are essentially constant throughout the year. Shifts in atmospheric chemistry can also change the rate of nitric acid (HNO_3) production; in particular seasonal differences in sunlight and temperature enhance heterogeneous N_2O_5 reactions (Geyer et al., 2001). In urban areas, with high [NO_x] (>20ppt) and large aerosol concentrations, NO_x removal through N_2O_5 reactions on aerosol surfaces increases (Brown et al., 2006; Riemer et al., 2003). A low boundary layer height can trap pollutants near the surface, in essence changing boundary layer chemistry, enhancing NO_3^- production rates and dry deposition rates (Sillman, 1999). Understanding which of these mechanisms is responsible for increased/decreased atmospheric nitrate loading in urban areas is important for scientists and air quality mangers goals of improving urban air quality.

Variations in stable isotope abundances in atmospheric nitrate may be a new way of inferring the relative importance of changing NO_x sources or shifts in seasonal changes in NO_x chemistry. The $\delta^{15}N$ values of atmospheric NO_3^- (where $\delta = [R_{sample}/R_{standard} -$

1]•1000 and R is the $^{15}N/^{14}N$ of the sample and the standard) have been used for NO_x source apportionment (Elliott et al., 2007; Hastings et al., 2003). Shifts in nitrate $\delta^{15}N$ values in rainwater from the Northeastern US have been attributed to an increase in stationary NO_x sources (i.e. power plants) relative to vehicle emissions (Elliott et al., 2007). Seasonal changes in nitrate $\delta^{15}N$ values in rainwater from Bermuda were attributed to atmospheric circulation transporting North American anthropogenic NO_x emissions in October – March and lightening NO_x in April – September (Hastings et al., 2003). In contrast, Freyer determined that isotope effects during the chemical reactions that form atmospheric nitrate, not changing NO_x sources, was controlling the seasonal variations in $\delta^{15}N$ of NO_3^- in rain water, HNO_3, and as $PM_{2.5}/PM_{10}$ (Freyer, 1991). However, no definite conclusions were made about which reactions might be controlling the seasonal pattern in nitrate $\delta^{15}N$, and they noted additional measurements were needed to constrain which isotopic mechanisms were important. Here we examine $\delta^{15}N$ of nitrate in PM_{10} and $PM_{2.5}$ collected in Tucson, AZ to evaluate the factors controlling seasonal changes in aerosol nitrate concentrations. An emissions mass balance and simple isotopic exchange equilibrium model were compared to test the NO_x source versus NO_x chemistry $\delta^{15}N$ hypotheses.

5.2. Study Area

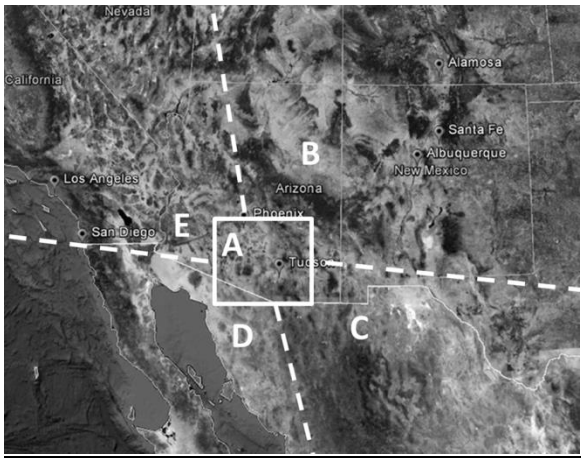

Figure 5.1. Study site is in Tucson, AZ (solid box, A) located in the Southwest U.S. and has a semi-arid climatology. Aerosol sampling site was NW of downtown Tucson. Dashed lines with letters represent sectors to different air mass source regions examined with HySplit back trajectories.

Particulate matter ($PM_{2.5}$ and PM_{10}) was collected in the urbanized, semi-arid Tucson Basin, in the southwestern United States (32.12°N, -110.92°W), beginning in 2006 for a 1 year period (Figure 5.1). The monitoring and collection site is located in a residential area with light industry NW of downtown Tucson. Site elevation is 680m ASL and there is greater than 270° of unrestricted airflow with the aerosol sampler inlet sitting 2.65m above the ground. The basin is bounded by the Santa Catalina, Rincon, and Tucson Mountain ranges (peak elevations of 2.7km, 2.6km, and 1.5km, respectively). Wind direction is affected by this topography, as well as the changing seasons and time of day. Air flows generally tend to be down-valley (from the SE) at night and during the

early morning hours and reverses to up-valley (from the NE) during the day (Day et al., 2012). Over the course of a year, temperature typically varies from 4°C – 40°C with hot summers (average daily above 34°C) from May through September and mild winters (average daily below 21°C). Tucson's metropolitan area has a population of ~1 million residents (U.S.Census Bureau, 2012). The majority of Tucson's industry is retail/business (41%) and smaller amounts from construction (9%), manufacturing (3%), mining, oil and gas extraction (0.2%) and agriculture (0.1%) (U.S.Census Bureau, 2010).

The Pima County Department of Environmental Quality (PDEQ) monitors criteria air pollutants throughout the Tucson metropolitan area in accordance with the National Ambient Air Quality Standards (NAAQS) set by the U.S. Environmental Protection Agency (USEPA). Criteria air pollutants include $PM_{2.5}$ (particulate matter <2.5μm in diameter) and PM_{10} (particulate matter <10μm in diameter), O_3, and NO_x. Since 1999 there have been eight recorded NAAQS violations of the PM_{10} standard (150μg/m^3) in Tucson. Main factors contributing to these violations include high winds, unusually long periods without rain, and natural events (i.e. forest fires, dust). $PM_{2.5}$ concentrations are typically 40% of the NAAQS standard (35μg/m^3) and there have been no violations since monitoring began in 1999 (Pima County Department of Environmental Quality (PDEQ), 2012). No significant changes have been observed in NO_x levels over the past 20 years and concentrations are roughly 30% of the NAAQS standard (0.053ppmv).

5.3. Methods

5.3.1. Aerosol and Emission Data at Site

Particulate matter was studied to understand NO_3^- dynamics within the Tucson Basin. Daily aerosol concentrations were determined by collecting $PM_{2.5}$ and PM_{10} using a Rupprecht & Parashnick Partisol FRM Model 2025 Sequential air sampler at a flow rate of 16.7 L/min with a sample collection time of 24 hours (Day et al., 2009). During the sampling period the criteria air monitoring instrumentation was not installed at the aerosol collection site therefore mixing ratios of O_3, CO, NO, and NO_2 as well as relative humidity, wind speed and direction, and outside temperature (Figure A5.1) were taken from a nearby monitoring location (~4.5km SE). The boundary layer height (BLH), which was taken as equivalent to the cloud condensation level, was estimated using temperature, relative humidity data, the Clausius – Clapeyron equation, and assuming a dry adiabatic lapse rate (Section 5.2.). Finally, emission inventories (anthropogenic and biogenic) for Pima County and surrounding areas were obtained from the USEPA (U.S.Environmental Protection Agency, 2012b).

5.3.2. Air Mass Trajectory Analysis

In order to evaluate if NO_x sourced outside of the basin was important in Tucson, air mass origin was determined using NOAA ARL HYSPLIT (Draxler et al., 2012). Daily two-day back trajectories ending in Tucson, AZ were computed for 2006 at ending altitudes (above ground level) of 0 m (surface), 1000 m (mixed layer) and 2000 m (boundary layer height). Back trajectories were group into five sectors (Figure 5.1) that could have significantly different NO_x sources. Trajectories from Sector A correspond to

those that spent at least a day of recirculation within the Tucson vicinity and would unlikely be influenced by external NO_x sources. Sector B are trajectories that originate northeast of Tucson and have several major cities, Albuquerque, NM (13,000 tons NO_x) and Santa Fe, NM (4,100 tons NO_x), but no other major NO_x sources. Air masses from Sector C originate from the Gulf of Mexico and also include areas of southern Texas and New Mexico. This area is dominated by the Chihuahuan Desert and other areas with low NO_x emissions but does include San Antonio, TX (42,000 tons NO_x). Sector D includes trajectories that begin in the Pacific Ocean and pass over the Baja California peninsula and the Gulf of California. These air masses can potentially be influenced from urban NO_x emissions from the city of Mexicali, Mexico (population 1 million). Trajectories originating from Sector E originated in the Pacific Ocean and were then transported over California or the western part of Nevada and the Mohave Desert. The major cities of San Diego, CA and Los Angeles, CA and their extensive urban sprawl lie within these trajectories and they have much greater NO_x emissions (54,000 and 200,000 tons NO_x, respectively) relative to the other sectors.

5.3.3. Chemical and Isotopic Analyses

Geochemical and isotopic analyses were carried out using established methods. In order to have sufficient NO_3^- for isotope analysis five sequential filters were combined and soluble NO_3^- was extracted in 50 mL of Millipore water. Nitrate samples were filtered (0.7μm) and stored frozen, then pre-concentrated by freeze drying and $\delta^{15}N$ analysis was performed using the denitrifier method and gold tube thermal reduction (Casciotti et al., 2002; Kaiser et al., 2007). Isotope ratios were measured using the Delta

V Plus ratio mass spectrometer that was calibrated using internal working reference standards that were previously calibrated to international standards USGS32, USGS35 and USGS34 (Riha et al., 2013). All subsequent $\delta^{15}N$ values are reported versus air N_2. Precision and accuracy of the $\delta^{15}N$ values were ±0.4‰ based on replicate analysis of the working standards and calibrations. Nitrate concentrations were measured using suppressed ion chromatography (Dionex IonPac® AS 14 Analytical Column interfaced with PeakSimple 3.29 software) and based on replicated analysis of standards uncertainty is ±0.33 mg/L.

5.4. Results

5.4.1 Seasonal amounts of particulate matter, nitrate, and NO_x in Tucson

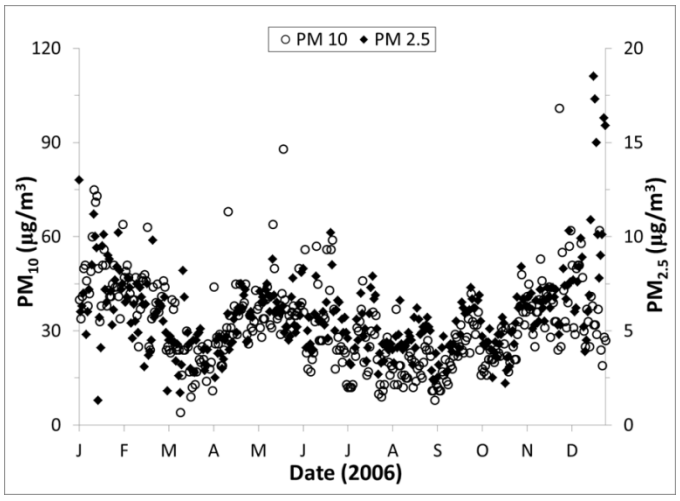

Figure 5.2. $PM_{2.5}$ and PM_{10} aerosol concentrations ($\mu g/m^3$) in Tucson AZ in 2006.

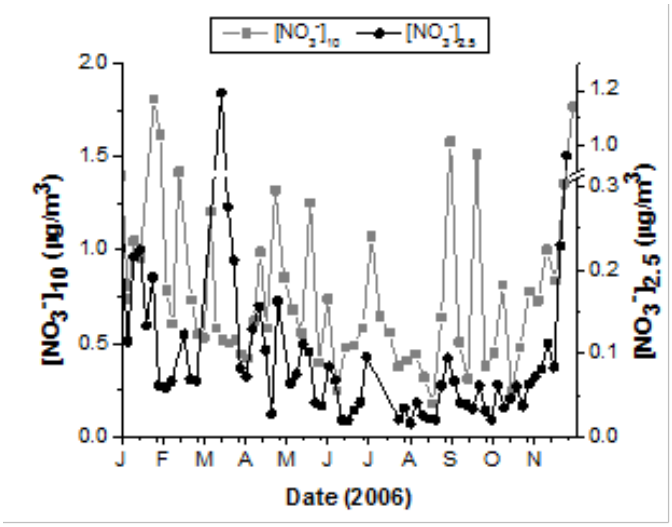

Figure 5.3. Seasonal trends in $[NO_3^-]_{2.5}$ (black circles and line, notice broken axis) and $[NO_3^-]_{10}$ (grey squares and line).

Particulate matter, $[NO_3^-]$ and NO_x concentrations all exhibited distinct seasonal variation. $PM_{2.5}$ and PM_{10} concentrations had a bimodal distribution (Figure 5.2), with higher concentrations during the winter and late spring ($PM_{2.5}$ = 10µg/m^3 and PM_{10} = 50µg/m^3) compared to early spring, summer and fall ($PM_{2.5}$ = 3µg/m^3 and PM_{10} = 10µg/m^3). In contrast, the ratio of $PM_{2.5}$ to PM_{10} is relatively constant throughout the year (0.2 ± 0.08) except during the monsoon seasons when the ratio increases (0.4 – 0.6). The concentration of nitrate in $PM_{2.5}$ (hereafter denoted $[NO_3^-]_{2.5}$) was typically higher in the winter and spring (0.1 – 0.25µg/m^3) compared to the summer (0.01 – 0.1µg/m^3), but there were two anonymously high peaks in March (1.19µg/m^3) and December (0.96µg/m^3). PM_{10} $[NO_3^-]$ (hereafter denoted $[NO_3^-]_{10}$) also had a seasonal trend, however had more intra-season variation, but generally maximums occurred in the winter and spring (0.8 –

1.8μg/m^3) while minimums were mainly in the summer and early fall (0.2 – 0.6μg/m^3) (Figure 5.3). Fraction $[NO_3^-]_{2.5}/PM_{2.5}$ ranged from 0.3 – 27% with a mean of 2% and the fraction of $[NO_3^-]_{10}/PM_{10}$ ranged from 0.7 – 7% with a mean of 2.5% (Figure A5.2). NO, NO_2 and total N oxides had pronounced seasonal trends with minimums in summer and maximums in winter (0.007 ± 0.008, 0.015 ± 0.006, and 0.021 ± 0.013ppmv, respectively) (Figure A5.1).

5.4.2 Nitrate $\delta^{15}N$ values of $PM_{2.5}$ and PM_{10}

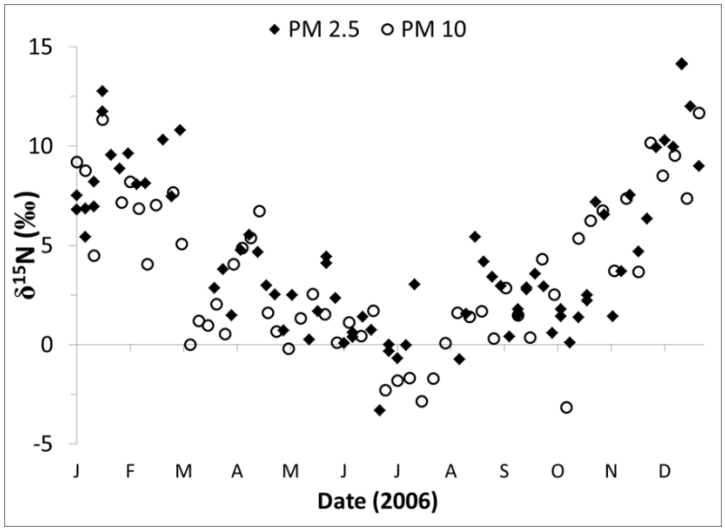

Figure 5.4. Pronounced seasonal trend in $\delta^{15}N$ of $[NO_3^-]_{2.5}$ and $[NO_3^-]_{10}$ with higher values in the summer and lower values in the winter.

The $\delta^{15}N$ values of $[NO_3^-]_{2.5}$ and $[NO_3^-]_{10}$ also exhibited a seasonal pattern (Figure 5.4). The $\delta^{15}N$ values were elevated during the winter in $[NO_3^-]_{2.5}$ (8 – 14‰) and $[NO_3^-]_{10}$ (8 – 12‰) relative to summer (-3 – 2‰, -3 – 0.5‰, respectively). The observed seasonal trends are similar to the $\delta^{15}N$ of rain water NO_3^- from the Midwestern and Northeastern

United States (Elliott et al., 2007) as well as $[NO_3^-]_{PM}$ from Germany (Freyer, 1991) but are opposite of rainwater nitrate from Bermuda (Hastings et al., 2003) that had higher $\delta^{15}N$ values in the winter compared to the summer.

5.4.3 Air Mass Trajectories

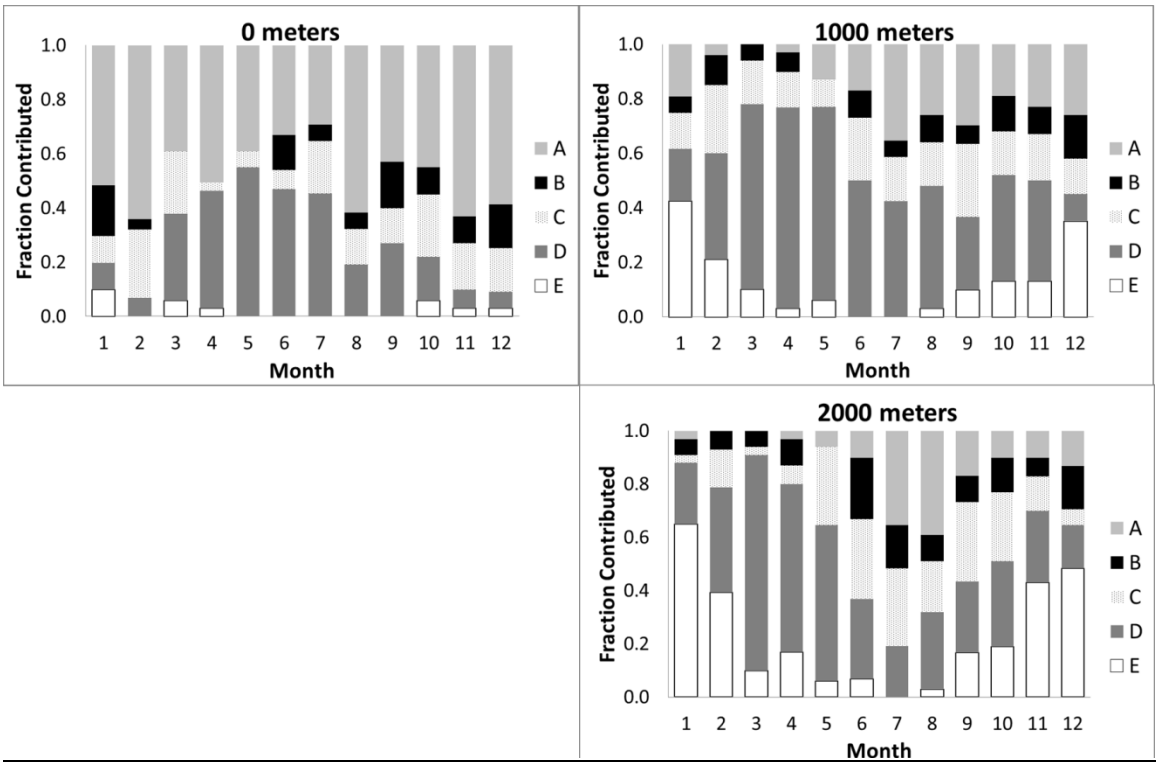

Figure 5.5. Relative frequencies of two-day air mass back trajectories passing through the five sectors (Figure 5.1) at three different ending altitudes (0, 1000, 2000 meters AGL) and arriving in Tucson, AZ.

There were several notable trends in the air mass trajectory analysis (Figure 5.5). Surface (0m) air mass origin was predominately local (Sector A: 29 – 64%) throughout the year but had significant contributions from the south-west during the spring and

summer (Sector D: 19 – 55%). The other surface sectors had minor contributions which accounted for less than 20% trajectories throughout the year. At 1000 ASL the majority of air masses originated from Sector D throughout the year with higher frequencies during the spring and summer (42 – 73%). Sector C had relatively constant contributions (10 – 27%). Whereas, Sectors A and E were more predominate during fall and winter (17 – 26% and 10 – 42%, respectively). At 2000 ASL the majority of air masses originated from Sector D with the highest contributions during the spring (58 – 81%). During the winter, a significant number of trajectories originated from southern California (Sector E; 39 – 65%). While during the summer Sectors A (13 – 35%), C and D made up the majority of the air mass origins. These 2000m trajectories correspond with the North American Monsoon system. Between July and September, intense and confined summer monsoon storms originating from the Gulf of Mexico and the eastern tropical Pacific Ocean as well as the Gulf of California account for roughly half of the annual precipitation in Tucson. Whereas, between November and March, lingering, sparse winter rains originate out of the Pacific Ocean (Sorooshian et al., 2011).

5.5. Discussion

5.5.1 Nitrate concentrations in $PM_{2.5}$ and PM_{10}

The cause for the bimodal distribution in the aerosol concentrations and seasonal variations in $[NO_3^-]_{PM}$ are most likely twofold: an increase in windblown dust and pollen during spring and a seasonal change in BLH. Across southern Arizona between April through July, a large fraction of $PM_{2.5}$ and PM_{10} is comprised of fine soil, which is attributed to agitated soils from agricultural activities, vehicles, construction, and mining

operations (Sorooshian et al., 2011). In the Tucson metropolitan area, O'Rourke et. al. observed a 4 fold increase in pollen concentrations during April (O'Rourke, 1990). While intact pollen grains are typically 15 – 40μm or larger (Monn, 2001), pollen allergens have been detected in the $PM_{2.5}$ size fraction (Rantio-Lehtimaeki et al., 1994; Solomon et al., 1983; Spieksma, 1990; Spieksma et al., 1995) possibly due to the release of subpollen particles (0.5 – 4.5μm) upon hydration of pollen grains (Bacsi et al., 2006; Monn, 2001). Both dust and pollen would lead to increased PM concentrations and can explain the observed spring time peak in PM that begins in April and continues through the beginning of July (Figure 5.2). Changes in the amount of surface level $PM_{2.5}$, PM_{10} and $[NO_3^-]_{PM}$ are also likely influenced by a change in BLH, from winter to summer. The estimated BLH exhibits a general seasonal trend, changing from ~1.5km during the winter to ~3.5km in the summer. The predicted BLH in July and August was suppressed relative to the other summer months and is probably due to large amounts of precipitation associated with the summer monsoon during this period (Figure 5.6). Evaporation of rainfall (both during transit and at the surface) results in an increased surface relative humidity, which in turn creates an artificially shallow cloud height in the BLH calculation, when in fact these are periods of intense convective mixing. The seasonal increase in BLH from winter to summer would causes pollutants to mix higher into the atmosphere diluting surface aerosol concentrations and $[NO_3^-]_{PM}$ and vice versa in the winter, consistent with our observed trend. This mechanism is supported by a comparison of $[NO_3^-]_{2.5}$ concentrations at the valley surface with those in the surrounding mountains. Matichuk et. al.(2006) observed that levels of $[NO_3^-]_{2.0}$ at Mt. Lemmon (2.7km above Tucson) in the summer are similar to those in Tucson (Figure 5.6, bottom). In the winter,

however, the $[NO_3^-]_{2.0}$ at the high elevation site are significantly less than in Tucson. Similar seasonal changes were observed in PM, elemental carbon, and organic carbon, changes that could not be explained by source changes but were instead driven by convective mixing in boundary layer. Thus, changes in BLH is prohibiting vertical mixing and can, in part, explain the observed seasonal trend in aerosol concentrations and $[NO_3^-]_{PM}$ at the surface in Tucson.

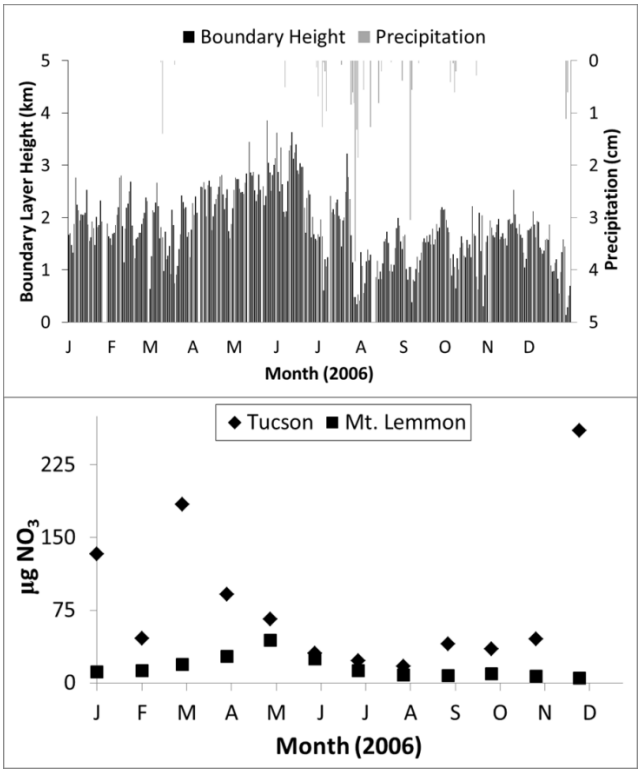

Figure 5.6. (top) Calculated change in boundary layer throughout the year with an artificial suppression in August due to the summer monsoon (bottom) Demonstration of change in boundary layer throughout the year in which vertical mixing induces equal loading of NO_3^- in Tucson (751m) and Mt. Lemmon (2700m) during summer months and increased at surface in the winter. Mt. Lemmon data taken from (Matichuk et al., 2006).

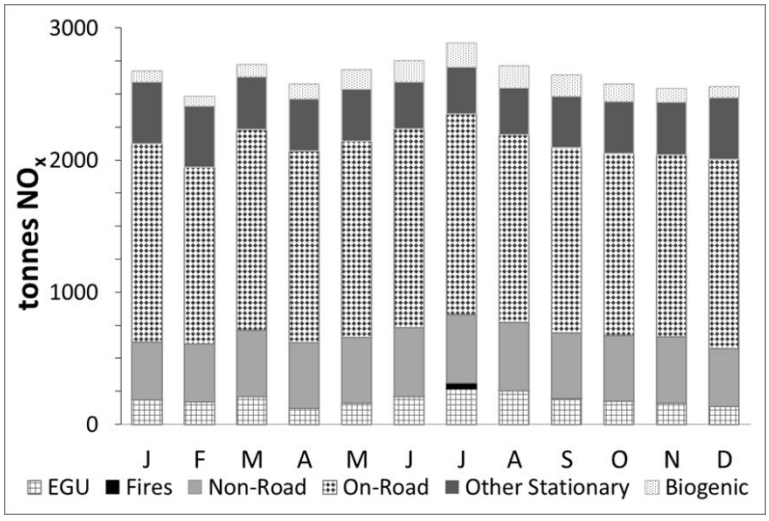

Figure 5.7. 2005 EPA NO_x Emission Inventory for Pima County, AZ indicating relatively constant NO_x emissions and little source variation throughout the year.

It is unlikely that increases/decreases in NO_x emissions are the cause of seasonal $[NO_3^-]_{PM}$, but shifts in atmospheric chemistry may be playing a role. The major NO_x sources surrounding Tucson (U.S.Environmental Protection Agency, 2012b) vary by less than 3 – 6% throughout the year (Figure 5.7) and thus cannot account for the observed 10 fold changes in $[NO_3^-]_{PM}$. Likewise, since seasonal NO_x emissions do not significantly vary, the observed seasonal trend in NO_x concentrations, which are similar to the $[NO_3^-]_{2.5}$ and $[NO_3^-]_{10}$ trends, are most likely due to dilution caused by changes in BLH and seasonal photochemistry that partitions NO_x into different forms of atmospheric N that were not measured (organic nitrate, PAN, HNO_3). Chemistry associated with regional increases in alkaline dust, typically found in southwestern AZ during April through July (Sorooshian et al., 2011), could increase the production of $[NO_3^-]_{PM}$ by two

mechanisms. First, the higher aerosol concentrations should enhance aerosol nitrate formation by heterogeneous hydrolysis because this depends linearly on aerosol surface area (Riemer et al., 2003). A weak (r^2 = 0.57 for $PM_{2.5}$) but statistically significant correlation between aerosol mass and nitrate content indicates higher winter nitrate concentrations can be explained, in part, by increased heterogeneous reactions driven by enhanced aerosol surface area during the winter. Second, the uptake of HNO_3 on alkali particles is a neutralizing reaction, trapping NO_3^- into the solid phase, enhancing surface $[NO_3]_{PM}$ during dust storms (Sullivan et al., 2007). Further discussion of the importance of HNO_3 formation pathways are beyond the scope of this paper, but will be the focus of a forthcoming paper examining oxygen isotopes in Tucson atmospheric nitrates.

The ratio $PM_{2.5}/PM_{10}$ also provides insight into aerosol mechanisms in the Tucson basin. The $PM_{2.5}/PM_{10}$ ratio remains relatively constant throughout the year but is lower during the dry seasons (0.17 ± 0.04) compared to the monsoon seasons (0.23 ± 0.08). This would suggest that during the dry season, mechanisms producing $PM_{2.5}$ and PM_{10} coupled. However, during the monsoon season, the ratio increases, which is likely due to washout efficiency of different sized PM. Because of droplet-aerosol impaction, the effectiveness of PM_{10} washout is 100 times higher compared to $PM_{2.5}$. Suppression of dust entrainment because of wet soil during the summer monsoon (June – September) may be playing a role in increasing the ratio. However, since the ratio goes down during latter stages of the monsoon, when dust suppression should be highest, it appears that size dependent washout in the primary mechanism for enhancing the $PM_{2.5}/PM_{10}$ ratio.

5.5.2 Nitrate $\delta^{15}N$ values of $PM_{2.5}$ and PM_{10}

In order to test the competing hypotheses that atmospheric nitrate $\delta^{15}N$ values change due to either increases/decreases in a particular NO_x source or because of shifts in seasonal NO_x chemistry, an emissions model and simple isotopic exchange equilibrium model were compared. The isotope mass balance model used the fraction of NO_x from each major source (U.S.Environmental Protection Agency, 2012b) and the mean observed (Ammann et al., 1999; Felix et al., 2012; Heaton, 1990; Li et al., 2008; Moore, 1977; Pearson et al., 2000) ranges of $\delta^{15}N$ values for those sources and assumed the $\delta^{15}N$ of atmospheric nitrate mirrored the $\delta^{15}N$ of the NO_x. It should be noted that the number of direct $\delta^{15}N$ measurements for all NO_x sources, across different regions and conditions, is sparse and should be a priority for future research. Given this caveat, the isotope mass balance equation: $\delta^{15}N_{NOx} = f_{EGU}\ \delta^{15}N_{EGU} + f_{nonroad}\ \delta^{15}N_{nonroad} + f_{road}\ \delta^{15}N_{road} + f_{biogenic}\ \delta^{15}N_{biogenic}$, was applied to calculate the expected nitrate $\delta^{15}N$ values in the Tucson basin (Figure 5.8), where f is the fraction of each NO_x source normalized to total NO_x emissions, and $\delta^{15}N_i$ the mean value for each NO_x source (i). Because Pima County's seasonal NO_x emissions and the NO_x source proportions are relatively constant (Figure 5.7), the predicted $\delta^{15}N$ of both $[NO_3^-]_{2.5}$ and $[NO_3^-]_{10}$ is also constant (mean -3.4 ± 0.4‰) (Figure 5.8). This is in stark contrast to the observed seasonal variation observed in both $\delta^{15}N$ of $[NO_3^-]_{2.5}$ and $[NO_3^-]_{10}$, (±5‰).

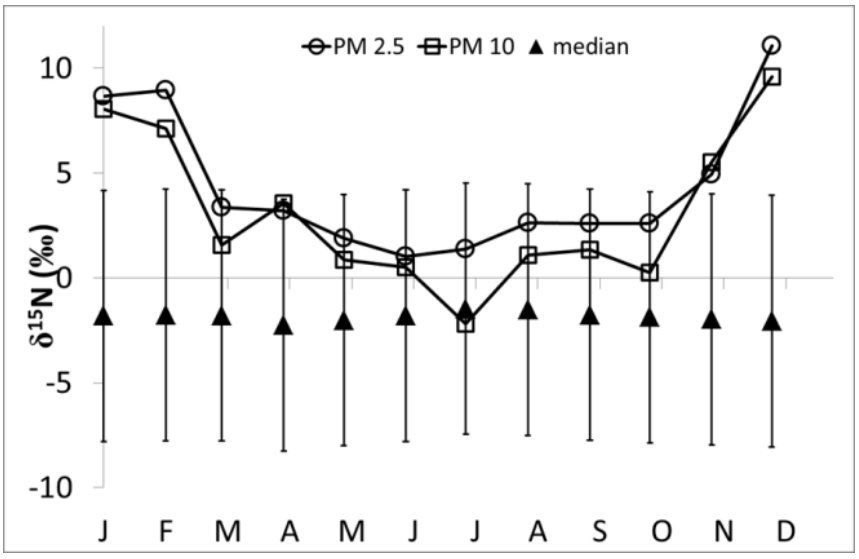

Figure 5.8. Expected $\delta^{15}N$ of NO_x (triangles) from emission mass balance and observed $\delta^{15}N$ of $[NO_3^-]_{2.5}$ (circles) and $[NO_3^-]_{10}$ (squares). $\delta^{15}N$ values of NO_x from coal fired power plants (EGU's): 6 – 13‰ (Heaton, 1990) and 9.8 – 19.8‰ (Felix et al., 2012), vehicle NO_x exhaust: 3.7 – 5.7‰ (Ammann et al., 1999; Moore, 1977; Pearson et al., 2000) (negative values have also been reported (-13 – -2‰) (Heaton, 1990)), biogenic NO_x emissions: -50 – -20‰ (Li et al., 2008). Triangles are the median calculated values of $\delta^{15}N_{NOx}$ emissions from the literature and the error bars represent the range of literature values given, this leads to a ± 0.2‰ spread that could be expected from the isotopic mass balance however no variations would be observed.

The hypothesis that nitrate $\delta^{15}N$ values arise because of the $\delta^{15}N$ of NO_x sources is also not supported by the back trajectory analysis. They indicate that the majority of the surface air (where aerosol sampling occurred) recirculated within the Tucson Basin (Figure 5.1) suggesting local emissions were primarily responsible for the observed

$[NO_3^-]_{PM}$ and their $\delta^{15}N$ values. There was also no seasonal trend within the remaining sectors at the surface that would account for the variations observed in $[NO_3^-]_{2.5}$ and $[NO_3^-]_{10}$. The seasonal trend at 2000 ASL that originated from Sectors D and E, which includes the populated cities of Los Angeles, CA and San Diego, CA, both of which have large NO_x emissions could be influencing $\delta^{15}N$ values of Tucson NO_3^-. Studies have shown, however, that HNO_3 produced in downtown Los Angeles was removed from the atmosphere within 242 km (Allen et al., 2009; Fenn et al., 2003a; Rao et al., 2009). Since, Tucson is located 775km from Los Angeles, it is unlikely that any HNO_3 or particulates could be effectively transported and mixed to the surface (Fenn et al., 2003a). Mixing from this height over Tucson would be challenging through an inversion layer by turbulent diffusion and would be minor relative to local urban NO_x loading within the basin. Lastly, California NO_x emissions are dominated by road vehicles (86% of yearly NO_x budget (U.S.Environmental Protection Agency, 2012b)) which if transported to Tucson, AZ would cause more depleted nitrate $\delta^{15}N$ values, which is opposite the observed $\delta^{15}N$ increase. To obtain the higher nitrate $\delta^{15}N$ values that are observed in the winter, NO_x emissions would have to come from EGU, which are sparse in California (0.92% of the yearly NO_x budget (U.S.Environmental Protection Agency, 2012b)). Therefore, NO_x emitted outside the Tucson basin and transported to it are not likely the cause of this seasonal $\delta^{15}N$ trend in the aerosol nitrate.

The influence of NO_x sources on the $\delta^{15}N$ value of atmospheric nitrate is also not evident in Tucson during seasonal forest fires. In late April (2006), a spike in CO concentrations (Figure A5.3) suggested that regional biomass burning (Galanter et al., 2000) may have impacted Tucson's air quality. We found this corresponded to a major

wildfire 420km north of Tucson. Increases in $[NO_3^-]_{2.5}$ and $[NO_3^-]_{10}$ (Figure 5.3) also occurred during the period, yet on-site monitoring showed no increase in $[NO_x]$ and there was no significant change in atmospheric nitrate $\delta^{15}N$ values (Figure 5.4). This would suggest that the increase in the $[NO_3^-]_{PM}$ was due to increased NO_x reactions occurring on wildfire soot/aerosols prior to its arrival in Tucson, but that the $\delta^{15}N$ value of that NO_x source was indistinguishable from the value of Tucson's regional NO_x. Thus, the data suggest that biomass burning NO_x also cannot explain the seasonal variation in atmospheric nitrate $\delta^{15}N$ values in Tucson. The alternative hypothesis used to explain the seasonal $\delta^{15}N$ variations observed in atmospheric nitrate is seasonal changes of NO_x chemistry.

A chemical reaction that could be controlling the seasonal trend in the $\delta^{15}N$ of $[NO_3^-]_{2.5}$ is the gas-particle equilibrium of $NH_4NO_3(s) \leftrightarrow HNO_3(g) + NH_3(g)$. This could help explain the $[NO_3^-]_{2.5}$ winter maximum and summer minimum, because $NH_4NO_3(s)$ is thermodynamically favored at cold temperatures while the gaseous phase is favored at warmer temperatures (Seinfeld et al., 2006). However, this hypothesis is not supported by the observed $\delta^{15}N$ values (Figure 5.4) or aerosol concentrations. At equilibrium, ^{15}N is usually preferentially in the particle phase (as suggested by (Freyer, 1991)) so the expected $[NO_3^-]_{2.5}$ $\delta^{15}N$ seasonal trend would be inverse of what was observed in Tucson (Figure 5.4). Also, $NH_4NO_{3(s)}$ is usually found in the $PM_{2.5}$ fraction of the total aerosol mass because gas to particle conversion produces sub-micron particles (Khoder, 2002). However, due to the high soil contribution to aerosol concentration (20% in $PM_{2.5}$ and 90% in PM_{10}) (Malm et al., 2007), studies have shown that in the southwest US $[NO_3^-]_{2.5}$ is mainly found as sodium or calcium nitrate resulting from the reaction of nitric acid

vapor with sea salt or soil dust (Malm et al., 2003). Sorooshian et. al. observed that $PM_{2.5}$ mass was mainly fine soil (32%) and organic carbon (29%, dust and biological aerosols such as bacteria and pollen) throughout the course of the year in Phoenix, AZ (Sorooshian et al., 2011). This suggests that in Tucson there is too little $[NO_3^-]_{2.5}$ as NH_4NO_3 to significantly alter its concentrations because of temperature driven phase partitioning. Therefore, it is concluded based on isotopic and mass considerations that gas-particle equilibrium of NH_4NO_3 is not the main chemical process controlling the $\delta^{15}N$ of $[NO_3^-]_{2.5}$.

Another possibility that might explain the seasonal change in atmospheric nitrate $\delta^{15}N$ values in Tucson is a gas phase isotopic equilibrium. The isotope exchange equilibrium between gaseous NO and NO_2 (Freyer, 1991):

$$^{15}NO + {}^{14}NO_2 \rightarrow {}^{14}NO + {}^{15}NO_2 \qquad (R1\text{-}k_1)$$

$$^{14}NO + {}^{15}NO_2 \rightarrow {}^{15}NO + {}^{14}NO_2 \qquad (R2 - k_2)$$

$$K_{eq} = \frac{k_1}{k_2} \qquad (EQ\ 5.1)$$

can occur if the exchange timescale is faster than the timescale of nitric acid formation through $NO_2 + OH \rightarrow HNO_3$ $_{(k3)}$. Using published rate constants ($k_1 = 8.13 \times 10^{-14}$ molecules/sec at 296K and $k_3 = 1 \times 10^{-11}$ molecules/sec at 298K, $k_{eq} = 8.13 \times 10^{-3}$) (Seinfeld et al., 2006; Sharma et al., 1970), the observed Tucson $[NO_x]$ and an estimated [OH] of 1 x 10^6 molecules/cm^3 for polluted atmospheres (Prinn et al., 1992) the ratio of exchange-to-reaction ranges from 400 to 3500 indicating complete isotopic exchange equilibrium

occurs in this environment. Additional NO_x removal, by hydrolysis of N_2O_5 during nighttime, occurs on a similar timescale as OH + NO_2 and thus would also not limit complete isotope exchange. We note that NO_x isotope equilibrium might not be attained in unpolluted environments where [NO] are at parts per trillion levels rather than the parts per billion that is observed in Tucson's urban atmosphere.

Isotopic mass balance and equilibrium enrichment was used to determine the $\delta^{15}N$ of NO_2 in the atmosphere assuming equilibrium with NO and using:

$$\delta^{15}N_{NO2} = [\delta^{15}N_{NOx} - f_{NO}(\delta^{15}N_{NO})]/f_{NO2} \quad \text{(EQ 5.2)}$$

$$\delta^{15}N_{NO} - \delta^{15}N_{NO2} = \varepsilon(T) \quad \text{(EQ 5.3)}$$

where f is the fraction of NO_x as NO or NO_2 (observed) and the enrichment factor ($\varepsilon(T)$) is calculated from the NO-NO_2 isotopic equilibrium constant K_{eq}, that was calculated from reduced partition functions (Richet et al., 1977) using known vibrational frequencies (Henry et al., 1978; Michalski et al., 2004b; Teffo et al., 1980). The $\varepsilon(T)$ factor for exchange is temperature dependent and ranges linearly from 37 to 45.8 ‰ over a scale of 46 to 7°C. The $\delta^{15}N_{NOx}$ is the expected value of NO_x emissions (-3.4‰) based on the emission inventory and using isotopic mass balance (Figure 5.8).

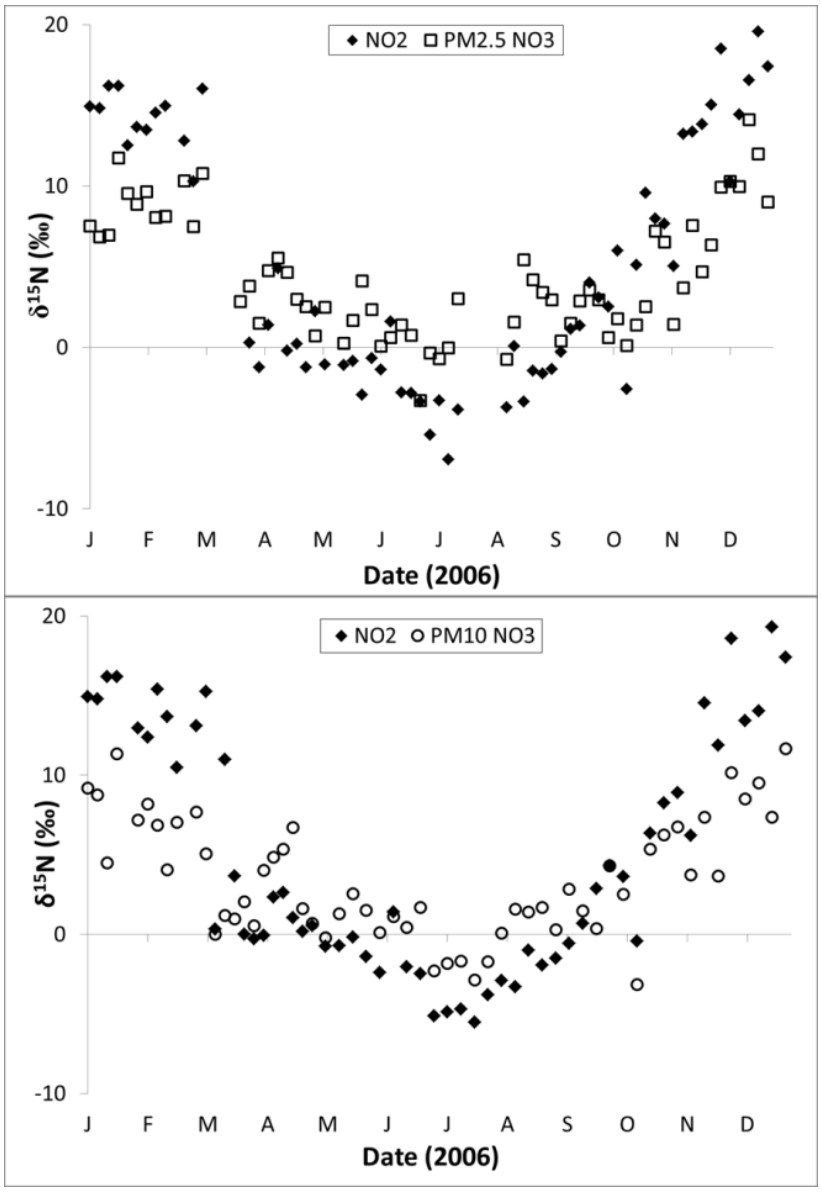

Figure 5.9. Calculated $\delta^{15}N$ of NO_2 (diamonds) undergoing isotopic equilibrium exchange compared to $\delta^{15}N$ of $[NO_3^-]_{2.5}$ (open squares) (top) and $\delta^{15}N$ of $[NO_3^-]_{10}$ (open circles) (bottom)

The calculated $\delta^{15}N$ of the precursor NO_2 using EQ 5.2 and 5.3 has a similar seasonal trend to the observed $\delta^{15}N$ of $[NO_3^-]_{2.5}$ and $[NO_3^-]_{10}$ (Figure 5.9). The small offset and deviations between the observed and calculated $\delta^{15}N$ values could be attributed to a second fractionation occurring during $NO_2 \rightarrow NO_3^-$ reactions. The calculated $\delta^{15}N$ of NO_2 suggests that the isotope exchange equilibrium between gaseous NO and NO_2, and not NO_x source apportionment, is the main process controlling the observed $\delta^{15}N$ of both $[NO_3^-]_{2.5}$ and $[NO_3^-]_{10}$ seasonal trends in the Tucson basin.

It has been determined that seasonal changes in NO_x sources had little influence on $[NO_3]_{PM}$ its $\delta^{15}N$ values in the Tucson metropolitan area. Instead, seasonal changes in boundary layer mixing and chemistry largely control $[NO_3^-]_{PM}$ and isotope exchange equilibrium between NO_x and is controlling its $\delta^{15}N$ values. NO_x sources must play some role in atmospheric nitrate $\delta^{15}N$ values in regions where significant shifts in source apportionment occur. However, interpreting seasonal nitrate $\delta^{15}N$ changes solely as source changes without accounting for meteorological and ambient atmospheric chemistry conditions is not justified. The problem should be approached by incorporating stable isotopes into regional 3D chemical transport models that can factor spatial and temporal changes in meteorology, chemistry, and NO_x sources. Stable isotopes may then provide insight not only into possible NO_x budgets but as an additional observational constraint for understanding oxidation chemistry in the atmosphere.

CHAPTER 6: LINKAGES BETWEEN THE ATMOSPHERIC AND BIOLOGIC NITROGEN CYCLES IN SEMI-ARID URBAN ECOSYSTEMS

6.1. Introduction

Arid and semi-arid regions are the most prevalent terrestrial ecosystem representing one third of the Earth's surface (Ezcurra, 2006) and are experiencing disproportionate increases in population growth and land use changes (Ezcurra, 2006). These alterations are straining already scarce water resources (Norman et al., 2009) and likely changing nitrogen biogeochemistry (Fenn et al., 2003a; Fenn et al., 2003b; Hall et al., 2011). How urbanization affects the biotic response to the reallocation of water and nitrogen in desert ecosystems is unclear (Lovett et al., 2005). Understanding interactions such as nitrification, N deposition, and N leaching, and their feedbacks on ecosystem function and services, will be critical to for developing science based management strategies to sustaining these limited resources.

Nitrate is often the main N compound in many ecosystems, is believed to be primarily from nitrification with only a small amount of nitrate deposited from the atmosphere. Urbanization in semi-arid regions may alter this proportion due to increases in N deposition in response to rapid increases in population and expanding urban areas (Fenn et al., 2003b) as well as increased impervious surfaces (Arnold et al., 1996) and the

emergence of catchment connectivity provided through stormwater infrastructure (Carle et al., 2005; Hatt et al., 2004). However, differentiating between biologic and atmospheric nitrate is impossible simply measuring changes in NO_3^- concentration in soils or streams. Therefore, it has been difficult to quantify the contribution of atmospheric relative to nitrification NO_3^- to an ecosystem, or to assess how the importance of these NO_3^- sources change under water limitation or urbanization. However, many studies in semi-arid ecosystems have suggested an increase of microbial processing upon soil wetting, leading to an accumulation of nutrients between runoff events and subsequent flushing (Austin et al., 2004; Welter et al., 2005), but they were not able to distinguish between biologic NO_3^- inputs versus atmospherically derived NO_3^-. Other studies have proposed increased dry deposited nitrate within urban catchments and due to limited soil water required for microbial processing, there is increased mobilization of nitrate during runoff (Lewis et al., 2007; McCrackin et al., 2008), but likewise these studies were unable to conclusively distinguish atmospheric from biologic NO_3^-. Yet, another study suggested that both processes are working together leading to high NO_3^- concentrations across a gradient of urbanized catchments (Gallo et al., 2012a), but again quantification of the two sources was lacking. These studies highlight that there needs to be better understanding on and quantification of the N cycle particularly related to N deposition and a better technique which can be used in semi-arid urbanized ecosystems (Adams, 2003).

Stable isotope abundance variations in nitrate can be useful in N biogeochemical studies as they can be used to infer changing NO_3^- sources or biogeochemistry. The small amount of research on tracing atmospheric NO_3^- deposition that has been done is mainly

in forested ecosystems (e.g. Durka et al., 1994; Mayer et al., 2002) using the dual isotope approach of $\delta^{15}N$ and $\delta^{18}O$ (where $\delta = (R_{sample}/R_{standard} - 1)\bullet 1000$). Most forested studies suggest no atmospheric NO_3^- deposition despite high N deposition rates but this could be due to the high variability of the $\delta^{18}O$ values of biologic and atmospheric NO_3^- which is often times a limiting factor is using the dual isotope approach in mixed systems (Michalski et al., 2004d). Triple oxygen isotopes are a new way to quantify the atmospheric fraction. Atmospheric NO_3^- is known to be anomalously enriched in ^{17}O (Michalski et al., 2003a). This ^{17}O enrichment is denoted by $\Delta^{17}O$, where $\Delta^{17}O = \delta^{17}O - 0.52(\delta^{18}O)$ (Miller, 2002b). Atmospheric NO_3^- $\Delta^{17}O$ values have only been measured in coastal and ocean environments and they range between 20 and 32 ‰. In contrast, NO_3^- produced by nitrification has a $\Delta^{17}O = 0$ and NO_3^- loss by denitrification/assimilation obey the mass dependent fractionation law, leaving the $\Delta^{17}O$ signal unaltered (Michalski et al., 2004a). Therefore, $\Delta^{17}O$ can be used as a conservative tracer of atmospheric NO_3^- and can be used to better understand the fate of atmospheric deposition in semi-arid urbanized ecosystems. It also can provide insights into the rate on microbial N turnover via the assimilation-mineralization-nitrification cycle.

The overall purpose of this research is to use stable isotopes in NO_3^- to understand how urbanization of desert biomes impacts coupled hydrologic – N biogeochemical processes. In particular, the following research questions were addressed: 1) How do precipitation NO_3^- isotopic abundances in semi-arid urban ecosystem compare to previous studies? 2) Do semi-arid urban streams have atmospheric NO_3^- present in waterways and if so does it compare to forested watersheds? 3) Are $\delta^{18}O$ and $\Delta^{17}O$

equally effective as an atmospheric tracer and can additional information be obtained through the coupled used of these two methods? 4) Can $\Delta^{17}O$ be used to obtain a gross nitrification rate in semi-arid urban catchments?

We hypothesized that urban streams would have higher atmospheric nitrate contributions because of augmented N emissions. In addition, impervious surfaces would reduce the N residence time in urbanized catchments' stream beds therefore limiting nitrate loss by microbial cycling during transport and creating a smaller reservoir of soil nitrate.

6.2. Study Catchments

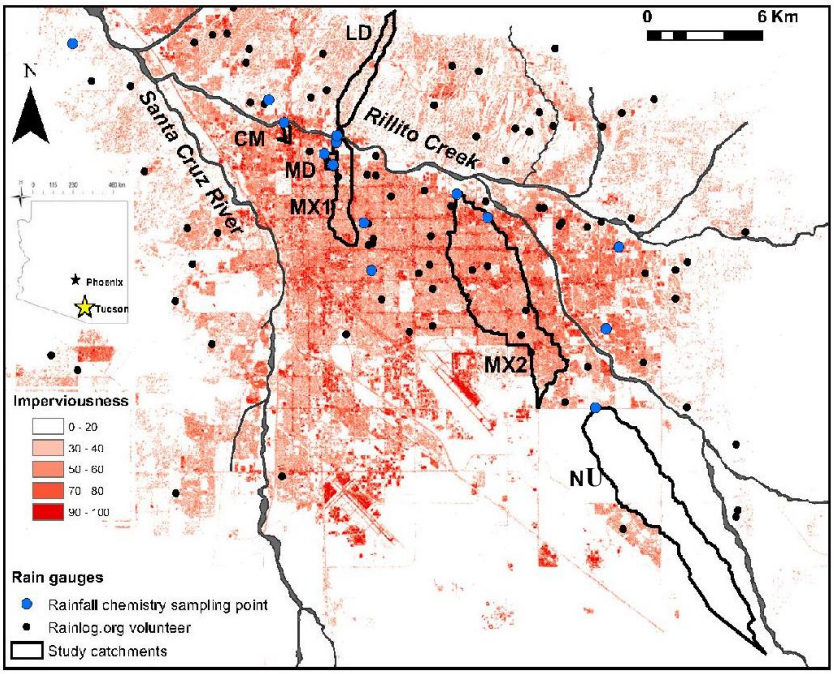

Figure 6.1. Location of the six study catchments (LD, CM, MD, MX_1, MX_2, and NU), rainfall gauges from Rainlog.org volunteer network (black dots), rainfall sampling locations nutrient and isotopic analyses and percent impervious cover within the Tucson Basin in south-eastern Arizona.

Study catchments are situated within the Tucson metropolitan area, AZ located in the southwestern United States (Figure 6.1). The Tucson metropolitan area is bounded by the Santa Catalina, Rincon, and Tucson Mountain ranges which form an alluvial basin. The basin is drained to the northeast by the ephemeral Santa Cruz River and its tributaries, the Canada del Oro, Rillito Creek, Pantano Wash and Tanque Verde Creek (Davidson, 1973). Climate in the Tucson basin is semi-arid with a mean annual temperature of 20°C (maximum 30°C in July and minimum 10°C in January). Mean annual precipitation is approximately 310mm and the region is affected by the North American Monsoon system in which precipitation occurs during two distinct rainy seasons. Between November and March, lingering, sparse winter rains originate out of the Pacific Ocean accounting for roughly half the annual precipitation. Whereas, between July and September, intense and confined summer-monsoon storms originating from the Gulf of Mexico and the eastern tropical Pacific Ocean as well as the Gulf of California (Gelt et al., 1999). Summer monsoonal rainfall is short in duration, high in intensity and highly spatially heterogeneous (Garcia et al., 2008; Morin et al., 2006; Syed et al., 2003). The current population of the Tucson metropolitan area is ~1 million residents and is projected to increase by 20% by 2030 (U.S.Census Bureau, 2012). Annual NO_x emissions (anthropogenic and biogenic) total 32,000 tonnes (U.S.Environmental Protection Agency, 2012b), modeled annual total N deposition was estimated at 7.5 – 15 kg $N \bullet ha^{-1} \bullet yr^{-1}$ (Fenn et al., 2003b) and measured annual total N deposition in nearby Phoenix, AZ was 4 – 7 kg $N \bullet ha^{-1} \bullet yr^{-1}$ of which 1 kg $N \bullet ha^{-1} \bullet yr^{-1}$ was estimated to be NO_3^- (Lohse et al., 2008).

Table 6.1. Land cover characteristics of the study catchments.

	Catchment					
	LD	MD	MX_1	CM	MX_2	NU
Catchment Area (km^2)	4.44	0.45	4.7	0.33	25.30	26.98
Impervious Cover (%)	21.84	40.64	45.78	90.70	50.63	2.92
Catchment Slope (%)	5.60	1.20	1.90	1.50		
Land Cover (%)						
Residential Housing						
Low Density	87.56	0.13	11.08	0.32	3.92	3.29
Medium Density	0.09	80.57	43.27	2.15	52.24	1.85
High Density	7.26	16.70	17.28	0	11.22	0.75
Commerical (office, retail, roads)	5.00	2.59	19.76	95.65	27.36	1.66
Open Space (parks, undeveloped)	0.08	0	2.78	1.87	5.26	92.45
Agriculture	0	0	5.54	0	0	0
Stream Channel Length (m)	12479	881	18634	1457	70496	146474
Impervious Channel Length (m)	1102	881	15021	1457	44748	1649
Pervious Channel Length (m)	11377	0	3613	0	25748	144825

Four of the urban catchments used in this study have been previously described and characterized by Gallo et. al. (Gallo et al., 2012a). Catchments were delineated and characterized for land cover properties in ArcMap 9.0 as described by Gallo et al. (2012a) using the stormwater drainage system, which encompasses engineered and natural, impervious and pervious attributes and does not share any infrastructure with sewer system. All of these catchments are hydrologically isolated and do not receive contributions from other sources (2012a). Land cover characteristics for each study catchment are summarized in Table 6.1 and vary in land use type, percent impervious cover, size, slope, and stream channel network and described in detail in Gallo et. al. (2012a). Briefly catchments consist of: a $4.44km^2$, majority low density housing (LD) catchment, a $0.45km^2$, majority medium density housing (MD) catchment, a small mixed density (MX_1) catchment ($4.7km^2$) with relatively equal contributions from all land uses,

a 0.33 km^2 commercial land use catchment (CM), a large mixed density (MX_2) catchment (25.3km^2) with relatively equal contributions from all land uses and a 26.98km^2 non-urban (NU) catchment of which 92% of the land use is open space.

6.3. Methods

6.3.1 Rainfall and runoff sample collection and analyses

Rainfall data (rainfall depth, duration, time since last rainfall) was obtained from 4 Pima County Flood Alert system monitoring sites (2380, 2350 6180 and 6190; http://rfcd.pima.gov/wrd/alertsys/index.htm) which were located in close proximity to the study catchments. Rainfall samples for isotope and inorganic N analyses were collected using a citizen scientist network of 21 people located throughout the Tucson Basin (see Gallo et al. (Gallo et al., 2012b)) as well as rainfall collectors at the outlet of the catchments from the 2007-2010 summer monsoon seasons.

Runoff samples were collected during the 2007 and 2010 summer monsoon season and analyzed for isotopes and geochemistry. Runoff was collected using automatic water samplers (ISCO 6712, Teledyne Technologies) installed at the outlet of each catchment. In 2007 they were programmed to collect a discrete sample every 20 minutes (for 4 hours), and in 2010, once stage height exceeded 1cm samples were collected every 10 minutes the first 40 minutes and every 20 minutes thereafter. Runoff samples were collected in acid washed combusted 1L glassware (2007) or plastic bottles with ProPak disposable sample bags (2010) retrieved within 24 hours of a storm event, placed in a dark cooler (~4°C) and immediately taken to the University of Arizona for processing. A split of the sample was filtered through a pre-combusted 0.7μm glass fiber

filter (Whatman GF/F) for nutrient and isotopic analyses. Aliquots for nitrate isotopic analysis were frozen shipped with ice packs overnight to Purdue Stable Isotope Facility (West Lafayette, IN). Ammonium-N analyses were carried out on a SmartChem Discrete Analyzer with a detection limit of 0.002 mg/L. Nitrate-N analysis was carried out on a Dionex Ion Chromatograph ICS-5000 with a detection limit of 0.005 mg/L. All concentrations are reported with respect to N (i.e. NO_3-N and NH_4-N). Nitrate samples were stored frozen until they were isotope analysis ($\delta^{15}N$, $\delta^{17}O$ and $\delta^{18}O$) was performed using the denitrifier gold tube thermal reduction (Casciotti et al., 2002; Kaiser et al., 2007; Riha et al., 2013) technique for, where $\delta = (R_{sample}/R_{standard} - 1)\bullet 1000$ and R is the ratio of the rare isotope relative to the abundant isotope of the sample and the standard. Isotope ratios were measured using the Delta V Plus ratio mass spectrometer that was calibrated using internal working reference standards that were previously calibrated to international standards USGS32, USGS35 and USGS34 (Riha et al., 2013). All subsequent $\delta^{15}N$ values are reported versus air N_2 and oxygen values ($\delta^{18}O$ and $\Delta^{17}O$) are reported with respect to VSMOW. The anomalous ^{17}O enrichment, denoted by $\Delta^{17}O$, was determined using (Miller, 2002b):

$$\Delta^{17}O = \left[ln\left(1 + \frac{\delta^{17}O}{1000}\right) - 0.52 \cdot ln\left(1 + \frac{\delta^{18}O}{1000}\right)\right] \cdot 1000$$

Precision of the $\delta^{15}N$ values were ±0.4‰, $\delta^{18}O$ values were ±1.0‰, and $\Delta^{17}O$ values were ±0.3‰ based on replicate analysis of the working standards and calibrations.

6.3.2 Isotopic mass balance

The fraction of atmospheric nitrate in urban runoff samples was determined using two mixing models, the first using $\Delta^{17}O$ values and the second using the $\delta^{18}O$ values. The first model employs the use of runoff NO_3^- $\Delta^{17}O$ values to determine the fraction of atmospheric (f_{atm}) and biologic (f_{bio}) nitrate in a sample through the use of isotope mass balance:

$$\Delta^{17}O_{runoff} = f_{bio}\,(\Delta^{17}O_{bio}) + f_{atm}\,(\Delta^{17}O_{atm})$$

where $\Delta^{17}O_{runoff}$, $\Delta^{17}O_{bio}$, and $\Delta^{17}O_{atm}$ are the isotopic compositions of NO_3^- in the urban runoff sample, biologically produced NO_3^-, and atmospherically produced NO_3^- (precipitation), respectively and $f_{atm} + f_{bio} = 1$ are the NO_3^- mole fractions. Atmospheric NO_3^- is known to be anomalously enriched in ^{17}O (Michalski et al., 2003a) while NO_3^- produced by nitrification has a $\Delta^{17}O = 0$ and NO_3^- loss by denitrification/assimilation obey the mass dependent fractionation law leaving the $\Delta^{17}O$ signal unaltered (Michalski et al., 2004a). This allows the isotopic mass balance is reduced to:

$$f_{atm} = \Delta^{17}O_{runoff}/\Delta^{17}O_{atm} \text{ and } f_{bio} = 1 - f_{atm}.$$

The second approach to determining fraction of atmospheric nitrate in runoff uses the $\delta^{18}O$ value as the atmospheric NO_3^- tracer (Chang et al., 2002; Durka et al., 1994; Kaushal et al., 2011; Kendall, 1998a; Mayer et al., 2002). A two component isotope mixing model yields:

$$f_{atm} = (\delta^{18}O_{runoff} - \delta^{18}O_{nit}) / (\delta^{18}O_{atm} - \delta^{18}O_{nit}).$$

where $\delta^{18}O_{runoff}$, $\delta^{18}O_{nit}$, and $\delta^{18}O_{atm}$ are the isotopic compositions of NO_3^- in the urban runoff, produced from nitrification and by atmospheric chemistry (precipitation),

respectively. A variety of models have been used to evaluate the $\delta^{18}O$ value of nitrification. The simplest assumes that O atoms from atmospheric O_2 ($\delta^{18}O$ = 23‰ and $\Delta^{17}O$ = -0.15‰) and soil water are incorporated into NO_3^- in a 1:2 ratio (Mayer et al., 2001). This ratio value has been recently challenged (Snider et al., 2010) suggesting that oxygen exchange between H_2O and NO_2^- controls the water to air incorporation ratio. It is likely that oxygen exchange between H_2O and NO_2^- would be minimal in these catchments due to the neutral to slightly basic soil conditions (7.5 ± 0.5) which limits the pH dependent exchange rate (Bunton et al., 1959) and the relatively small timescale that soil water is available in semi-arid systems. Precipitation during this study had a $\delta^{18}O$ = -5.6 ± 4‰ (*unpublished data*), which would result in a $\delta^{18}O_{nit}$ value of 4 ± 2.6‰.

These two mixing models were evaluated to determine f_{atm} (and f_{bio}) three different ways depending on the availability of isotope data for precipitation NO_3^- during a particular storm. If the runoff event had a single corresponding precipitation NO_3^- $\Delta^{17}O$ and $\delta^{18}O$ value, then that data were used in the isotopic mass balance model. Runoff events in which multiple precipitation NO_3^- $\Delta^{17}O$ and $\delta^{18}O$ values were available, the averaged $\Delta^{17}O$ and $\delta^{18}O$ values were used. In the case where no precipitation NO_3^- $\Delta^{17}O$ and $\delta^{18}O$ values were available owing to the highly spatially heterogeneous distribution of rainfall, the seasonally averaged values were used. For example, while all catchments contained at least one rainfall collector at the outlet of the catchment, it was quite possible for it to rain at the upper portion of the catchment but to be dry at the outlet precipitation collector. Uncertainties arising because of the assumptions in these three approaches are detailed in the discussion.

Nitrate fractional contributions (f_{atm} and f_{bio}) can be used to remove the atmospheric nitrate contribution from runoff samples (Dejwakh et al., 2012; Michalski et al., 2004d) and allow better constraint on the biological NO_3^- dual isotope plot. Since $\delta^{18}O$ values of atmospheric NO_3^- are elevated but $\delta^{15}N$ values are similar to terrestrial sources, even a small f_{atm} would lead to scatter in the dual isotope plot. Removing the atmospheric $\delta^{18}O$ and $\delta^{15}N$ components from runoff NO_3^- allows assessment of other NO_3^- sources or losses by assimilation or denitrification. To assess biological NO_3^- sources and NO_3^- processing, runoff NO_3^- samples were transformed with the $\Delta^{17}O$ and $\delta^{15}N$ and $\delta^{18}O$ values of atmospheric NO_3^- to obtain $\delta^{15}N$ and $\delta^{18}O$ values of biologic NO_3^- (Dejwakh et al., 2012). This isotope transform (40) is applied to find the biological $\delta^{15}N$ and $\delta^{18}O$ values of NO_3^- were obtained from the following isotopic mass balances:

$$\delta^{18}O_{bio} = (\delta^{18}O_{runoff} - f_{atm}(\delta^{18}O_{atm})) / f_{bio}$$

$$\delta^{15}N_{bio} = (\delta^{15}N_{runoff} - f_{atm}(\delta^{15}N_{atm})) / f_{bio}$$

6.4. Results

6.4.1 Precipitation NO_3^- $\Delta^{17}O$ and $\delta^{18}O$ values

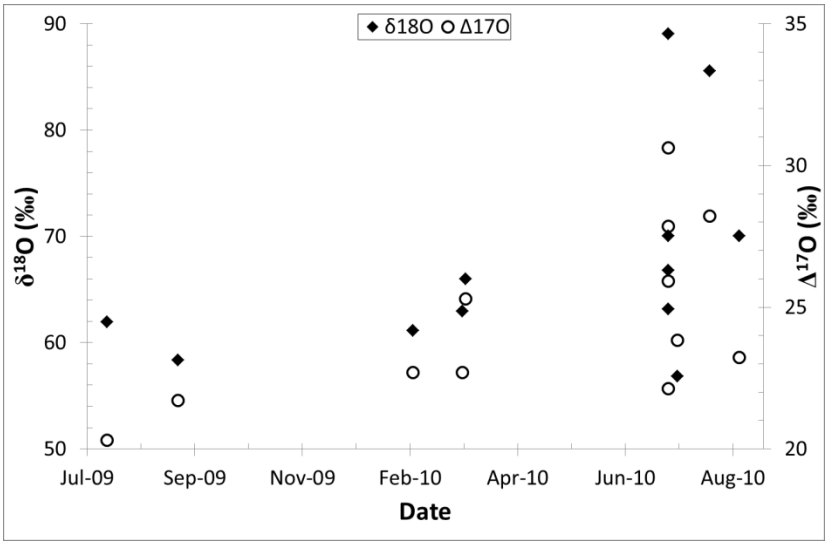

Figure 6.2. $\Delta^{17}O$ (open circles) and $\delta^{18}O$ (closed diamonds) values of NO_3^- in precipitation collected throughout the Tucson Basin during the study period.

The $\Delta^{17}O$ and $\delta^{18}O$ values of NO_3^- in precipitation varied spatially within storms and between consecutive storm events in Tucson during the study period (Figure 6.2). Between July 2009 and September 2010 (n=12), rainfall NO_3^- $\Delta^{17}O$ values ranged from 20.3 – 30.6‰ and averaged 24.5‰. The $\delta^{18}O$ values had a wider spread and ranged from 55.2 – 89‰, averaging 57‰. There was a significant correlation between precipitation NO_3^- $\delta^{18}O$ and $\Delta^{17}O$ values (r = 0.85, slope = 0.25). There was a large spatial variation in the NO_3^- $\delta^{18}O$ (63.1 – 89‰) and $\Delta^{17}O$ (22.1 – 30.6‰) values within the same storm from samples collected at different sites across Tucson. The inter-storm NO_3^- $\delta^{18}O$ and $\Delta^{17}O$ correlation was significant and similar to the seasonal (r = 0.83, slope = 0.21). Isotope

data for precipitation NO_3^- was not obtained for all storms during the summer because of either limited rainfall or low NO_3^- concentration resulted in insufficient NO_3^- for isotopic analysis. Rainfall NH_4^+/NO_3^- ratios ranged from 0 – 2 (mean = 0.9 ± 0.7).

6.4.2 Atmospheric NO_3^- fractional contribution based on $\Delta^{17}O$

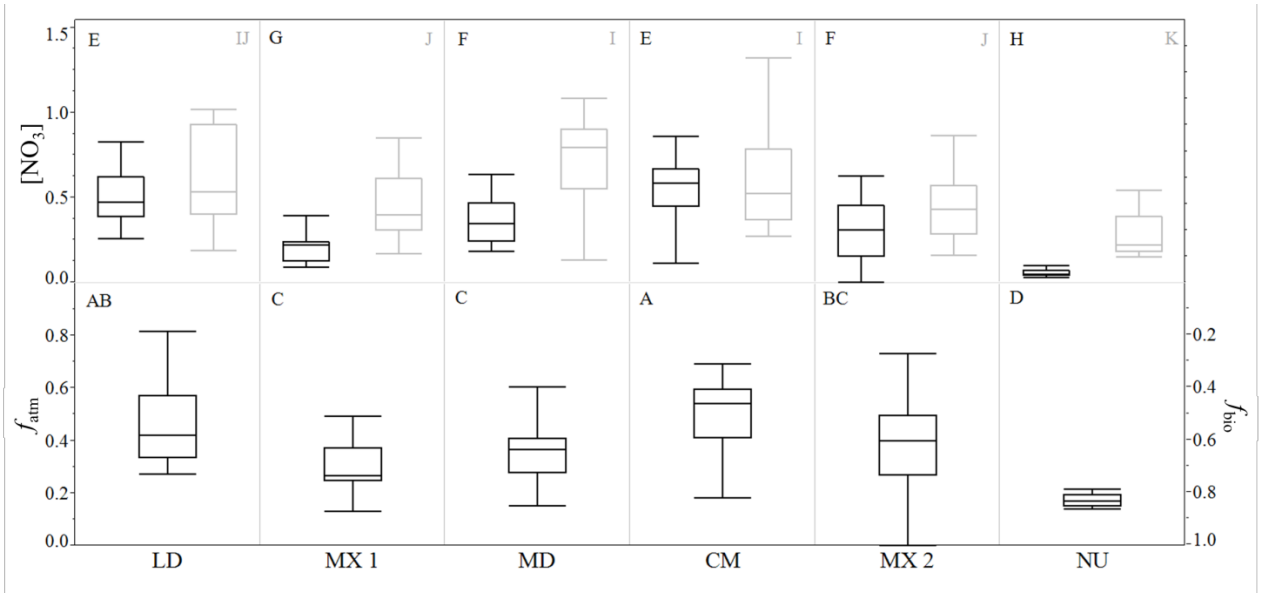

Figure 6.3. $[NO_3^-]_{atmo}$ (black) and $[NO_3^-]_{bio}$ (grey) runoff samples from each urban catchment ($[NO_3^-]_{atmo} = f_{atm}[NO_3^-]$) (Top) and the f_{atm} (fraction atmospheric NO_3^- - left y-axis) and f_{bio} (fraction biologic NO_3^- - right y-axis) for runoff samples from each urban catchment (Bottom). Quantile box plots, where the whiskers represent the minimum and maximum, box is the 25th and 75th quartiles, and the horizontal line is the sample median. Box plots sharing the same letter are not significantly different from each other ($p \leq 0.05$).

The f_{atm} were similar between catchments and storm events. For all catchments f_{atm} ranged from 0 – 0.82 (mean = 0.38, σ = 0.16, n = 179) and differed slightly depending on which model ($\Delta^{17}O$ average, storm specific) was used to calculate f_{atm}. Individual catchment f_{atm} are shown in Figure 6.3, with the highest atmospheric NO_3^- fractions observed in the CM and LD catchments and the lowest observed in the NU catchment. The MD, MX_1 and MX_2 catchments all had similar f_{atm} in runoff. However, total the f_{atm} variation from the six catchments were not significantly different from each other (t-test, $p<0.05$) (Figure 6.3).

Whereas f_{atm} were similar amongst catchments, the corresponding fraction weighted NO_3^- concentrations varied substantially among catchment to catchment (Figure 6.3). Fraction weighted NO_3^- is $[NO_3^-]_{atmo} = f_{atm}[NO_3^-]$ and $[NO_3^-]_{bio} = f_{bio}[NO_3^-]$. Highest $[NO_3^-]_{atmo}$ were found in the CM and LD catchments and the lowest in the NU catchment. The MD catchment tended to have higher $[NO_3^-]_{atmo}$ than both MX_1 and MX_2. Highest $[NO_3^-]_{bio}$ were observed in the MD catchment. The CM, LD, and both MX_1 and MX_2 catchments had similar $[NO_3^-]_{bio}$ with large variations whereas the NU catchment had the lowest $[NO_3^-]_{bio}$ of all study catchments.

6.4.3 Biologic NO_3^- sources and processing

Table 6.2. Mean (±SD) $\delta^{15}N$ and $\delta^{18}O$ values of biologic NO_3^- (obtained by isotopic transform) and corresponding NO_3^- source and slope of the dual isotope plot representative of NO_3^- processing (assimilation (slope = 1 (Granger et al., 2004a)) and denitrification (slope = 0.5 (Kendall, 1998b))). Mean (±SD) of runoff NH_4^+ and DOC concentrations used in the interpretation of biologic NO_3^- processing. Means sharing the same superscript across variables are not significantly different from each other ($p \leq 0.05$).

Catchment	$\delta^{18}O$ (‰)	$\delta^{15}N$ (‰)	Source	event based slope	NH_4^+ (mgN/L)	DOC (mg/L)
LD	16.3 (± 14.8)^{A}	4.7 (± 6.7)^{D}	NH_4^+/soil	−1.44 - 1.09	0.29 (± 0.19)^{C}	15.7 (± 7)^{C}
MD	16.8 (± 23.7)^{AB}	13.7 (± 16.7)^{C}	NH_4^+/soil	0.12 - 1.13	0.59 (± 0.41)^{A}	15.9 (± 10.5)^{BC}
MX_1	8.9 (± 6.9)^{B}	9.3 (± 6.5)^{C}	soil	−0.23 - 1.35	0.20 (± 0.19)^{B}	9.9 (± 7.8)^{E}
CM	13.5 (± 11.6)^{A}	−0.5 (± 11.5)^{AB}	NH_4^+/soil	−0.39 - 1.07	0.65 (± 0.33)^{A}	30.1 (± 18)^{D}
MX_2	4.4 (± 13.4)^{C}	2.4 (± 6.1)^{AD}	NH_4^+/soil	−1.31 - 0.89	0.18 (± 0.21)^{B}	22.2 (± 13.4)^{A}
NU	−0.11 (± 6.2)^{C}	−5.6 (± 12.5)^{B}	NH_4^+/soil	0.29 - 0.43	0.02 (± 0.03)^{D}	18.6 (± 5.4)^{AB}

Nearly all transformed $\delta^{15}N$ and $\delta^{18}O$ values fell within the range of nitrate derived from nitrification in soils (i.e. NH_4^+ and soil N) with a few event based $\delta^{15}N$ and $\delta^{18}O$ values falling within the fertilizer NO_3^- range (Table 6.2). Highest ^{15}N enrichments were observed in the MD and MX_1 catchment, whereas ^{15}N depletions were seen in CM and NU catchments. The highest transformed $\delta^{18}O$ values were observed in MD and LD catchments whereas MX_1 and NU showed low transformed $\delta^{18}O$ values. NO_3^- processing was detected in CM, LD and MD catchments and was primarily assimilation with minor contributions of denitrification.

6.5. Discussion

6.5.1 Precipitation NO_3^- $\Delta^{17}O$ and $\delta^{18}O$ values

The precipitation NO_3^- $\Delta^{17}O$ and $\delta^{18}O$ values are similar to other reported values but the high degree of inter-storm spatial variation and intra-storm variation over the monsoon season was not expected. The precipitation NO_3^- $\Delta^{17}O$ and $\delta^{18}O$ values are in similar to annual PM_{10} (particulate matter <10 mm diameter) collected in Tucson during 2006 (Riha et al. *in preparation*). The PM_{10} NO_3^- $\delta^{18}O$ and $\Delta^{17}O$ values (n= 57) were highly correlated with the same slope as the precipitation NO_3^- $\delta^{18}O$ and $\Delta^{17}O$ values (slope = 0.25, r = 0.94). PM_{10} NO_3^- had an annual average $\delta^{18}O$ value of 70.9‰ (± 13.5) and an annual average $\Delta^{17}O$ value of 27.2‰ (± 3.7), and summer (n= 11) $\delta^{18}O$ values of 55.2‰ (± 10.9) and $\Delta^{17}O$ values of 22.3‰ (± 2.4). Precipitation NO_3^- $\Delta^{17}O$ and $\delta^{18}O$ values reported here are also similar to those reported in Southern California (Michalski et al., 2003b; Michalski et al., 2004d), and $\delta^{18}O$ values are also comparable to those observed in the Northeastern United States (Burns et al., 2009; Elliott et al., 2009). The small scale $\delta^{18}O$ and $\Delta^{17}O$ variation (in time and space) in atmospheric NO_3^- has not previously been reported at other locals. However, these studies did not collect spatial and temporal sets of precipitation samples and therefore variability amongst precipitation NO_3^- $\Delta^{17}O$ and $\delta^{18}O$ values could not have been observed and cannot be compared to the current dataset.

Possible reasons for this variation include contamination of dry deposition in wet deposition samples or heterogeneity of storm centers causing fractionations during washout of nitrate. Due to the unpredictability of the summer monsoon rains (short in

duration, intense and spatially heterogeneous) precipitation collectors were left out in between storm events and therefore are considered a combined sample of wet and dry deposition. This combined sample can, in part, explain some of the variability observed in the precipitation NO_3^- $\Delta^{17}O$ and $\delta^{18}O$ values. In between precipitation events dry deposited collects particulate $NO_3^-{}_{(s)}$, and $HNO_{3(g)}$ could volatilize due to high temperatures therefore causing the residual $NO_3^-{}_{(s)}$ to become enriched in ^{18}O. This enrichment followed by a precipitation event could cause a mixture of fractionated dry deposited $NO_3^-(p)$ and current wet deposited $NO_3^-(aq)$ whose NO_3^- $\Delta^{17}O$ and $\delta^{18}O$ values would be a function of 1) dry deposition rate (how much $NO_3^-(p)$ is deposited in the collector), 2) the time between precipitation events (how much fractionation has occurred), and 3) wet deposition rate (how much $NO_3^-(aq)$ is deposited). However, this explanation would not justify the variation in $\Delta^{17}O$ as any post-depositional processing would likely obey the mass dependent fractionation law, leaving the $\Delta^{17}O$ unaltered (Michalski et al., 2004d). Therefore, this variation most likely is a reflection of localized changes in chemistry based on the position of the precipitation collector (near road versus residential area) and its location within the Tucson Basin. The range of precipitation NO_3^- $\Delta^{17}O$ values reported here suggest site specific varying importance HNO_3 formation pathways (Michalski et al., 2003b). This is most likely due to heterogeneity of NO_x and VOC emissions within the Tucson Basin (Diem et al., 2001), such that during a precipitation event the time scale from local emissions to conversion to HNO_3 and subsequent deposition is too short to allow for a homogenized mixture across the Basin therefore resulting in different precipitation NO_3^- $\Delta^{17}O$ and $\delta^{18}O$ values. Unfortunately there was not enough data (n=12) to determine if there were trends in precipitation NO_3^-

$\Delta^{17}O$ and $\delta^{18}O$ values throughout the course of the summer monsoon season. As a result, these variations can cause uncertainty in the calculated f_{bio} and f_{atm} when averaged precipitation NO_3^- $\Delta^{17}O$ and $\delta^{18}O$ values are used in the absence of actual event based data in the isotope mass balance model. Fractional contribution errors induced by utilization of seasonal averaged precipitation NO_3^- $\Delta^{17}O$ and $\delta^{18}O$ values versus event based can be both large and variable ($\Delta^{17}O$: +3 to -10% and $\delta^{18}O$: -9 to -45%).

6.5.2 Atmospheric NO_3^- contribution

The fraction of atmospheric NO_3^- exported from all the urban catchments, throughout the study period, were substantially higher (regardless of $\Delta^{17}O$ or $\delta^{18}O$ approach), than in nearly all other ecosystems. Most studies trying to quantify atmospheric NO_3^- export have attempted to use elevated $\delta^{18}O$ values (50 – 90‰) in atmospheric NO_3^- as the tracer, and have focused on forested and alpine ecosystems and have shown almost little to no contribution of atmospheric NO_3^- to total N. Throughout 16 major watersheds in the northeastern U.S., atmospheric NO_3^- contributions were considered negligible because high microbial N cycling erased the atmospheric $\delta^{18}O$ tracer (Mayer et al., 2002). In more humid forested systems, atmospheric NO_3^- accounted for 1 – 30% of total stream NO_3^- (Barnes et al., 2008; Campbell et al., 2006; Spoelstra et al., 2001; Williard et al., 2001). Unlike these forested catchments, all but one of our urban catchments have a significant fraction of atmospheric NO_3^- during the entire hydrograph (averaging 34 to 53%) and does not recede at the end of the storms as is observed in forested systems. The NU catchment, which is non-urbanized and majority

open space (92%), had low f_{atm} similar to forested catchments, however, unlike forested catchments f_{atm} did not recede at the end of the storm event.

The high f_{atm} NO_3^- in runoff observed in Tucson (Figure 6.3) has been found in several ecosystems with perennial waterways, but often as transient pulses during peak discharge with low f_{atm} NO_3^- observed during baseflow conditions. During peak snowmelt flows, 45 – 48% of the nitrate load was determined to be atmospheric NO_3^- in forested watersheds in the Eastern US. However, low atmospheric NO_3^- contributions, ≤7% were observed during the majority of flow conditions (Goodale et al., 2009; Pardo et al., 2004; Sebestyen et al., 2008). In northeast Bavaria, significant amounts of atmospheric NO_3^- contributions (14 – 46%) were also observed in forest spring water (Durka et al., 1994). High f_{atm} values were found in declining forests, and it was suggested that acidic forest soils were inhibiting nitrification. $\Delta^{17}O$ was used to detect high atmospheric NO_3^- fractions (4 – 40%) in Southern California (Michalski et al., 2004d), a semiarid climate similar to Tucson. While this range is closer to those found in Tucson, the highest f_{atm} were observed during peak discharge and they quickly diminished during baseflow conditions. These high peak flow atmospheric NO_3^- concentrations were primarily attributed to flushing of atmospheric NO_3^- deposition (*e.g.* plants and soil) during prolonged dry periods.

The difference in the amounts of atmospheric NO_3^- in Tucson relative to other mainly forested ecosystems must be a function of N deposition and N cycling rates. NO_3^- deposition in northeastern US watersheds were estimated at 4 – 8 kg $N \bullet ha^{-1} \bullet yr^{-1}$ (Mayer et al., 2002), which is higher than both the modeled NO_3^- deposition rate

(4 kg N•ha^{-1}•yr^{-1}) in Tucson (Fenn et al., 2003b) and the measured rate(1kg N•ha^{-1}•yr^{-1}) in nearby Phoenix (Lohse et al., 2008), which should be similar to Tucson. Therefore, major differences in atmospheric NO_3^- deposition rate between Tucson and eastern forests cannot explain higher atmospheric NO_3^- in Tucson's runoff. It is hypothesized that in urban catchments imperviousness limits N residence time and reduces the amount of exposed soil, thus decreasing the rate of assimilation/denitrification of deposited N and reducing nitrification rate.

6.5.2.1 Assessing f_{atm} using $\delta^{18}O$ versus $\Delta^{17}O$

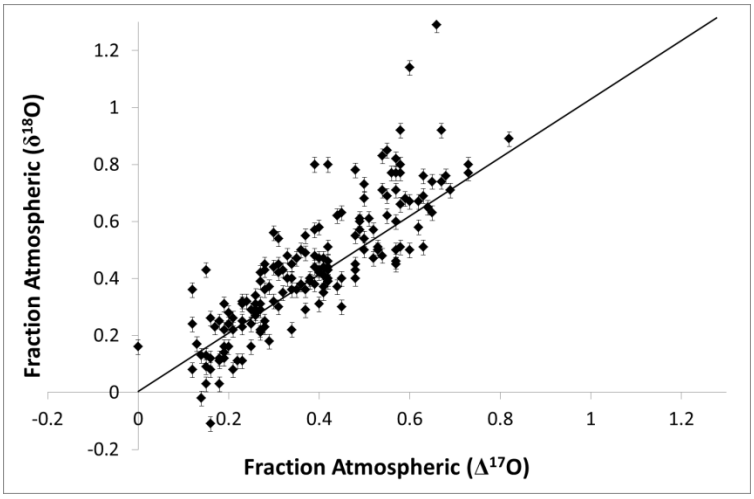

Figure 6.4. Mass balance estimates of the fraction atmospheric NO_3^- in runoff samples using an average $NO_3^-_{atmo}$ $\delta^{18}O$ = 57‰ and $\Delta^{17}O$ = 24.3‰ and a nitrification NO_3^- $\delta^{18}O$ of 4‰ and $\Delta^{17}O$ = -0.1‰. Solid 1:1 correlation line represents if the $\delta^{18}O$ method and $\Delta^{17}O$ method gives the same fraction of atmospheric NO_3^- contribution. Error bars represent the possible range of nitrification $\delta^{18}O$ values.

Comparing of the $\Delta^{17}O$ and $\delta^{18}O$ mass balance approaches to determine f_{atm} (Figure 6.4) yields additional information about the varying importance of nitrification within urban catchments. There was a strong correlation ($r^2 = 0.71$) between methods, and this suggests that the primary mechanism controlling runoff NO_3^- $\delta^{18}O$ and $\Delta^{17}O$ values in Tucson runoff are likely the same, i.e., deposition of atmospheric NO_3^-. However, the $\delta^{18}O$ method overestimates f_{atm} by approximately 10% and overestimations/underestimations of f_{atm} were ubiquitous and could be quite large (±40%) and suggests secondary mechanisms are altering the isotopic composition of runoff NO_3^- $\delta^{18}O$ values (Figure 6.4). In catchments where f_{atm} was high (CM, LD, MD), the $\delta^{18}O$ method often over predicts f_{atm}. In catchments where f_{atm} was low (MX_1 and MX_2), the $\delta^{18}O$ method was comparable to the $\Delta^{17}O$ method, and in the non-urbanized NU catchment, the $\delta^{18}O$ method underpredicted f_{atm}. Deviations from the 1:1 are not likely caused by variability of $\delta^{18}O_{atm}$. The atmospheric $\delta^{18}O/\Delta^{17}O$ ratio remains relatively constant during the summer monsoon season (Figure 6.2) suggesting that any inter-storm deviation in the $\delta^{18}O_{atm}$ value would also change the $\Delta^{17}O_{atm}$ value and thus alters the f_{atm} by the same amount. The deviation from the 1:1 line in the f_{atm} plot suggests that there is varying importance of nitrification within each catchment that is being reflected in the NO_3^- $\delta^{18}O$ values.

We hypothesize that the deviations are most likely due to seasonal variability in the $\delta^{18}O_{nit}$ values themselves. The $\delta^{18}O$ values of NO_3^- produced from nitrification is mainly controlled by the oxygen sources participating in the oxidation reaction and it is

believed to occur in a 2:1 ratio of H_2O and O_2 in a mass balance (Bohlke et al., 1997; Durka et al., 1994; Kendall, 1998a; Mayer et al., 2001; Wassenaar, 1995):

$$\delta^{18}O_{NO3} = \frac{2}{3}(\delta^{18}O_{H2O}) + \frac{1}{3}(\delta^{18}O_{O2}) \quad \text{(EQ. 1)}$$

Tucson precipitation $\delta^{18}O$ values vary seasonally particularly during the transition to the monsoon seasons (Wright, 2001) and the $\delta^{18}O$ of O_2 is taken as a constant of 23.5‰ (Horibe et al., 1973; Kroopnick et al., 1972). The variation if H_2O $\delta^{18}O$ values is a function of moisture sources (Pacific versus Gulfs of Mexico/California), storm size (large – sourced outside basin, small – recycled within basin) and rain magnitude (Wright, 2001). If nitrification occurs after a previous storm with a lower precipitation $\delta^{18}O$ value relative to the precipitation generating the runoff, then f_{atm} would be overestimated because improperly calculating the $\delta^{18}O_{nit}$ value (EQ.1). Conversely, evaporation leads to elevated water $\delta^{18}O$ values (Gazis et al., 2004), so if nitrification occurs after evaporative loss of soil water, f_{atm} calculated using $\delta^{18}O$ values would be underestimated because the H_2O $\delta^{18}O$ value used in EQ. 1 would be too low. One test of the hypothesis is that the variance in the 1:1 plot should increase in watersheds where higher fractions of soil nitrification might be expected. The urbanized catchments had lowest variance (MD – r^2 = 0.82, MX_1 – r^2 = 0.80, CM – r^2 = 0.72, LD – r^2 = 0.77), whereas the two sites with the largest open space land cover contribution (NU and MX_2) had the greatest variance (NU – r^2 = 0.10, MX_2 – r^2 = 0.52) and had the largest underestimations of f_{atm} (NU – 0.27, MX_2 – 0.15). This increase in variance with increasing soil surface area supports the hypothesis that variability in the $\delta^{18}O_{nit}$ values is contributing to deviation in calculated f_{atm} when using runoff NO_3^- $\delta^{18}O$ values instead of

the $\Delta^{17}O$ values. This indicates that nitrification is more important in catchments with a large fraction of its surface area as exposed soil (relative to impervious surfaces). This supports our hypothesis that nitrification rates in urban environments are a function of impervious surface area that decrease N turnover rate.

6.5.3 Biologic NO_3^- contribution

While the presence of a significant f_{bio} nitrate across all catchments is not surprising, it is remarkable that this holds true for the CM catchment, where 90.7% of the land cover is impervious (Figure 6.3). We hypothesize that this is due to nitrification occurring in soil particles deposited as dust between storms. The f_{bio} could be derived from grass medians in the parking lots and a few small areas of exposed soil (0.006 km^2) located within the watershed. However, these potential nitrification sources are scattered throughout the watershed and should appear as biogenic NO_3^- "pulses" in runoff, depending on their hydrologic connectivity to the remainder of the watershed (i.e. runoff arrival time to the sampler). This is not the observed, rather there is consistent ~30% biologic fraction that suggests that the biologic source of nitrate is evenly distributed across the watershed. This nitrification contribution may be nitrification occurring on dust previously deposited on the impervious surfaces. It has been shown that ammonia oxidizing bacteria (Prosser, 2011) can attach and colonize soil aggregates, thus nitrification could proceed if there is NH_4^+ within the dust. NH_4^+ may have been concentrated on soil particulate matter after its entrainment in the atmosphere by reacting with atmospheric $NH_{3(g)}$ and then nitrified. If true, the ratio of NH_4^+/NO_3^- in wet deposition should be higher compared to the ratio in runoff (wet + dry deposition) due to

loss of NH_4^+ during nitrification occurring since the last storm. For the CM catchment, the average ratio of NH_4^+/NO_3^- in wet deposition was 0.96 whereas in runoff it was 0.75, the 0.21 difference nearly matching the 0.30 nitrification fraction observed, suggesting that nitrification is occurring between storm events. This is consistent with results from other studies in the region (Sullivan et al., 2012). Volatilization of NH_4NO_3 from the surface would not decrease the ratio since HNO_3 is also lost during volatilization. Decreases in the NH_4^+/NO_3^- ratio as a function of stream length in semi-arid, urban watersheds has been interpreted as in-stream nitrification (Welter et al., 2005). If true at the CM site, we would expect to see an increase in the biologic fraction as a function of runoff arrival time. However, this was not observed in CM or in any of the study catchments, and is consistent with the finding by Gallo et. al. (Gallo et al., 2012c) who showed that storm runoff residence times are not long enough for water column processes to significantly alter runoff hydrochemistry. We conclude then that the most robust explanation of a substantial f_{bio} is nitrification of intra-storm dry deposited dust. Thus while impervious surface area may limit water soil interactions and retard N cycling, it does not completely eliminate it.

6.5.4 Biologic NO_3^- sources and processing

To improve the understanding of nitrogen cycling dynamics in semi-arid urban streams, it is important to know the source of N that is generating the biologic nitrate. This is possible by utilizing the dual isotope technique, where the nitrate $\delta^{15}N$ and $\delta^{18}O$ values are used in an isotope mixing plot (Kendall, 1998b). The majority of biologic nitrate was sourced from nitrification (i.e. NH_4^+ or soil N range) with minimal

contributions from fertilizer (Table 6.2). This is not surprising as the stormwater and sewer system infrastructure are separate entities and do not share infrastructure therefore septic or manure derived NO_3^- would not be expected in these catchments. Also, only one catchment (MX_1) has agricultural land use ($0.26km^2$); however, unexpectedly this catchment was not representative of any of the events that contain fertilizer NO_3^-. Fertilizer NO_3^- was within catchments that had the greatest amounts of low residential and ranch land uses (MX_2) suggesting citizen lawn fertilizer application contamination. While other catchments (LD and CM) had elevated $\delta^{15}N$ and $\delta^{18}O$ values that could be indicative of fertilizer, these values occur at peak discharge and then at the recession of the hydrograph biologic nitrate has isotopic signatures representative of nitrification (NH_4^+ and soil N). A possible explanation is volatilization of NH_4^+ in between runoff events and then nitrification of this enriched NH_4^+ during dry periods and subsequent flushing (peak discharge) and then the lower values during the recession can be attributed to nitrification of current NH_4^+ in rainfall with current H_2O incorporation from rainfall inputs.

The dual isotope approach can also be used to differentiate between denitrification and assimilation loss of nitrate (Boettcher et al., 1990; Sebilo et al., 2003b). Understanding nitrate loss by denitrification is important because it removes nitrogen from the system, which reduces downstream contamination potential of recharged groundwater. If denitrification is occurring both the $\delta^{15}N$ and $\delta^{18}O$ of the residual nitrate will increase along a trend line with a slope of 0.5 (Chen et al., 2005; Kendall, 1998b). Conversely, assimilation by plants or microbes acts as a temporary holding reservoir for nitrate, which can then be regenerated by mineralization/

nitrification downstream. If assimilation is taking place, both the $\delta^{15}N$ and $\delta^{18}O$ of the residual nitrate will increase along a trend line with a slope of 1 (Granger et al., 2004a). The relative importance of these two loss processes can be inferred using these two different isotope slopes. Nitrate processing was mainly evident in smaller catchments (MD, CM, LD and MX_1) (Table 6.2). NO_3^- assimilation was prevalent in cases where there was a runoff event the previous day. The first rainfall-runoff event could have caused a growth of microbial populations between events causing nutrients to become depleted (Austin et al., 2004). While [NH_4^+] remained relatively constant between the two events [DOC] increased (Table 6.2), this would have increased C:N ratios causing microbial populations to assimilate nitrate to sustain growth during the following water pulse event (Austin et al., 2004). Events showing evidence of denitrification were from catchments with majority pervious stream channels and lower catchment slopes (MX_1 and NU) and were recently preceded by another rain event. It is often observed in semi-arid landscapes that areas of low elevation (*e.g.* riparian zones, ephemeral washes) provide patchiness in soil resources and microbial biomass due to pooling of resource availability (i.e. water retention and NO_3^-) and provide 'hot spots' and 'hot moments' of potential denitrification (Harms et al., 2008).

6.5.5 Gross nitrification

6.5.5.1 $\Delta^{17}O$ mass balance to estimate watershed gross nitrification

Here we show that $\Delta^{17}O$ values can be used to estimate the gross nitrification rate at the catchment scale. Since the main NO_3^- removal mechanisms, denitrification, assimilation and nitrification, are all mass-dependent isotope processes, the NO_3^- $\Delta^{17}O$

values remain unchanged under their influence. In essence, using $\Delta^{17}O$ to assess gross nitrification is analogous to ^{15}N isotope dilution techniques, but where the tracer is naturally applied. On the contrary, residual NO_3^- $\delta^{18}O$ values increase after NO_3^- loss by these processes and can be used to assess the importance of NO_3^- removal (net nitrification). In order to determine gross nitrification, an isotopic mass balance was calculated similar to that previously used to determine the NO_3^- fractional contributions:

$$\Delta^{17}O_{runoff} = Q_{bio} (\Delta^{17}O_{bio}) + Q_{atm} (\Delta^{17}O_{atm})$$

where Q_{bio} and Q_{atm} are now the gross rate fractions in units of $kgNO_3^-•km^{-2}•day^{-1}$:

Q_{bio} = Gross Nitrification rate / (Gross Nitrification rate + Deposition rate)

Q_{atm} = Deposition rate / (Gross Nitrification rate + Deposition rate) = $\Delta^{17}O_{runoff} / \Delta^{17}O_{atm}$

and therefore $Q_{bio} + Q_{atm} = 1$. This model assumes that rainfall depth is heterogeneous across the study catchment and that all biologic NO_3^- in runoff is from dissolution and transport of near surface soil salts and therefore representative of nitrification occurring in the active layer since the last runoff event. It also assumes that there is sufficient exchange with the soil surface such that runoff would be representative of soil water (nitrification derived NO_3^-) and precipitation (atmospheric derived NO_3^-) however, if overland flow is occurring then poor exchange would be occurring and therefore GNR would be underestimated. The Q_{atm} (deposition rate) is both dry and wet deposition. A constant dry deposition rate of 1.2 $kgNO_3^-•km^{-2}•day^{-1}$ was used (Fenn et al., 2003b). The amount of NO_3^- from daily wet deposition was obtained from the precipitation $[NO_3^-]$ and normalized to time between precipitation events. Substituting Q_{bio} and Q_{atm} into the original mass balance and solving for the Gross Nitrification rate yields:

$$\text{Gross Nitrification Rate (GNR)} = \text{Deposition rate} \bullet [1 / (\Delta^{17}O_{runoff} / \Delta^{17}O_{atm}) - 1]$$

6.5.5.2 Gross nitrification results

Table 6.3. Mean (±SD) of event based gross nitrification rates calculated using average fractional atmospheric contribution, where *n* is the number of events per catchment. NO_3^- dry deposition rate was assumed to be constant (Fenn et al., 2003b). NO_3^- wet deposition was obtained from event based precipitation [NO_3^-] and normalized time between rain events. Means sharing the same superscript across variables are not significantly different from each other ($p \leq 0.05$).

Catchment	n	Dry Deposition (kgN/km^2d)	Wet Deposition (kgN/km^2d)	Total Deposition (kgN/km^2d)	Gross Nitrification Rate (kgN/km^2d)
LD	3	1.2	2.8 (±2)	4.0 (±2)	$4.68\ (\pm 2)^{C}$
MD	5	1.2	2.0 (±2)	3.2 (±2)	$6.21\ (\pm 2)^{BD}$
MX_1	3	1.2	1.3 (±1)	2.5 (±1)	$5.87\ (\pm 4)^{CD}$
CM	5	1.2	1.9 (±2)	3.1 (±2)	$3.04\ (\pm 2)^{E}$
MX_2	4	1.2	1.8 (±0.3)	3 (±0.3)	$6.22\ (\pm 5)^{AB}$
NU	2	1.2	1.3 (±0.3)	2.5 (±0.3)	$10.15\ (\pm 1)^{A}$

The GNR support the hypothesis that soil surface area and N residence time are the key factors controlling nitrification in Tucson. The highest GNR is in the NU catchment (10.15 ± 1 $kgNO_3^- \bullet km^{-2} \bullet day^{-1}$) whereas CM statistically had the lowest (3.04 ± 2 $kgNO_3^- \bullet km^{-2} \bullet day^{-1}$) (Table 6.3). This would be expected based on our hypothesis: NU has highest soil surface and CM has the least. And while MX_2 has a soil surface area in-

between these two extremes, it has a GNR similar to NU, which must be related to catchment characteristics which enhances nitrification. The remaining three catchments (LD, MD, and MX1) all have low soil surface area and similar GNR. In semi-arid systems, minimal studies have reported gross nitrification rates and focus has been on net nitrification rates. However, those that have been measured were conducted using the ^{15}N dilution method on intact soil cores in fields and there it has been shown that GNR is dependent on water pulses, depth to wetting, and time since wetting on gross nitrification rates (Dijkstra et al., 2012; Saetre et al., 2005). In the semi-arid Central Plains Experimental Range (Colorado), gross nitrification rates were highest after 3 days following an initial wetting (220 – 360 $kgNO_3^-•km^{-2}•day^{-1}$) and rates were near negligible after 10 days (Dijkstra et al., 2012). These GNR are similar to those observed GNR in forested ecosystems in New Mexico and Oregon which ranged from 25 – 300 $kgNO_3^-•km^{-2}•day^{-1}$(Stark et al., 1997). The GNR in forested and natural, semi-arid systems are 5-100 times larger than those observed in these semi-arid, urbanized study catchments. Whereas the reported GNR in the urban study catchments are similar to those reported in a Japanese mineral forest soil (0 – 61 $kgNO_3^-•km^{-2}•day^{-1}$) (Kuroiwa et al., 2011). And while C:N ratios were not reported in for those studies in natural semi-arid and forested ecosystems, the urban study catchments have C:N ratios ranging from 10 – 13 (*unpublished data*). This suggests that similar competition mechanisms could be occurring in Tucson due to carbon limitations and that upon NH_4^+ availability it will be immobilized rather than available for nitrification. A notable difference in these study catchments from other studies reporting GNR are that they are urbanized which could greatly alter GNR and these effects have yet to be studied. However, in near-by urbanized

Phoenix, it has been shown that urbanization and its subsequent land conversion from desert to lawns will significantly increase soil N_2O emissions (by-product of both nitrification and denitrification) and speed N cycling (Hall et al., 2008). Similarly, throughout the Tucson metropolitan area, some of the highest ever reported N_2O fluxes immediately following wetting of ephemeral streambeds (3121μg N_2O-N•m^{-2}•hr^{-1}) (Gallo et al., 2013). It has also been shown in semi-arid landscapes that areas of low elevation (*e.g.* riparian zones, ephemeral washes) provide 'hot spots' and 'hot moments' of potential denitrification due to patchiness in soil resources (*e.g.* pooling of microbial biomass, nutrient resources, and water) (Harms et al., 2008). These studies combined with the low GNR suggest that less nitrified NO_3^- is present in urban catchments due to competing N cycling processes or that nitrification processes are 'leaky' in which complete conversion of NH_3 to NO_3^- does not occur. These much higher GNR are further evidence of the lack of atmospheric nitrate contributions in forested ecosystems where microbial turnover is higher therefore 'erasing' atmospheric $\delta^{18}O$ contributions. Whereas in Tucson, gross nitrification rates are significantly lower and therefore atmospheric nitrate contributions prevail.

6.6. Conclusion

In this study we show conclusively for the first time, in semi-arid urban environments, the fractional contributions of atmospherically versus biologically derived nitrate. Urban runoff showed a significant fraction of atmospherically derived NO_3^- from all catchments (0 – 0.82, mean = 0.38) with higher fractions from more impervious catchments and lower from non-urban catchments. Our results are in agreement with the

previous “build and flush” model for both nitrate fractions. It was observed that during dry periods, atmospheric nitrate was depositing and accumulating on surfaces and biologic nitrate (produced via nitrification) in soils as well and were subsequently flushed to waterways following the next rainfall/runoff event. The results presented here suggest increased impervious surface area allows for more atmospheric NO_3^- to reach urban waterways due to inefficient N cycling within the catchment. Whereas, increased soil surfaces in catchments allows for nitrification and therefore atmospheric NO_3^- deposition is not as prevalent. The continued urban sprawl and further modification of ephemeral streams to augment a limited water supply in semi-arid regions will continue to modify N cycling.

CHAPTER 7: CONCLUSIONS

The research presented in this dissertation focused on developing an improved technique for multiple isotope analysis of nitrate and used that technique to measure nitrates from a range of environments to understand the relative importance of different nitrate sources in order to better understand the N cycle. The denitrifier method coupled with gold tube thermal decomposition has been shown to be a fully compatible method for the simultaneous measurements of $^{15}N/^{14}N$, $^{17}O/^{16}O$ and $^{18}O/^{16}O$ of nitrate. New isotopic references have been made and encompass the isotopic range of environmental samples, this eliminates the need to extrapolate calibration curves and helps reduce error. Linearities and offsets were observed amongst all isotope values and therefore it is important to bracket samples within the desired ranges of references to obtain proper calibration. Also, the importance of consistent NO_3^- sample size during analysis to further eliminate errors as different sample sizes yield different isotopic values for the same sample of interest, and while this can be corrected for by a linearity correction, it should be avoided. Pre-concentration of nitrate samples using evaporation methods has been proven to have minimal effects on isotopic values provided that samples are neutralized.

This method has been used to analyze atmospheric nitrate (aerosols and precipitation), synthetic fertilizers and soil extracts in order to constrain nitrate sources

utilized in the dual isotope approach as well as the development of a three isotope mixing model approach. While measured nitrate source isotopic values ($\delta^{15}N$ and $\delta^{18}O$) from this study fell within the range of those previously published, they had a narrower range. Previously published values have likely lead to the underestimation of atmospheric nitrate contributions. These new values will lead to better separation between sources and also allows for more accurate isotopic values for studies conducted outside of forested and coastal regions. However, there is still the chance that deconvoluting original sources will be difficult due to mixing of sources or processing. Here we presented the use of the triple oxygen isotope composition ($\Delta^{17}O$) and developed a three isotope mixing model approach to better allow for better separation of nitrate sources.

These NO_3^- source constraints and mixing models have been used in a case study to determine the effects of urbanization on the coupled nitrogen hydrologic cycle in the semi-arid urban city of Tucson, AZ. It was found that, contrary to an abundant amount of literature, variations in atmospherically derived NO_3^- was not controlled by changes in NO_x source emissions but rather by shifts in meteorological conditions and atmospheric chemistry. This has important implications for environmental policy specifically regarding emission reduction. Previous studies, which have saturated the literature, suggest NO_x source emissions caused variations in atmospherically derived NO_3^- and have also suggested that $\delta^{15}N$ can be used to monitor progress toward NO_x stationary source reduction goals. Previous studies, which have saturated the literature, suggest NO_x source emissions caused variations in atmospherically derived NO_3^- and have also suggested that $\delta^{15}N$ can be used to monitor progress toward NO_x stationary source reduction goals. However, these studies do not take into consideration local atmospheric

chemistry and even with NO_x emission reduction it is unlikely that these variations will change since it is possible that local isotopic exchange will 'erase' any individual NO_x emission isotopic signatures.

We show conclusively for the first time, in semi-arid urban environments, the fractional contributions of atmospherically versus biologically derived nitrate. Urban runoff showed a significant fraction of atmospherically derived NO_3^- from all catchments with higher fractions from more impervious catchments and lower from non-urban catchments. Our results are in agreement with the previous "build and flush" model for both nitrate fractions. It was observed that during dry periods, atmospheric nitrate was depositing and accumulating on surfaces and biologic nitrate (produced via nitrification) in soils as well and were subsequently flushed to waterways following the next rainfall/runoff event. The results presented here suggest increased impervious surface area allows for more atmospheric NO_3^- to reach urban waterways due to inefficient N cycling within the catchment. Whereas, increased soil surfaces in catchments allows for nitrification and therefore atmospheric NO_3^- deposition is not as dominant. The continued urban sprawl and further modification of ephemeral streams to augment a limited water supply in semi-arid regions will continue to modify N cycling.

Future research needs include determining the degree of isotopic inter-storm spatial variation and intra-storm variation of precipitation of NO_3^-. The high degree of observed variation over the monsoon season during this study was not expected nor has any other study presented similar results. This is mainly due to previous studies examining atmospheric NO_3^- (precipitation or aerosols) utilize existing monitoring networks (*e.g.* NADP, CASNET) which do not collect at the high resolutions (spatially

and temporally) in which we have presented here and therefore the isotopic signatures would have been diluted out. Also, many N biogeochemical studies also rely on these monitoring networks or if precipitation sampling occurs they do not collect at the high resolutions. These large variations, if not unique to monsoonal systems, have likely led to large over/underestimations of atmospheric contributions.

BIBLIOGRAPHY

Abe, O. and N. Yoshida, Partial pressure dependency of $^{17}O/^{16}O$ and $^{18}O/^{16}O$ of molecular oxygen in the mass spectrometer, *Rapid Comm. Mass Spectrom., 17*, 395-400, 2003.

Adams, M. B., Ecological issues related to N deposition to natural ecosystems: research needs, *Environment International, 29*(2-3), 189-199, 2003.

Alexander, B., M. G. Hastings, D. J. Allman, J. Dachs, J. A. Thornton and S. A. Kunasek, Quantifying atmospheric nitrate formation pathways based on a global model of the oxygen isotopic composition ($\Delta^{17}O$) of atmospheric nitrate, *Atmos. Chem. Phys., 9*(14), 5043-5056, 2009.

Allen, E. B., L. E. Rao, R. J. Steers, A. Bytnerowicz and M. E. Fenn, Impacts of atmospheric nitrogen deposition on vegetation and soils in Joshua Tree National Park, in The Mojave Desert: Ecosystem Processes and Sustainability., edited by R. H. Webb, L. F. Fenstermaker, J. S. Heaton, D. L. Hughson, E. V. McDonald and D. M. Miller, University of Nevada Press, Las Vegas, NV, 2009.

Ammann, M., R. Siegwolf, F. Pichlmayer, M. Suter, M. Saurer and C. Brunold, Estimating the uptake of traffic-derived NO_2 from ^{15}N abundance in Norway spruce needles, *Oecologia, 118*(2), 124-131, 1999.

Amoroso, A., F. Domine, G. Esposito, S. Morin, J. Savarino, M. Nardino, M. Montagnoli, J. M. Bonneville, J. C. Clement, A. Ianniello and H. J. Beine, Microorganisms in Dry Polar Snow Are Involved in the Exchanges of Reactive Nitrogen Species with the Atmosphere, *Environ. Sci. Technol., 44*, 714-719, 2010.

Anderson, I. C. and J. S. Levine, Relative rates of nitric oxide and nitrous oxide by nitrifiers, denitrifiers, and nitrate respirers, *Appl. Environ. Microbiol., 51*, 938-945, 1986.

Andersson, K. K. and A. B. Hooper, O_2 and H_2O are each the source of one O in NO_2^- produced from NH_3 by Nitrosomonas: ^{15}N-NMR evidence, *FEBS Lett., 164*, 236-240, 1983.

Appl, M., Ammonia, 2. Production Processes, in Ullmann's Encyclopedia of Industrial Chemistry, Wiley-VCH, 2011.

Arnold, C. L. and C. J. Gibbons, Impervious surface coverage - the emergence of a key environmental indicator, *J. Am. Plan. Assoc., 62*(2), 243-258, 1996.

Austin, A. T., L. Yahdjian, J. M. Stark, J. Belnap, A. Porporato, U. Norton, D. A. Ravetta and S. M. Schaeffer, Water Pulses and Biogeochemical Cycles in Arid and Semiarid Ecosystems, *Oecologia, 141*(2), 221-235, 2004.

Bacsi, A., B. K. Choudhury, N. Dharajiya, S. Sur and I. Boldogh, Subpollen particles: Carriers of allergenic proteins and oxidases, *J. Allergy Clin. Immunol., 118*(4), 844-850, 2006.

Barford, C. C., J. P. Montoya, M. A. Altabet and R. Mitchell, Steady-State Nitrogen Isotope Effects of N_2 and N_2O Production in Paracoccus denitrificans, *Appl. Environ. Microbiol., 65*(3), 989-994, 1999.

Barnes, R. T., P. A. Raymond and K. L. Casciotti, Dual Isotope Analyses Indicate Efficient Processing of Atmospheric Nitrate by Forested Watersheds in the Northeastern U.S., *Biogeochemistry, 90*(1), 15-27, 2008.

Bergersen, F. J., G. L. Turner, N. Amarger, F. Mariotti and A. Mariotti, Strain of Rhizobium lupini determines natural abundance of 15N in root nodules of Lupinus spp, *Soil Biol. Biochem., 18*(1), 97-101, 1986.

Bigeleisen, J., The effects of isotopic substitiution on the rates of chemical reactions, *J. Phys. Chem., 56*(7), 823-828, 1952.

Bigeleisen, J., Chemistry of Isotopes, *Science, 147*(3657), 463-471, 1965.

Boettcher, J., O. Strebel, S. Voerkelius and H. L. Schmidt, Using isotope fractionation of nitrate-nitrogen and nitrate-oxygen for evaluation of microbial denitrification in a sandy aquifer, *J. Hydrol., 114*(3-4), 413-424, 1990.

Bohlke, J. K., G. E. Ericksen and K. Revesz, Stable isotpe evidence for an atmospheric origin of desert nitrate deposits in northern Chile and southern Califonia, USA, *Chem. Geol., 136*(135), 152, 1997.

Bohlke, J. K., S. J. Mroczkowski and T. B. Coplen, Oxygen isotopes in nitrate: new reference materials for ^{18}O:^{17}O:^{16}O measurements and observations on nitrate-water equilibration, *Rapid Comm. Mass Spectrom., 17*, 1835-1846, 2003.

Bothe, H., S. J. Ferguson and W. E. Newton, Biology of the Nitrogen Cycle, Elsevier, Amsterdam, 2007.

Bottcher, J., O. Strebel, S. Voerkelius and H. L. Schmidt, Using isotope fractionation of nitrate-nitrogen and nitrate-oxygen for evaluation of microbial denitrification in a sandy aquifer, *J. Hydrol. (Amsterdam, Neth.), 114*, 413-424, 1990.

Bowen, G. J. and J. Revenaugh, Interpolating the isotopic composition of modern meteroric precipitation, *Water Resources Research, 39*(10), 1299, 2003.

Bowen, G. J. and B. Wilkinson, Spatial distribution of $\delta^{18}O$ in meteoric precipitation, *Geology, 30*(4), 315-318, 2002.

Brand, W. A., Mass Spectrometer Hardware for Analyzing Stable Isotope Ratios, in Handbook of Stable Isotope Analytical Techniques, edited by P.A.de Groot, pp. 835-856, 2004.

Bremmer, J. M. and A. M. Blackmer, Nitrous oxide: emission from soils during nitrification of fertilizer nitrogen, *Science, 199*, 295-296, 1978.

Brown, S. S., T. B. Ryerson, A. G. Wollny, C. A. Brock, R. Peltier, A. P. Sullivan, R. J. Weber, W. P. Dube, M. Trainer, J. F. Meagher, F. C. Fehsenfeld and A. R. Ravishankara, Variability in Nocturnal Nitrogen Oxide Processing and Its Role in Regional Air Quality, *Science, 311*(5757), 67-70, 2006.

Bryan, B. A., G. Shearer, J. L. Skeeters and D. H. Kohl, Variable Expression of the Nitrogen Isotope Effect Associated with Denitrification of Nitrite, *J. Biol. Chem., 258*(14), 8613-8617, 1983.

Buchwald, C. and K. L. Casciotti, Oxygen isotopic fractionation and exchange during bacterial nitrite oxidation, *Limnol. Oceanogr., 55*(3), 1064-1074, 2010.

Bunton, C. A., E. A. Halevi and D. R. Llewellyn, Oxygen exchange between nitric acid and water. Part 1, *J. Chem. Soc.,*(0), 4913-4916, 1952.

Bunton, C. A., E. A. Halevi and D. R. Llewellyn, Oxygen exchange between nitric acid and water. Part III. Catalysis by nitrous acid, *J. Chem. Soc.,*(0), 2653-2657, 1953.

Bunton, C. A., D. R. Llewellyn and G. Stedman, Oxygen exchange between Nitrous Acid and Water, *J. Chem. Soc.,* 1959.

Burgin, A. J. and S. K. Hamilton, Have we Overemphasized the Role of Denitrification in Aquatic Ecosystems? A Review of Nitrate Removal Pathways, *Frontiers in Ecology and the Environment, 5*(2), 89-96, 2007.

Burns, D. A., E. W. Boyer, E. M. Elliott and C. Kendall, Sources and Transformations of Nitrate from Streams Draining Varying Land Uses: Evidence from Dual Isotope Analysis, *J. Environ. Qual., 38*, 1149-1159, 2009.

Campbell, J. L., M. J. Mitchell and B. Mayor, Isotopic assessment of NO_3^- and SO_4^{2-} mobility during winter in two adjacent watersheds in the Adirondack Mountains, New York, *Journal of Geophysical Research, 111*, 2006.

Carle, M. V., P. N. Halpin and C. A. Stow, Patterns of watershed urbanization and impacts on water quality, *J. Am. Water Resour. Assoc., 41*(3), 693-708, 2005.

Casciotti, K. L. and M. McIlvin, Isotopic analyses of nitrate and nitrite from reference mixtures and application to Eastern Tropical North Pacific waters, *Mar. Chem., 107*, 184-201, 2007.

Casciotti, K. L., D. M. Sigman, M. G. Hastings, J. K. Bohlke and A. Hilkert, Measurement of the Oxygen Isotopic Composition of Nitrate in Seawater and Freshwater Using the Denitrifier Method, *Anal. Chem., 74*(19), 4905-4912, 2002.

Casciotti, K. L., Inverse kinetic isotope fractionation during bacterial nitrite oxidation, *Geochimica et Cosmochimica Acta, 73*, 2061-2076, 2009.

Casciotti, K. L., M. McIlvin and C. Buchwald, Oxygen isotopic exchange and fractionation during bacterial ammonia oxidation, *Limnology and Oceanography, 55*(2), 753-762, 2009.

Casciotti, K. L., D. M. Sigman and B. B. Ward, Linking Diversity and Stable Isotope Fractionation in Ammonia-Oxidizing Bacteria, *Geomicrobiol. J., 20*, 335-353, 2003.

Chang, C. C. Y., C. Kendall, S. R. Silva, W. A. Battaglin and D. H. Campbell, Nitrate stable isotopes: tools for determining nitrate sources among different land uses in the Mississippi River Basin, *Canadian Journal of Fish Aquatic Science, 59*, 1874-1885, 2002.

Chen, D. J. Z. and K. T. B. MacQuarrie, Correlation of $\delta^{15}N$ and $\delta^{18}O$ in NO_3^- during denitrification in groundwater, *J. Environ. Eng. Sci., 4*, 221-226, 2005.

Coplen, T. B., J. A. Hopple, J. K. Bohlke, H. S. Peiser, S. E. Rieder, H. R. Krouse, K. J. R. Rosman, T. Ding, R. D. Vocke, K. M. Revesz, A. Lamberty, P. Taylor and P. De Bievre, Compilation of Minimum and Maximum Isotope Ratios of Selected Elements in Naturally Occurring Terrestrial Materials and Reagents, U.S. Department of the Interior, U.S. Geological Survey, 2002.

Crimmins, M. A. and A. C. Comrie, Interactions between antecedent climate and widfire variability across south-eastern Arizona, *Int. J. Wildland Fire, 13*, 455-466, 2004.

Criss, R. E., Principles of Stable Isotope Distribution, Oxford University Press, Inc, New York, 1999.

Crutzen, P. J., The role of NO and NO_2 in the chemistry of the troposphere and stratosphere, *Annu. Rev. Earth Planet. Sci., 7*, 443-472, 1979.

Davidson, E. S., Geohydrology and Water Resources of the Tuscon Basin, Arizona, edited by United States Geological Survey, United States Government Printing Office, Washington D.C., 1973.

Day, A., R. Valadez, S. Bronson, R. Carroll and R. Elias, 2009 Ambient Air Monitoring Five Year Network Assessment and Plan, Pima Department of Environmental Quality, Tucson, AZ, 2009.

Day, A., R. Valadez, S. Bronson, R. Carroll and R. Elias, 2011 Air Quality Summary Report for Pima County, Arizona, 2012.

Dejwakh, N. R., T. Meixner, G. Michalski and J. McIntosh, Using ^{17}O to investigate Nitrate Sources and Sinks in a Semi-Arid Groundwater System, *Environmental Science and Technology, 46*, 745-751, 2012.

Delwiche, C. C. and P. L. Steyn, Nitrogen Isotope Fractionation in Soils and Microbial Reactions, *Environ. Sci. Technol., 4*(11), 929-935, 1970.

Dentener, F. J., G. R. Carmichael, Y. Zhang, J. Lelieveld and P. J. Crutzen, Role of mineral aerosol as a reactive surface in the global troposphere, *J. Geophys. Res. : Atmos., 101*(D17), 22869-22889, 1996.

Dentener, F. J. and P. J. Crutzen, Reaction of N_2O_5 on Tropospheric Aerosols: Impact on the Global Distributions of NO_x, O_3, and OH, *J. Geophys. Res., 98*(D4), 7149-7168, 1993.

Diem, J. E. and A. C. Comrie, Allocating anthropogenic pollutant emissions over space: appliaction to ozone pollution management, *J. Environ. Manage., 63*, 425-447, 2001.

Dijkstra, F. A., D. J. Augustine, P. Brewer and J. C. von Fischer, Nitrogen cycling and water pulses in semiarid grasslands: are microbial and plant processes temperally asynchronous?, *Ecosystem Ecology, 170*, 799-808, 2012.

Draxler, R. R. and G. D. Rolph, HYSPLIT (HYbrid Single-Particle Lagrangian Integrated Trajectory) Model, NOAA Air Resources Laboratory, Silver Springs, MD, 2012.

Durka, W., E.-D. Schulze, G. Gebauer and S. Voerkelius, Effects of forest decline on uptake and leaching of deposited nitrate determined from ^{15}N and ^{18}O measurements, *Nature, 372*, 765-767, 1994.

Elliott, E. M., C. Kendall, E. W. Boyer, D. A. Burns, G. G. Lear, H. E. Golden, K. Harlin, A. Bytnerowicz, T. J. Butler and R. Glatz, Dual nitrate isotopes in dry deposition: Utility for partitioning NO_x source contributions to landscape nitrogen deposition, *Journal of Geophysical Research, 114*, 2009.

Elliott, E. M., C. Kendall, S. D. Wankel, D. A. Burns, E. W. Boyer, K. Harlin, D. J. Bain and T. J. Butler, Nitrogen Isotopes as Indicators of NO_x Source Contributions to Atmospheric Nitrate Deposition Across the Midwestern and Northeastern United States, *Environ. Sci. Technol., 41*, 7661-7667, 2007.

Ezcurra, E., Global deserts outlook, United Nations Environment Programme, Nairobi, Kenya, 2006.

Felix, J. D., E. M. Elliott and S. L. Shaw, Nitrogen Isotopic Composition of Coal-Fired Power Plant NO_x: Influence of Emission Controls and Implications for Global Emission Inventories, *Environ. Sci. Technol., 46*, 3528-3535, 2012.

Fenn, M. E., J. S. Baron, E. B. Allen, H. M. Rueth, K. R. Nydick, L. Geiser, W. D. Bowman, J. O. Sickman, T. Meixner, D. W. Johnson and P. Neitlich, Ecological Effects of Nitrogen Deposition in the Western United States, *Bioscience, 53*(4), 404-420, 2003a.

Fenn, M. E., R. Haeuber, G. S. Tonnesen, J. S. Baron, S. Grossman-Clarke, D. Hope, D. A. Jaffe, S. Copeland, L. Geiser, H. M. Rueth and J. O. Sickman, Nitrogen Emissions, Deposition, and Monitoring in the Western United States, *Bioscience, 53*(4), 391-403, 2003b.

Finlayson-Pitts, B. and J. N. Pitts, Atmospheric chemistry: fundamentals and experimental techniques, Wiley, New York, 1986.

Freyer, H. D., Seasonal-Variation of N-15-N-14 Ratios in Atmospheric Nitrate Species, *Tellus, Ser. B, 43*(1), 30-44, 1991.

Galanter, M., H. Levy and G. R. Carmichael, Impacts of biomass burning on tropospheric CO, NO_x, and O_3, *J. Geophys. Res. : Atmos., 105*(D5), 6633-6653, 2000.

Gallo, E. L., P. D. Brooks, K. A. Lohse and J. E. T. McLain, Land cover controls on summer discharge and runoff solution chemistry of semi-arid urban catchments, *Journal of Hydrology,* 2012a.

Gallo, E. L., P. D. Brooks, K. A. Lohse and J. E. T. McLain, Temporal patterns and controls on runoff magnitude and solution chemistry of urban catchments in the semiarid southwestern United States, *Hydrological Processes,* 2012b.

Gallo, E. L., K. A. Lohse, P. D. Brooks, C. M. Ferlin and T. Meixner, Physical and biological controls on biogeochemical processes of semi-arid urban ephemeral waterways, *Biogeochemistry,* 2013.

Gallo, E. L., K. A. Lohse, P. D. Brooks, J. C. McIntosh, T. Meixner and J. E. T. McLain, Quantifying the effects of stream channels on storm water quality in a semi-arid urban environment, *Journal of Hydrology, 470-471*, 98-110, 2012c.

Galloway, J. N. and E. B. Cowling, Reactive Nitrogen and The World: 200 Years of Change, *Ambio, 31*(2), 2002.

Galloway, J. N., W. H. Schlesinger, H. Levy, A. Michaels and J. L. Schnoor, Nitrogen fixation: Anthropogenic enhancement-environmental response, *Global Biogeochemical Cycles, 9*(2), 235-252, 1995.

Garcia, M., C. D. Peters-Lidard and D. C. Goodrich, Spatial interpolation of precipitation in a dense gauge network for monsoon storm events in the southwestern United States, *Water Resour. Res., 44*(5), 2008.

Gat, J. R., Oxygen and hydrogen isotopes in the hydrologic cycle, *Ann. Rev. Earth Planet. Sci., 24*, 225-262, 1996.

Gazis, C. and X. Feng, A stable isotope study of soil water: evidence for mixing and preferential flow paths, *Geoderma, 119*, 97-111, 2004.

Gelt, J., J. Henderson, K. Seasholes, B. Tellman, G. Woodard, K. Carpenter, C. Hudson and S. Sherif, Water in the Tucson Area: Seeking Sustainability, pp. 1-55, The University of Arizona, Water Resources Research Center, 1999.

Geyer, A., R. Ackermann, R. Dubois, B. Lohrmann, T. Muller and U. Platt, Long-term observation of nitrate radicals in the continental boundary layer near Berlin, *Atmos. Chem., 35*, 3619-3631, 2001.

Goodale, C. L., S. A. Thomas, G. Fredriksen, E. M. Elliott, K. M. Flinn, T. J. Butler and M. T. Walter, Unusual seasonal patterns and inferred processes of nitrogen retention in forested headwaters of the Upper Susquehanna River, *Biogeochemistry, 93*, 197-218, 2009.

Goreau, T. J., W. A. Kaplan, S. C. Wofsy, M. B. McElroy, F. W. Valois and S. W. Watson, Production of NO_2^- and N_2O by nitrifying bacteria at reduced concentrations of oxygen., *Appl. Environ. Microbiol., 40*, 526-532, 1980.

Granger, J., D. M. Sigman, J. A. Needoba and P. J. Harrison, Coupled nitrogen and oxygen isotope fractionation of nitrate during assimilation by cultures of marine phytoplankton, *Limnology and Oceanography, 49*(5), 1763-1773, 2004a.

Granger, J. and D. M. Sigman, Removal of nitrite with sulfamic acid for nitrate N and O isotope analysis with the denitrifier method, *Rapid Communications in Mass Spectrometry, 23*, 3753-3762, 2009.

Granger, J., D. M. Sigman, J. A. Needoba and P. J. Harrison, Coupled nitrogen and oxygen isotope fractionation of nitrate during assimilation by cultures of marine phytoplankton, *Limnol. Oceanogr., 49*(5), 1763-1773, 2004b.

Granger, J., D. M. Sigman, M. G. Prokopenko, M. F. Lehmann and P. D. Tortell, A method for nitrite removal in nitrate N and O isotope analyses, *Limnol. Oceanogr. : Methods, 4*, 205-212, 2006.

Hall, S. J., D. Huber and N. B. Grimm, Soil N_2O and NO emissions from an arid, urban ecosystem, *J. Geophys. Res., 113*(G01016), 2008.

Hall, S. J., R. Sponseller, N. B. Grimm, D. Huber, J. P. Kaye, C. Clark and S. L. Collins, Ecosystem response to nutrient enrichment across an urban airshed in the Sonoran Desert, *Ecological Applications, 21*(3), 640-660, 2011.

Harms, T. K. and N. B. Grimm, Hot spots and hot moments of carbon and nitrogen dynamics in a semiarid riparian zone, *J. Geophys. Res., 113*(G01020), 2008.

Harrison, J. A., The Nitrogen Cycle: Of Microbes and Men, 2003.

Hastings, M. G. and D. M. Sigman, Isotopic evidence for source changes of nitrate in rain at Bermuda, *J. Geophys. Res., 108*(D24), 2003.

Hatt, B. E., T. D. Fletcher, C. J. Walsh and S. L. Taylor, The Influence of Urban Density and Drainage Infrastructure on the Concentrations and Loads of Pollutants in Small Catchments, *Environ. Manage., 34*(1), 112-124, 2004.

Heaton, T. H. E., $^{15}N/^{14}N$ ratios of NO_x from vehicle engines and coal-fired power stations, *Tellus, 42B*, 304-307, 1990.

Henry, A., M. F. Le Moal, Ph. Cardinet and A. Valentin, Overtone Bands of $^{14}N^{16}O$ and Determination of Molecular Constants, *J. Mol. Spectrosc., 70*, 18-26, 1978.

Hoch, M. P., M. L. Fogel and D. L. Kirchman, Isotope fractionation associated with ammonium uptake by a marine bacterium, *Limnol. Oceanogr., 37*(7), 1447-1459, 1992.

Hoering, T. C. and H. T. Ford, The Isotope Effect in the Fixation of Nitrogen by Azobacter, *J. Amer. Chem. Soc., 82*, 376-378, 1960.

Hogberg, P., Tansley Review No. 95: ^{15}N natural abundance in soil-plant systems, *New Phytol., 137*, 179-203, 1997.

Hollocher, T. C., Source of the oxygen atoms of nitrate in the oxidation of nitrite by Nitrobacter agilis and evidence against a P-O-N anhydride mechanism in oxidative phosphorylation, *Arch. Biochem. Biophys., 233*, 721-727, 1984.

Hooper, A. B., T. Vannelli, D. J. Bergmann and D. M. Arciero, Enzymology of the oxidation of ammonia to nitrite by bacteria, *Antonie van Leeuwenhoek, 71*, 56-67, 1997.

Horibe, Y., K. Shigehara and Y. Takakuwa, Isotopic separation factors of carbon-dioxide-water system and isotopic composition of atmospheric oxygen, *J. Geophys. Res., 78*, 2625-2629, 1973.

Jarvis, J., M. G. Hastings, E. Steig and S. A. Kunasek, Isotopic ratios in gas-phase HNO_3 and snow nitrate at Summit, Greenland, *J. Geophys. Res., 114*, 2009.

Kaiser, J., M. G. Hastings, B. Z. Houlton, T. Rockmann and D. M. Sigman, Triple Oxygen Isotope Analysis of Nitrate Using the Denitrifier Method and Thermal Decomposition of N_2O, *Anal. Chem., 79*(2), 599-607, 2007.

Kaushal, S. S., P. M. Groffman, L. E. Band, E. M. Elliott, C. A. Shields and C. Kendall, Tracking Nonpoint Source Nitrogen Pollution in Human-Impacted Watersheds, *Environmental Science and Technology, 45*, 8225-8232, 2011.

Keeney, D. R. and J. L. Hatfield, The Nitrogen Cycle, Historical Perspective, and Current and Potential Furute Concerns, in Nitrogen in the Environment: Sources, Problems, and Management, edited by R. F. Follett and J. L. Hatfield, pp. 3-16, Elsevier Science B.V., Amsterdam, 2001.

Kendall, C., Tracing nitrogen sources and cycling in catchments, in Isotope tracers in catchment hydrology, edited by C. Kendall and J. J. McDonnell, pp. 519-576, Elsevier, Amsterdam, 1998a.

Kendall, C., Tracing Nitrogen Sources and Cycling in Catchments, in Isotope Tracers in Catchment Hydrology, edited by C. Kendall and J. J. McDonnell, pp. 519-576, Elsevier Science, Amsterdam, 1998b.

Khoder, M. I., Atmospheric conversion of sulfur dioxide to particulate sulfate and nitrogen dioxide to particulate nitrate and gasous nitric acid in an urban area, *Chemosphere, 49*, 675-684, 2002.

Kool, D. M., N. Wrage, O. Oenema, C. Van Kessel and J. W. Van Groenigen, Oxygen exchange with water alters the oxygen isotopic signature of nitrate in soil ecosystems, *Soil Biology & Biochemistry, 43*, 1180-1185, 2011.

Kroopnick, P. and H. Craig, Atmospheric oxygen: Isotopic composition and solubility fractionation, *Science, 175*, 54-55, 1972.

Kumar, S., D. J. D. Nicholas and E. H. Williams, Definitive ^{15}N NMR evidence that water serves as a source of 'O' during nitrite oxidation by Nitrobacter agilis, *FEBS Lett., 152*(1), 71-74, 1983.

Kuroiwa, M., K. Koba, K. Isobe, R. Tateno, A. Nakanishi, Y. Inagaki, H. Toda, S. Otsuka, K. Senoo, Y. Suwa, M. Yoh, R. Urakawa and H. Shibata, Gross nitrification rates in four Japanese forest soils: heterotrophic versus autotrophic and the regulation factors for the nitrification, *J. For. Res., 16*, 363-373, 2011.

Lassey, D. and N. Harvey, Nitrous oxide: the serious side of laughing gas, *Water Atmosph., 15*(10), 11, 2007.

Ledgard, S. F., Nutrition, moisture and rhizobial strain influence isotopic fractionation during N_2 fixation in pasture legumes, *Soil Biol. Biochem., 21*(1), 65-68, 1989.

Leighton, P. A., Photochemistry of air pollution, Academic Press, New York, 1961.

Lewis, D. B. and N. B. Grimm, Hierarchical regulation of nitrogen export from urban catchments: interactions of storms and landscapes, *Ecological Applications, 17*(8), 2347-2364, 2007.

Li, D. and X. Wang, Nitrogen isotopic signature of soil-released nitric oxide (NO) after fertilizer application, *Atmos. Environ., 42*, 4747-4754, 2008.

Lohse, K. A., D. Hope, R. Sponseller, J. O. Allen and N. B. Grimm, Atmospheric deposition of carbon and nutrients across an arid metropolitan area, *Science of the Total Environment, 402*, 95-105, 2008.

Lovett, G. M., C. G. Jones, M. G. Turner and K. C. Weathers, Ecosystem Function in Heterogeneous Landscapes, Springer, New York, 2005.

Luz, B. and E. Barkan, The isotopic ratios $^{17}O/^{16}O$ and $^{18}O/^{16}O$ in molecular oxygen and their significance in biogeochemistry, *Geochim. Cosmochim. Acta, 69*(5), 1099-1110, 2005.

Luz, B., E. Barkan, M. L. Bender, M. H. Thiemens and K. A. Boering, Triple-isotope composition of atmospheric oxygen as a tracer of biosphere productivity, *Nature, 400*, 547-550, 1999.

Malm, W. C., D. E. Day, S. M. Kreidenweis, J. L. Collett and T. Lee, Humidity-dependent optical properties of fine particles during the Big Bend Regional Aerosol and Visibility Observational Study, *J. Geophys. Res., 108*(D9), 4279, 2003.

Malm, W. C., M. L. Pitchford, C. McDade and L. L. Ashbaugh, Coarse particle speciation at selected locations in the continental United States, *Atmos. Environ., 41*, 2225-2239, 2007.

Mariotti, A., J. C. Germon, P. Hubert, P. Kaiser, R. Letolle, A. Tardieux and P. Tardieux, Experimental determination of nitrogen kinetic isotope fractionation: some principles; illustration for the denitrification and nitrification processes, *Plant Soil, 62*, 413-430, 1981.

Matichuk, R., B. Barbaris, E. A. Betterton, M. Hori, N. Murao, S. Ohta and D. Ward, A Decade of Aerosol and Gas Precursor Chemical Characterization at Mt. Lemmon, Arizona (1992 to 2002), *J. Meteorol. Soc. Jpn., 84*(4), 653-670, 2006.

Mayer, B., S. M. Bollwerk, T. Mansfeldt, B. Hutter and J. Veizer, The oxygen isotope composition of nitrate generated by nitrification in acid forest floors, *Geochim. Cosmochim. Acta, 65*(16), 2743-2756, 2001.

Mayer, B., E. W. Boyer, C. L. Goodale, N. A. Jaworski, N. Van Breemen, R. W. Howarth, S. Seitzinger, G. Billen, K. Lajtha, K. Nadelhoffer, D. Van Dam, L. J. Hetling, M. Nosal and K. Paustian, Sources of nitrate in rivers draining sixteen watersheds in the northeastern U.S.: Isotopic constraints, *Biogeochemistry, 57/58*, 171-197, 2002.

McCalley, C. K. and J. P. Sparks, Controls over Nitric Oxide and Ammonia Emissions from Mojave Desert Soils, *Oecologia, 156*(4), 871-881, 2008.

McCrackin, M. L., T. K. Harms, N. B. Grimm, S. J. Hall and J. P. Kaye, Responses of Soil Microorganisms to Resource Availability in Urban, Desert Soils, *Biogeochemistry, 87*(2), 143-155, 2008.

Meador, T. B., L. I. Aluwihare and C. Mahaffey, Isotopic heterogeneity and cycling of organic nitrogen in the oligotrophic ocean, *Limnol. Oceanogr., 52*(3), 934-947, 2007.

Meijer, H. A. J. and W. J. Li, The Use of Electrolysis for Accurate $\delta^{17}O$ and $\delta^{18}O$ Isotope Measurements in Water, *Isoto. Envir. Health Stud., 34*(4), 349-369, 1998.

Michalski, G., T. Meixner, M. Fenn, L. Hernandez, A. Sirulnik, E. Allen and M. Thiemens, Tracing atmospheric nitrate deposition in a complex semiarid ecosystem using $\Delta^{17}O$, *Envir. Sci. Tech., 38*(7), 2175-2181, 2004a.

Michalski, G., Z. Scott, M. Kabiling and M. Thiemens, First Measurements and Modeling of $\Delta^{17}O$ in Atmospheric Nitrate, *Geophys. Res. Lett., 30*(16), (1870), 2003a.

Michalski, G. M., Purification procedure for $\delta^{15}N$, $\delta^{18}O$, $\Delta^{17}O$ analysis of nitrate, *Int. J. Environ. Anal. Chem., 90*(7), 586-590, 2010.

Michalski, G. M., R. Jost, D. Sugny, M. Joyeux and M. Thiemens, Dissociation energies of six NO2 isotopologues by laser induced flourescence spectroscopy and zero point energy of some triatomic molecules, *J. Chem. Phys., 121*(15), 7153-7161, 2004b.

Michalski, G., J. G. Bockheim, C. Kendall and M. Thiemens, Isotopic Composition of Antarctic Dry Valley nitrate: Implications for NO_y sources and cycling in Antarctica, *Geophys. Res. Lett., 32*, 2005.

Michalski, G., J. K. Bohlke and M. Thiemens, Long term atmospheric deposition as the source of nitrate and other salts in the Atacama Desert, Chile: New evidence from mass-independent oxygen isotopic compositions, *Geochimica et Cosmochimica Acta, 68*(20), 4023-4038, 2004c.

Michalski, G., T. Meixner, M. Fenn, L. Hernandez, A. Sirulnik, E. Allen and M. Thiemens, Tracing Atmospheric Nitrate Deposition in a Complex Semiarid Ecosystem Using $\Delta^{17}O$, *Environ. Sci. Technol., 38*(7), 2175-2181, 2004d.

Michalski, G. and K. Riha, Spatial and temporal variations in oxygen isotopes during ammonia oxidation: Isoscapes of nitrification, *in review* .

Michalski, G., J. Savarino, J. K. Bohlke and M. Thiemens, Determination of the Total Oxygen Isotopic Composition of Nitrate and the Calibration of a $\Delta^{17}O$ Nitrate Reference Material, *Anal. Chem., 74*, 4989-4993, 2002.

Michalski, G., Z. Scott, M. Kabiling and M. Thiemens, First Measurements and Modeling of $\Delta^{17}O$ in Atmospheric Nitrate, *Geophys. Res. Lett., 30*(16), 2003b.

Miller, D. A. and R. A. White, A Conterminous United States Multi-Layer Soil Characteristics Data Set for Regional Climate and Hydrology Modeling, 1998.

Miller, M. F., Isotopic fractionation and the quantification of O-17 anomalies in the oxygen three-isotope system: an appraisal and geochemical significance, *Geochim. Cosmochim. Acta, 66*, 1881-1889, 2002a.

Miller, M. F., Isotopic fractionation and the quantification of O-17 anomalies in the oxygen three-isotope system: an appraisal and geochemical significance, *Geochim. Cosmochim. Acta, 66*(11), 1881-1889, 2002b.

Monn, C., Exposure assessment of air pollutants: a review on spatial heterogeneity and indoor/outdoor/personal exposure to suspended particulate matter, nitrogen dioxide and ozone, *Atmos. Environ., 35*, 1-32, 2001.

Moore, H., The Isotopic Composition of Ammonia, Nitrogen Dioxide and Nitrate in Atmosphere, *Atmos. Environ. (1967-1989), 11*(12), 1239-1243, 1977.

Morin, E., D. C. Goodrich, R. A. Maddox, X. Gao, H. V. Gupta and S. Sorooshian, Spatial patterns in thunderstorm rainfall events and their coupling with watershed hydrological response, *Adv. Water Resour., 29*(6), 843-860, 2006.

Morin, S., J. Erbland, J. Savarino, F. Domine, J. Bock, U. Friess, H. W. Jacobi, H. Sihler and M. F. Martins, An isotopic view on the connection between photolytic emissions of NO_x from the Arctic snowpack and its oxidation by reactive halogens, *J. Geophys. Res., 117*, 2012.

Morin, S., J. Savarino, M. M. Frey, F. Domine, H. W. Jacobi, L. Kaleschke and J. M. F. Martins, Comprehensive isotopic composition of atmospheric nitrate in the Atlantic Ocean boundary layer from 65° S to 79° N, *J. Geophys. Res., 114*, 2009.

Morin, S., J. Savarino, M. M. Frey, N. Yan, S. Bekki, J. W. Bottenheim and J. M. F. Martins, Tracing the Origin and Fate of NO_x in the Arctic Atmosphere Using Stable Isotopes in Nitrate - Supporting Online Material, *Science, 322*(730), 2008.

Needoba, J. A. and P. J. Harrison, Influence of low light and a light:dark cycle on NO_3^- uptake, intracellular NO_3^-, and nitrogen isotope fractionation by marine phytoplankton, *J. Phycol., 40*, 505-516, 2004.

Norman, L. M., M. Feller and D. P. Guertin, Forecasting urban growth across the United States-Mexico border, *Comput. Environ. Urban Syst., 33*(2), 150-159, 2009.

Norton, J. M. and J. M. Stark, Regulation and Measurement of Nitrification in Terrestrial Systems, in Methods in Enzymology, edited by M. G. Klotz, pp. 343-368, Academic Press, Burlington, 2011.

O'Rourke, M. K., Comparative pollen calendars from Tucson, Arizona: Durham vs. Burkard samplers, *Aerobiologia, 6*(2), 136-140, 1990.

Ostrom, N. E., A. Pitt, R. Sutka, P. H. Ostrom, A. S. Grandy, K. M. Huizinga and G. P. Robertson, Isotopologue effects during N_2O reduction in soils and in pure cultures of denitrifiers, *J. Geophys. Res., 112*(G2), 2007.

Ostwald, W., Improvements in the Manufacture of Nitric Acid and Nitrogen Oxides, 1902.

Pardo, L. H., C. Kendall, J. Pett-Ridge and C. C. Y. Chang, Evaluating the source of streamwater nitrate using $\delta^{15}N$ and $\delta^{18}O$ in nitrate in two watersheds in New Hampshire, USA, *Hydrological Processes, 18*, 2699-2712, 2004.

Pearson, J., D. M. Wells, K. J. Seller, A. Bennett, A. Soares, J. Woodall and M. J. Ingrouille, Traffic exposure increases natural ^{15}N and heavy metal concentrations in mosses, *New Phytol., 147*(2), 317-326, 2000.

Pima County Department of Environmental Quality (PDEQ), Environmental Monitoring for Public Access and Community Tracking (EMPACT), 2012.

Pope, C. A. and D. W. Dockery, Health Effects of Fine Particulate Air Pollution: Lines that Connect, *J. Air Waste Manage. Assoc., 56*, 709-742, 2006.

Poth, M., Dinitrogen production from nitrite by a Nitrosomonas isolate, *Appl. Environ. Microbiol., 52*, 957-959, 1986.

Prinn, R., D. Cunnold, P. Simmonds, F. Alyea, R. Boldi, A. Crawford, P. Fraser, D. Gutzler, D. Hartley, R. Rosen and R. Rasmussen, Global Average Concentration and Trend for Hydroxyl Radicals Deduced From ALE/GAGE Trichloroethane (Methyl Chloroform) Data for 1978-1990, *J. Geophys. Res., 97*(D2), 2445-2461, 1992.

PRISM Climate Group, U.S. Maximum Temperature Normals, Oregon State University, 2004.

Prosser, J. I., Soil Nitrifiers and Nitrification, in Nitrification, edited by B. B. Ward, D. J. Arp and M. G. Klotz, pp. 347-362, American Society for Microbiology, 2011.

Rabalais, N. N., Nitrogen in Aquatic Ecosystems, *Ambio., 31*(2), 102-112, 2002.

Rantio-Lehtimaeki, A., M. Viander and A. Koivikko, Air-borne birch pollen antigens in difference particle sizes, *Clinical and Experimental Allergy, 24*, 23-28, 1994.

Rao, L. E., D. R. Parker, A. Bytnerowicz and E. B. Allen, Nitrogen mineralization across an atmospheric nitrogen depostion gradient in Southern California deserts, *Journal of Arid Environments, 73*, 920-930, 2009.

Ravishankara, A. R., J. S. Daniel and R. W. Portman, Nitrous oxide (N_2O): the dominant ozone-depleting substance emitted in the 21st century, *Science, 326*(123), 125, 2009.

Reddy, K. R., W. H. Patrick and F. E. Broadbent, Nitrogen transformations and loss in flooded soils and sediments, *CRC Critical Reviews in Environmental Control, 13*(4), 273-309, 1984.

Richardson, D., H. Felgate, N. Watmough, A. Thomson and E. Baggs, Mitigating release of the potent greenhouse gas N_2O from the nitrogen cycle: could enzymic regulation hold the key?, *Trends Biotechnol., 27*, 388-397, 2009.

Richet, P., Y. Bottinga and M. Javoy, A review of hydrogen, carbon, nitrogen, oxygen, sulphur, and chlorine stable isotope fractionation among gaseous molecules, *Annu. Rev. Earth Planet. Sci., 5*, 65-110, 1977.

Riemer, N., H. Vogel, B. Vogel, B. Schell, I. Ackermann, C. Kessler and H. Hass, Impact of the heterogeneous hydrolysis of N_2O_5 on chemistry and nitrate aerosol formation in the lower troposphere under photosmog conditions, *Journal of Geophysical Research, 108*(D4), 4144, 2003.

Riha, K., M. Z. King and G. Michalski, Standardization of $\Delta^{17}O$ and $\delta^{15}N$ using the denitrifer method and gold tube thermal decomposition, *in review*.

Saetre, P. and J. M. Stark, Microbial Dynamics and Carbon and Nitrogen Cycling following Re-Wetting of Soils beneath Two Semi-Arid Plant Species, *Oecologia, 142*(2), 247-260, 2005.

Sebestyen, S. D., E. W. Boyer, J. B. Shanley, C. Kendall, D. H. Doctor, G. R. Aiken and N. Ohte, Sources, transformations, and hydrological processes that control stream nitrate and dissolved organic matter concentrations during snowmelt in an upland forest, *Water Resources Research, 44*, 2008.

Sebilo, M., G. Billen, M. Grably and A. Mariotti, Isotopic composition of nitrate-nitrogen as a marker of riparian and benthic denitrification at the scale of the whole Seine River system, *Biogeochemistry, 63*(1), 35-51, 2003a.

Sebilo, M., G. Billen, M. Grably and A. Mariotti, Isotopic composition of nitrate-nitrogen as a marker of riparian and benthic denitrification at the scale of the whole Seine River system, pp. 35-51, 2003b.

Seinfeld, J. H. and S. N. Pandis, Atmospheric Chemistry and Physics: From Air Pollution to Climate Change, John Wiley & Sons, Inc, Hoboken, New Jersey, 2006.

Sharma, B. and R. C. Ahlert, Nitrification and Nitrogen Removal, *Water Research, 11*, 897-925, 1977.

Sharma, H. D., R. E. Jervis and K. Y. Wong, Isotopic Exchange Reactions in Nitrogen Oxides, *J. Phys. Chem., 74*(4), 923-933, 1970.

Sigman, D. M., K. L. Casciotti, M. Andreani, C. Barford, M. Galanter and J. K. Bohlke, A Bacterial Method for the Nitrogen Isotopic Analysis of Nitrate in Seawater and Freshwater, *Anal. Chem., 73*(17), 4145-4153, 2001.

Sillman, S., The relation between ozone, NO_x, and hydrocarbons in urban and polluted rural environments, *Atmos. Environ., 33*, 1821-1845, 1999.

Singh, H. B., Reactive nitrogen in the troposphere Chemistry and transport of NO_x and PAN, *Environ. Sci. Technol., 21*(4), 1987.

Snider, D. M., J. Spoelstra, S. L. Schiff and J. J. Venkiteswaran, Stable Oxygen Isotope Ratios of Nitrate Produced from Nitrification: ^{18}O-Labeled Water Incubations of Agricultural and Temperate Forest Soils, *Environ. Sci. Technol., 44*, 5358-5364, 2010.

Socolow, R. H., Nitrogen management and the future of food: lessons from the management of energy and carbon, *Proc. Natl. Acad. Sci., 96*, 6001-6008, 1999.

Solomon, W. R., H. A. Burge and M. L. Muilenberg, Allergen carriage by atmospheric aerosol. I: Ragweed pollen determinants in smaller micron fractions, *J. Allergy Clin. Immunol., 72*, 443-447, 1983.

Sorooshian, A., A. Wonaschutz, E. G. Jarjour, B. I. Hashimoto, B. A. Schichtel and E. A. Betterton, An aerosol climatology for a rapidly growing arid region (southern Arizona): Major aerosol species and remotely sensed aerosol properties, *J. Geophys. Res., 116*, 2011.

Spieksma, F. Th. M., Evidence of grass-pollen allergenic activity in the smaller micronic atmospheric aerosol fraction, *Clinical and Experimental Allergy, 20*, 273-280, 1990.

Spieksma, F. Th. M., B. H. Nikkels and J. H. Dijkman, Seasonal appearance of grass pollen allergen in natural paucimicronic aerosol of various size fractions. Relationship with airbourne grass pollen concentrations., *Clinical and Experimental Allergy, 25*, 234-239, 1995.

Spoelstra, J., S. L. Schiff, R. J. Elgood, R. G. Semkin and D. S. Jeffries, Tracing the Sources of Exported Nitrate in the Turkey Lakes Watershed Using $^{15}N/^{14}N$ and $^{18}O/^{16}O$ isotopic ratios, *Ecosystems, 4*, 536-544, 2001.

Spoelstra, J., S. L. Schiff, D. S. Jeffries and R. G. Semkin, Effect of Storage on the Isotopic Composition of Nitrate in Bulk Precipitation, *Environ. Sci. Technol., 38*, 4723-4727, 2004.

Stark, J. M., Modeling the Temperature Response of Nitrification, *Biogeochemistry, 35*(3), 433-445, 1996.

Stark, J. M. and S. C. Hart, High rates of nitrification and nitrate turnover in undisturbed coniferous forests, *Nature, 385*(6611), 61-64, 1997.

Steele, K. W., P. M. Bonish, R. M. Daniel and G. W. O'Hara, Effect of Rhizobial Strain and Host Plant on Nitrogen Isotopic Fractionation in Legumes, *Plant Physiology, 72*(4), 1001-1004, 1983.

Sullivan, B. W., P. C. Selmants and S. C. Hart, New evidence that high potential nitrification rates occur in soils during dry seasons: Are microbial communities metabolically active during dry seasons?, *Soil Biology and Biogeochemistry, 53*, 28-31, 2012.

Sullivan, R. C., S. A. Guazzotti, D. A. Sodeman and K. A. Prather, Direct observations of the atmospheric processing of Asian mineral dust, *Atmos. Chem. Phys., 7*, 1213-1236, 2007.

Syed, K. H., D. C. Goodrich, D. E. Myers and S. Sorooshian, Spatial characteristics of thunderstorm rainfall fields and their relation to runoff, *J. Hydrol., 271*(1-4), 1-21, 2003.

Teffo, J. L., A. Henry, Ph. Cardinet and A. Valentin, Determination of Molecular Constrants of Nitric Oxide from (1-0), (2-0), (3-0) Bands of the $^{15}N^{16}O$ and $^{15}N^{18}O$ Isotopic Species, *J. Mol. Spectrosc., 82*, 348-363, 1980.

Thiemens, M. H., History and Applications of Mass-Independent Isotope Effects, *Annu. Rev. Earth Planet. Sci., 34*, 217-262, 2006.

Thiemens, M. H. and J. E. Heidenreich, The Mass-Independent Fractionation of Oxygen: A Novel Isotope Effect and its Possible Cosmochemical Implications, *Science, 219*(4588), 1073-1075, 1983.

Tilman, D., D. Wedin and J. Knops, Productivity and sustainability influenced by biodiversity in grassland ecosystems, *Nature, 379*, 1996.

U.S.Census Bureau, 2010 MSA Business Patterns (NAICS), 2010.

U.S.Census Bureau, Tucson, Arizona, 2012.

U.S.Environmental Protection Agency, Inorganic Chemical Industry, in Compilation of Air Pollutant Emission Factors - AP 42, U.S.Environmental Protection Agency, Washington D.C., 1995.

U.S.Environmental Protection Agency, National Ambient Air Quality Standards (NAAQS), 2012a.

U.S.Environmental Protection Agency, The National Emissions Inventory, 2012b.

Venterea, R. T. and D. E. Rolston, Mechanistic modeling of nitrite accumulation and nitrogen oxide gas emissions during nitrificaiton, *J. Environ. Qual., 29*, 1741-1751, 2000.

Vitousek, P. M., J. D. Aber, R. W. Howarth, G. E. Likens, P. A. Matson, D. W. Schindler, W. H. Schlesinger and D. G. Tilman, Human Alteration of the Global Nitrogen Cycle: Sources and Consequences, *Ecological Applications, 7*(3), 737-750, 1997.

Wankel, S. D., Y. Chen, C. Kendall, A. Post and A. Paytan, Sources of aerosol nitrate to the Gulf of Aqaba: Evidence from $\delta^{15}N$ and $\delta^{18}O$ of nitrate and trace metal chemistry, *Mar. Chem., 120*(1-4), 90-99, 2010.

Waser, N. A., K. Yin, Z. Yu, K. Tada, P. J. Harrison, D. H. Turpin and S. E. Calvert, Nitrogen isotope fractionation during nitrate, ammonium and urea uptake by marine diatoms and coccolithophores under various conditions of N availability, *Mar. Ecol. Prog. Ser., 169*, 29-41, 1998.

Wassenaar, L. I., Evaluation of the origin and fate of nitrate in the Abbotsford Aquifer using the isotopes of ^{15}N and ^{18}O in NO_3^-, *Appl. Geochem., 10*, 391-405, 1995.

Welter, J. R., S. G. Fisher and N. B. Grimm, Nitrogen transport and retention in an arid land watershed: influence of storm charateristics on terrestiral-aquatic linkages, *Biogeochemistry, 76*, 421-440, 2005.

Westerling, A. L., H. G. Hidalgo, D. R. Cayan and T. W. Swetnam, Warming and Earlier Spring Increase Western U.S. Forest Wildfire Activity, *Science, 313*, 2006.

Williams, M. W., J. S. Baron, N. Caine, R. Sommerfeld and R. Sanford, Nitrogen Saturation in the Rocky Mountains, *Environmental Science and Technology, 30*, 640-646, 1996.

Williard, K. W. J., D. R. DeWalle, P. J. Edwards and W. E. Sharpe, ^{18}O isotopic separation of stream nitrate sources in mid-Appalachian forested watersheds, *Journal of Hydrology, 252*, 174-188, 2001.

Wright, W. E., δD and $\delta^{18}O$ in Mixed Conifer Systems in the U.S. Southwest: The Potential of $\Delta^{18}O$ in Pinus ponderosa Tree Rings as a Natural Environmental Recorder, PhD The University of Arizona, Ann Arbor, MI, 2001.

Yoshida, N., ^{15}N-depleted N_2O as a product of nitrification, *Nature, 355*(528), 529, 1988.

APPENDIX: SUPPLEMENTARY DATA CHAPTER 5

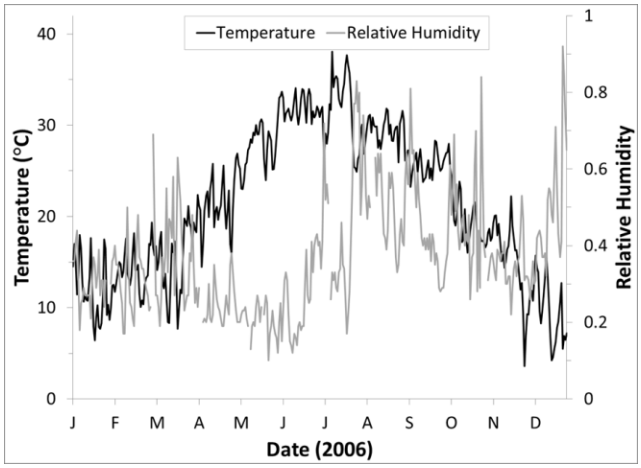

Figure A5.1. Daily average temperature (°C) and daily average relative humidity data for sampling period.

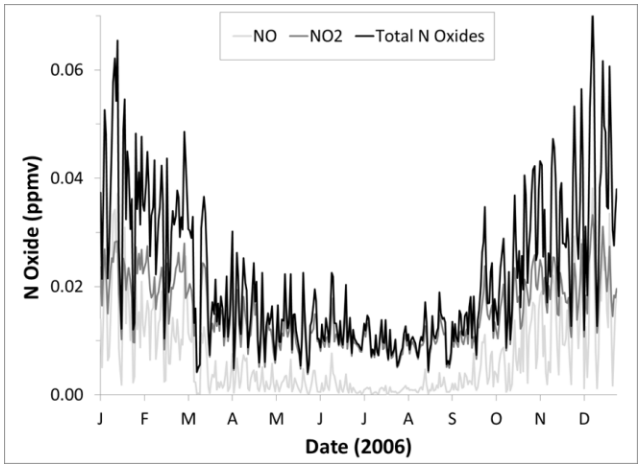

Figure A5.2. Prominent seasonal trends in monitored NO, NO_2 and Total N Oxides, with higher concentrations during the winter compared to summer, at the aerosol collection site.

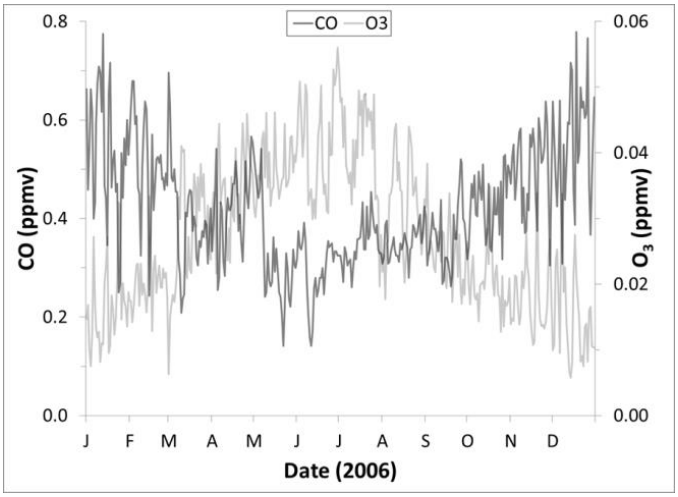

Figure A5.3. Noticeable seasonal trends in monitored CO and O_3 at the aerosol collection site. Higher concentrations of CO were observed in the winter compared to summer due to temperature inversion layers and inhibited vertical mixing. Whereas, higher concentrations of O_3 were detected in the summer compared to winter due intense sunlight and heat as well as abundance of precursor pollutants (NO_x and VOCs). The increase in CO during April corresponds to the Sand fire, just north of Tucson, which had a perimeter of 5.2km^2 and began on April 21, 2006 and was suppressed April 30, 2006.

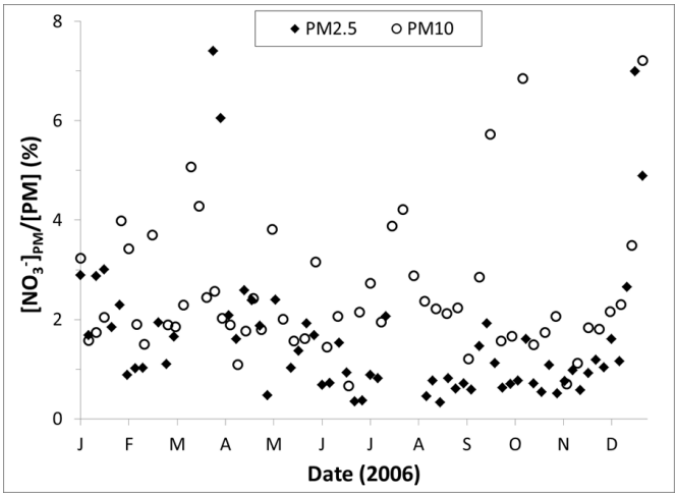

Figure A5.4. Percent $[NO_3^-]_{PM}/[PM]$, $PM_{2.5}$ (mean 1.2% ± 1.4) with less seasonal variation that PM_{10} (mean 2.5% ± 1.3). Anonymously high March $PM_{2.5}$ value of 27% removed from graph to avoid a skewed scale.

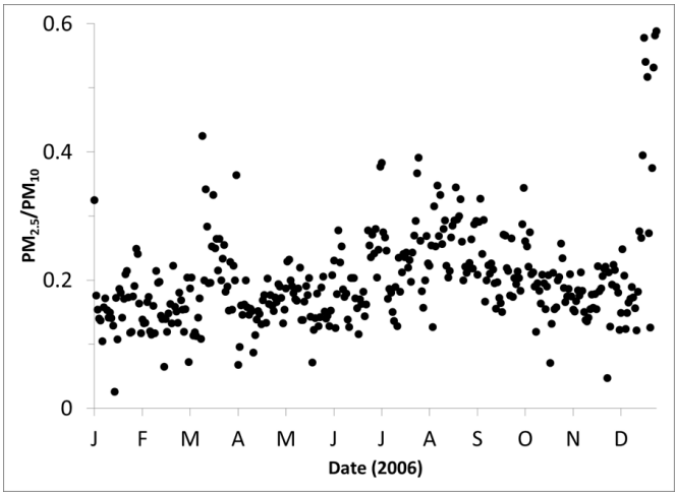

Figure A5.5. The constant ratio of $PM_{2.5}/PM_{10}$ during the dry seasons suggests that the same production mechanisms are controlling both PM fractions. Whereas, during the monsoon seasons, higher ratios are indicative of washout of predominately PM_{10}.

VITA

Krystin M. Riha

kriha@purdue.edu

Education: **PhD in Ecological Science and Engineering, May 2013**
Purdue University – West Lafayette, Indiana

Masters of Science in Chemistry, May 2008
Western Illinois University – Macomb, Illinois

Bachelor of Science in Chemistry and French, May 2006
Western Illinois University – Macomb, Illinois

Peer reviewed papers (First Author):

Riha, K.; King, M.Z.; and Michalski, G., **Standardization of $\Delta^{17}O$ and $\delta^{15}N$ using the denitrifier method and gold tube thermal decomposition.** *Rapid Communications in Mass Spectrometry* (in review).

Riha, K and Michalski, G., **Seasonal variations in NO_3^- $\delta^{15}N$ of $PM_{2.5}$ and PM_{10}: Insights into isotope exchange during NO_x chemistry**. *Environmental Science and Technology* (in review).

Riha, K.; Mase, D.; Lohse, K. A.; and Michalski, G. **Assessing seasonal changes in nitrogen oxidation pathways in the southwestern US using oxygen isotopes** *Atmospheric Environment* (in prep)

Riha, K.M.; Lohse, K.A.; Gallo, E.L.; Brooks, P.D.; Meixner, T.; and Michalski, G. **Linkages between the atmospheric and biospheric nitrogen cycles in arid urban ecosystems**. *Biogeochemistry* (in prep)

Riha, K.M.; Filley, T.R.; Dalzell, B.J.; and Michalski, G. **Effects of environmental change on carbon and nitrogen fluxes from a Midwestern agricultural watershed**. (in prep)

Peer reviewed papers (Co-Author):
Michalski. G.; Mase, D.; Riha, K.; and Waldschmidt, H. **Assessing peroxy radical chemistry and N_2O_5 uptake using oxygen isotope anomalies in atmospheric nitrate**. *Proceedings of the National Academy of Sciences – Physical Science* (in review).

Michalski, G. and Riha, K. **Spatial and temporal variations in oxygen isotopes during ammonia oxidation: Isoscapes of nitrification**. *Ecosphere* (in prep)

Michalski, G.; Li, B.; and Riha, K. **Multiple isotope mixing model for source apportionment of nitrate** *Agriculture, Ecosystems, and Environment.* (in prep)

Michalski, G.; Kolanowski, M; and Riha, K. **Triple oxygen isotope composition of fertilizer nitrate** *Environmental Science and Technology* (in prep)

Michalski, G.; Mase, D.; Riha, K.; Wang, F.; Kolanowski, M; **The global isotopic composition of nitrate in precipitation** *Atmospheric Chemistry and Physics* (in prep)
Hale R., Turnbull, L.,Earl, S., Moratto, S., Shorts, D., Grimm, NB., Michalski, G., and Riha, K. **Stormwater infrastructure effects on urban nitrogen budgets** *Biogeochemistry* (In prep)

Poster Presentations (First Author):
Riha, K.M.; Michalski, G.M.; Hale, R. L.; Earl, S.; Turnbull, L.; and Grimm, N.B. (2011) Use of Multiple Stable Isotopes to Quantify N Deposition in Arid-Urban Ecosystems, Abstract B43E-0326 presented at 2011 Fall Meeting, AGU, San Francisco, Calif. 5-9 Dec.

Riha, K.M.; Michalski, G.M.; Hale, R. L.; Earl, S.; Turnbull, L.; and Grimm, N.B. (2011) Use of Multiple Stable Isotopes to Quantify N Deposition in Arid-Urban Ecosystems. Ecological Science and Engineering Symposium. West Lafayette, IN. 2011

Riha, K.M.; Michalski, G.M.; Lohse, K.A.; Gallo, E.L.; Brooks, P.D.; and Meixner, T. (2010) Geochemical and Isotopic Composition of Aerosols in Tucson. Purdue Climate Change Research Center. West Lafayette, IN. 2011

Riha, K.M.; Michalski, G.M.; Lohse, K.A.; Gallo, E.L.; Brooks, P.D.; and Meixner, T. (2010) Geochemical and Isotopic Composition of Aerosols in Tucson. Department of Earth and Atmospheric Sciences Graduate Expo. West Lafayette, IN. 2010

Riha, K.M.; Michalski, G.M.; Lohse, K.A.; Gallo, E.L.; Brooks, P.D.; and Meixner, T. (2010) Geochemical and Isotopic Composition of Aerosols in Tucson. Abstract B51H-0457 presented at 2010 Fall Meeting, AGU, San Francisco, Calif. 13-17 Dec.

Riha, K.M.; Michalski, G.; Filley, T.R.; and Dalzell, B.J. (2009), Effects of Environmental Change on Carbon and Nitrogen Fluxes from a Midwestern Agricultural

Watershed. 31st Annual Indiana Water Resources Association Conference. West Lafayette, IN. 2010

Riha, K.M.; Michalski, G.; Filley, T.R.; and Dalzell, B.J. (2009), Effects of Environmental Change on Carbon and Nitrogen Fluxes from a Midwestern Agricultural Watershed. *Eos Trans.AGU, 90* (52), Fall Meet. Suppl., Abstract H53D-0962

Riha, K.M.; Michalski, G.; Filley, T.R.; and Dalzell, B.J. (2009), Effects of Environmental Change on Carbon and Nitrogen Fluxes from a Midwestern Agricultural Watershed. Ecological Science and Engineering Symposium. West Lafayette, IN. 2009

Riha, K.M.; Michalski, G.; Filley, T.R.; and Dalzell, B.J. (2009), Effects of Environmental Change on Carbon and Nitrogen Fluxes from a Midwestern Agricultural Watershed. Department of Earth and Atmospheric Sciences Graduate Expo. West Lafayette, IN. 2008

Riha, K.M.; Michalski, G.; Filley, T.R.; and Dalzell, B.J. (2009), Effects of Environmental Change on Carbon and Nitrogen Fluxes from a Midwestern Agricultural Watershed. Ecological Science and Engineering Symposium. West Lafayette, IN. 2008

Riha, K.M.; McConnell, J.S.; Altfillisch, C.J.; Bilderback, S.L.; Brink, M.T.; Maness, L.A.; and Stenger, S.M. (2008) Distribution and dynamics of nitrate-nitrogen as influenced by long-term nitrogen fertilizer application and irrigation method in an Alfisol cropped to cotton. Abstract ENVR 215, 235th National American Chemical Society Meeting. New Orleans, LA. 6-10 Apr.

Poster Presentations (Co-Author):

Mase, D.F., Riha, K.M., Waldschmidt, H., and Michalski, G.M. (2011) Seasonal trends of $\Delta^{17}O$, $\delta^{18}O$ and $\delta^{15}N$ in atmospheric NO_3^- of the Midwestern United States, Abstract B43E-0324 presented at 2011 Fall Meeting, AGU, San Francisco, Calif. 5-9 Dec.

Werayawarangura, W.; Riha, K.; Michalski, G.; and Mickelbart, M. (2011) Plant Nitrogen Use Efficiency, Summer Undergraduate Research Fellowship Research Symposium, Purdue University, 3 Aug.

Oral Presentations (Co-Contributor):

Mickelbart, M.; Werayawarangura, W.; Riha, K.; Gosney, M.J.; and Michalski, G. (2012) Using Stable Isotopes to Quantify Nitrogen Fates in Container Plants, American Society for Horticultural Science, Miami, FL. 31 Jul. – Aug 3.

Lohse, K.A.; Gallo, E.; Carlson, M.; Riha, K.M.; Brooks, P.D.; McIntosh, J.C.; Sorooshian, A.; Michalski, G.M.; and Meixner, T. (2011) *invited* Abstract H51P-08 presented at 2011 Fall Meeting, AGU, San Francisco, Calif. 5-9 Dec.

Undergraduate Mentoring:

Purdue University Summer Undergraduate Research Fellowships (SURF) – 2011
Purdue Undergraduate Research experience – 5 students over 5 years

Experience: Teaching Assistant
Department of Earth, Atmospheric, and Plantary Sciences, Purdue University

Planet Earth (January 2013 – May 2013):
- Graded assignments, tests, and research papers.
- Maintained class gradebook and posted grades online.
- Held office hours for student questions.

Oil (August 2012 – December 2012):
- Graded assignments, tests, and research papers.
- Posted class materials and grades online.
- Held office hours for student questions.

Geology (January 2009 – May 2009):
- Taught two lab sections.
- Graded assignments, tests, and lab reports.
- Held office hours for student questions.

Oceanography (August 2008 – December 2008):
- Graded assignments, tests, and research papers.
- Posted class materials and grades online.
- Held office hours for student questions.

Research Assistant, August 2009 – May 2012
Department of Earth, Atmospheric, and Planetary Sciences, Purdue University
- Maintained the denitrifier method.
- Aided other students in use of the denitrifier method.
- Maintained headspace extraction apparatus and conflow interface to the isotope ratio mass spectrometer.

Intern, May 2007 – August 2007
UOP Honeywell – Des Plaines, IL
- Prepared catalysts for several selective hydrogenation processes.
- Modified the support, incorporated metal onto the support and finished the catalyst.
- Discussed problems that occurred throughout experiment with supervisor and possible ways to fix them.

Graduate Assistant, August 2006 – May 2008
Department of Chemistry, Western Illinois University
- Instructed and tutored three weekly inorganic labs of 24 students.
- Graded lab reports, tests, and quizzes.
- Prepared chemicals and other lab materials for organic labs.

Research Assistant: Purdue University, West Lafayette, Indiana
Studying the effects of urbanization on the coupled nitrogen-hydrologic cycle in semi-arid urban environments under the supervision of Dr. Greg Michalski.

Western Illinois University, Macomb, Illinois
Collaborated with Dr. J. Scott McConnell to determine the effect of different fertilizer treatments on the acidity of soil.

Community Outreach 2011-2012
Station organizer for the bi-annual Wabash River sampling blitz. Wabash River Enhancement Corporation. http://www.wabashriver.net/wabash-sampling-blitz
Collect samples from blitz volunteers for nitrate isotope analysis